

**COPY 1** c  
REPORT NO. FAA-RD-75-13

# A COMPUTER STUDY AND SITE ANALYSIS OF THE BUFFALO, NEW YORK RUNWAY 23 GLIDESLOPE SITE

A. F. Zahorchak

**FAA  
LIBRARY  
1277**



December 1974

Released April 1977

Phase II

Interim Report.

Document is available to the U.S. public through  
the National Technical Information Service,  
Springfield, Virginia 22161.

Prepared for

**U.S. DEPARTMENT OF TRANSPORTATION  
FEDERAL AVIATION ADMINISTRATION  
Systems Research & Development Service  
Washington, D.C. 20590**

FAA WJH Technical Center



00090251

NOTICE

This document is disseminated under the sponsorship of the Department of Transportation in the interest of information exchange. The United States Government assumes no liability for its contents or use thereof.

1. Report No. FAA-RD-75-13		2. Government Accession No.		3. Recipient's Catalog No.	
4. Title and Subtitle A COMPUTER STUDY AND SITE ANALYSIS OF THE BUFFALO, NEW YORK RUNWAY 23 GLIDE SLOPE SITE				5. Report Date December 1974 <b>Released April 1977</b>	
				6. Performing Organization Code	
7. Author(s) A. F. ZAHORCHAK				8. Performing Organization Report No.	
9. Performing Organization Name and Address WESTINGHOUSE DEFENSE & ELECTRONIC SYSTEMS CENTER AEROSPACE & ELECTRONICS SYSTEMS DIVISION BALTIMORE, MARYLAND 21203				10. Work Unit No. (TRAVIS)	
				11. Contract or Grant No. DOT-FA74WA-3360	
12. Sponsoring Agency Name and Address U.S. Department of Transportation Federal Aviation Administration Systems Research and Development Service Washington, D.C. 20590				13. Type of Report and Period Covered INTERIM REPORT MARCH 1974-DEC. 1974	
				14. Sponsoring Agency Code	
15. Supplementary Notes					
16. Abstract  The possibility of achieving Category II performance at Buffalo Runway 23 is investigated in this report. Optimum antenna performance is obtained by compensation, increased coning and the evaluation of terrain effects for each antenna site. These techniques resulted in the probable attainment of Category II performance at Buffalo.					
17. Key Words INSTRUMENT LANDING SYSTEMS Glideslope                      Broadside Sidelobe                         Terrain Compensation                    Coning Waveguide Antenna              Powerline Modeling			18. Distribution Statement  Document is available to the U.S. public through the National Technical Information Service, Springfield, Virginia 22161.		
19. Security Classif. (of this report) UNCLASSIFIED		20. Security Classif. (of this page) UNCLASSIFIED		21. No. of Pages 73	22. Price

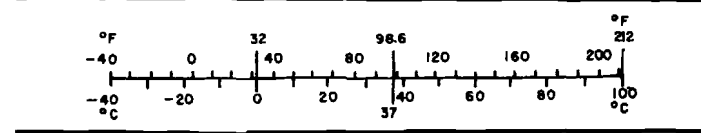
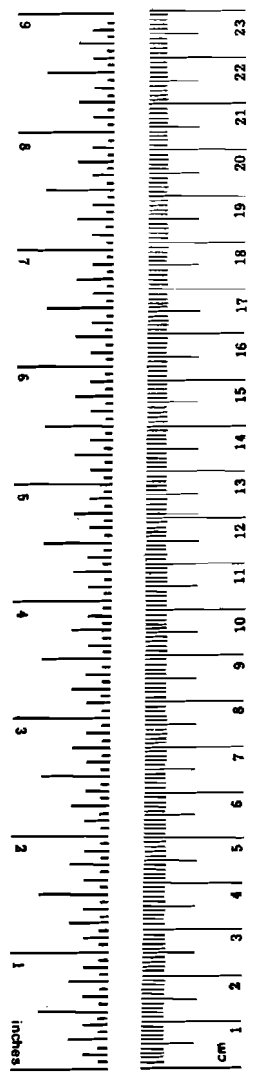
## METRIC CONVERSION FACTORS

### Approximate Conversions to Metric Measures

Symbol	When You Know	Multiply by	To Find	Symbol
<b>LENGTH</b>				
in	inches	*2.5	centimeters	cm
ft	feet	30	centimeters	cm
yd	yards	0.9	meters	m
mi	miles	1.6	kilometers	km
<b>AREA</b>				
in <sup>2</sup>	square inches	6.5	square centimeters	cm <sup>2</sup>
ft <sup>2</sup>	square feet	0.09	square meters	m <sup>2</sup>
yd <sup>2</sup>	square yards	0.8	square meters	m <sup>2</sup>
mi <sup>2</sup>	square miles	2.6	square kilometers	km <sup>2</sup>
	acres	0.4	hectares	ha
<b>MASS (weight)</b>				
oz	ounces	28	grams	g
lb	pounds	0.45	kilograms	kg
	short tons (2000 lb)	0.9	tonnes	t
<b>VOLUME</b>				
tsp	teaspoons	5	milliliters	ml
Tbsp	tablespoons	15	milliliters	ml
fl oz	fluid ounces	30	milliliters	ml
c	cups	0.24	liters	l
pt	pints	0.47	liters	l
qt	quarts	0.95	liters	l
gal	gallons	3.8	liters	l
ft <sup>3</sup>	cubic feet	0.03	cubic meters	m <sup>3</sup>
yd <sup>3</sup>	cubic yards	0.76	cubic meters	m <sup>3</sup>
<b>TEMPERATURE (exact)</b>				
°F	Fahrenheit temperature	5/9 (after subtracting 32)	Celsius temperature	°C

### Approximate Conversions from Metric Measures

Symbol	When You Know	Multiply by	To Find	Symbol
<b>LENGTH</b>				
mm	millimeters	0.04	inches	in
cm	centimeters	0.4	inches	in
m	meters	3.3	feet	ft
m	meters	1.1	yards	yd
km	kilometers	0.6	miles	mi
<b>AREA</b>				
cm <sup>2</sup>	square centimeters	0.16	square inches	in <sup>2</sup>
m <sup>2</sup>	square meters	1.2	square yards	yd <sup>2</sup>
km <sup>2</sup>	square kilometers	0.4	square miles	mi <sup>2</sup>
ha	hectares (10,000 m <sup>2</sup> )	2.5	acres	
<b>MASS (weight)</b>				
g	grams	0.035	ounces	oz
kg	kilograms	2.2	pounds	lb
t	tonnes (1000 kg)	1.1	short tons	
<b>VOLUME</b>				
ml	milliliters	0.03	fluid ounces	fl oz
l	liters	2.1	pints	pt
l	liters	1.06	quarts	qt
l	liters	0.26	gallons	gal
m <sup>3</sup>	cubic meters	35	cubic feet	ft <sup>3</sup>
m <sup>3</sup>	cubic meters	1.3	cubic yards	yd <sup>3</sup>
<b>TEMPERATURE (exact)</b>				
°C	Celsius temperature	9/5 (then add 32)	Fahrenheit temperature	°F



\*1 in = 2.54 (exactly). For other exact conversions and more detailed tables, see NBS Misc. Publ. 286, Units of Weights and Measures, Price \$2.25, SD Catalog No. C13.10:286.

## TABLE OF CONTENTS

	<u>PAGE</u>
1.0 INTRODUCTION	1-1
2.0 VERIFICATION OF MODEL	2-1
2.1 Modeling Techniques	2-1
2.2 Uncompensated Pattern Matching	2-5
2.3 Terrain Modeling	2-9
2.4 Compensated Pattern Matching	2-9
3.0 PREDICTION OF ILS PERFORMANCE	
3.1 Long Term Derogation	3-1
3.2 Short Term Derogation	3-1
3.3 Powerlines	3-15
4.0 REFERENCES	4-1
<u>APPENDIX</u>	<u>Page</u>
A.1.0 DETERMINATION OF MAXIMUM PLATE SIZE FOR TERRAIN MODELING	A-1
A.2.0 POWERLINE MODELING	A- 4

## LIST OF ILLUSTRATIONS

<u>FIGURE</u>		<u>PAGE</u>
2.1	U.S.GEOLOGICAL SURVEY MAP OF THE BUFFALO INTER- NATIONAL AIRPORT AREA	2-2
2.2	U.S. GEOLOGICAL SURVEY MAP OF THE BUFFALO INTERNATIONAL AIRPORT AREA	2-3
2.3	NON-LEVEL TERRAIN MODELING	2-4
2.4	DETERMINATION OF NORMALIZATION FACTOR	2-6
2.5	COMPARISON OF MEASURED AND CALCULATED 0 dB CONED ANTENNA PATTERNS (UNCOMPENSATED)	2-7
2.6	COMPARISON OF MEASURED AND CALCULATED 6 dB CONED ANTENNA PATTERNS (UNCOMPENSATED)	2-8
2.7	DATA POINTS FROM SIX TYPICAL R.T.T. RUNS MEASURED AT BUFFALO	2-11
2.8	FLY-IN ASSUMING DEROGATION DUE TO AN INFINITE FLAT PLANE	2-12
2.9	RUNWAY EMBANKMENT MODELED	2-13
2.11	TERRAIN CROSS-SECTION IN FRONT OF ANTENNA	2-14
2.10	FENCE PARALLEL TO RUNWAY MODELED	2-15
2.12	DEROGATION DUE TO AN INFINITE TILTED PLANE SUPERIMPOSED ON MEASURED DATA	2-16
2.13	POSSIBLE DEROGATION HALF-WAVELENGTHS OCCURRING IN MEASURED DATA CURVE	2-17
2.14	DETERMINATION OF DIRECTION OF DEROGATING ENERGY	2-18
2.15	AREA OF POSSIBLE DEROGATION SOURCES DUE TO A DEROGATION WAVELENGTH OF <u>4000 FEET</u>	2-19
2.16	<u>OF 7200 FEET</u>	2-20
2.17	<u>OF 13000 FEET</u>	2-21
2.18	<u>OF 8000 FEET</u>	2-22
2.19	METHOD OF MODELING THRUWAY	2-23
2.20	COMPARISON OF MEASURED DATA TO CALCULATED DATA WITH THRUWAY MODELED	2-24

FIGURELIST OF ILLUSTRATIONSPAGE

2.21	COMPARISON OF MEASURED AND CALCULATED 6 dB COMPENSATED ANTENNA PATTERNS	2-26
2.22	COMPARISON OF MEASURED AND CALCULATED 9 dB COMPENSATED ANTENNA PATTERNS	2-27
3.1	COMPARISON OF COMPENSATED AND UNCOMPENSATED FLY-INS AT ORIGINAL ANTENNA SITE AND WITH ORIGINAL ANTENNA CHARACTERISTICS	3-2
3.2-3.12	SEE TABLE 2-1, Page 3-3	3-4 to 3-14
3.13	REDUCTION OF FAST TERM DEROGATION BY INCREASED CONING (4 dB to 9 dB)	3-16
3.14	LOCATION OF SIX POSSIBLE ANTENNA SITES	3-17
3.15 - 3.20	FLY-INS FOR EACH OF THE ANTENNA SITES INDICATED IN FIGURE 3.14	3-18 to 3-23
3.21	OPTIMUM FLY-IN WITH ALL SIGNIFICANT TERRAIN MODELED	3-24
3.22	RELATION OF AIRCRAFT PATH TO POWERLINES	3-25
3.23- 3.25	DEROGATION DUE TO POWERLINES FOR THREE RADII	3-27 to 3-29
A.1.1	DESCRIPTION OF COMPONENTS OF PHYSICAL OPTICS EQUATION	A-2
A.1.2	DETERMINATION OF MAXIMUM PLATE SIZE	A-3
A.2.1	IDEALIZED REPRESENTATION OF A POWERLINE ILLUMINATED BY A PLANE WAVE	A-5

## 1.0 INTRODUCTION AND SUMMARY

The primary purpose of this study is to determine if the modified waveguide antenna will provide Category II guidance at Buffalo Runway 23. This problem can be divided into two portions: first; verification of the computer model, second; prediction of antenna performance using this model.

The first step in the verification process is determining an analytical model of the antenna which calculates antenna patterns, structure runs and other pertinent data which can be compared to measured data. An existing computer program was modified to accomplish this task.

The antenna characteristics were adjusted so that calculated antenna patterns matched measured antenna patterns taken at Buffalo in 1967. Measured RTT runs were averaged and this average compared to calculated fly-ins. Agreement was attained by calculating the effect of a thruway located approximately 1300 feet from the runway threshold and cutting diagonally across the aircraft approach path. This verified the computer model of the uncompensated antenna.

Compensated antenna patterns were measured at the Westinghouse antenna range. These measured patterns were matched by calculated patterns for 6 dB coning and 9 dB coning.

The modeled compensated antenna was then used to calculate fly-ins at the original antenna site with 4 dB coning. It was felt that further improvement could be realized by increased coning and a larger backset from threshold. At this point, several variables were controlled to optimize ILS performance. These were:

Antenna position, coning, antenna height, backtilt and side tilt. Three antenna positions were investigated along with 6 dB and 9 dB coning. The remaining variables were judiciously adjusted at each site to give maximum performance. The best conditions were determined to be:

Backset of 800 feet, offset of 650 feet, 9 dB coning, antenna height of 43.1 feet, back tilt of  $4.11^{\circ}$  and side tilt of  $.5^{\circ}$ .

A trip to Buffalo was made to examine the proposed site in more detail. The tentative location was found to be unsuitable so six more locations at less offset were investigated using more reliable terrain information. The final position was determined to be:

850 feet backset, 500 feet offset, 42.5 feet height,  $4.113^{\circ}$  back tilt and  $.5^{\circ}$  side tilt.

The effect of power lines in the vicinity of Runway 23 was investigated and found to be negligible.

## 2.0 VERIFICATION OF MODEL

### 2.1 Modeling Techniques

A computer program, already in existence, which calculates antenna patterns, structure runs and level runs for the uncompensated and compensated waveguide antenna was modified and used in the analysis of Buffalo Runway 23.

Upon examination of terrain maps, the only major terrain feature in the far zone of the antenna is a down slope of approximately  $.5^\circ$  at a range of 14,000 to 15,000 feet. Figures 2.1 and 2.2 show portions of a U.S. geological survey map of the area around the greater Buffalo International Airport. This down slope, since it is such a great distance from the antenna, will have very little effect on the guidance, so any terrain modeling will occur close to the antenna.

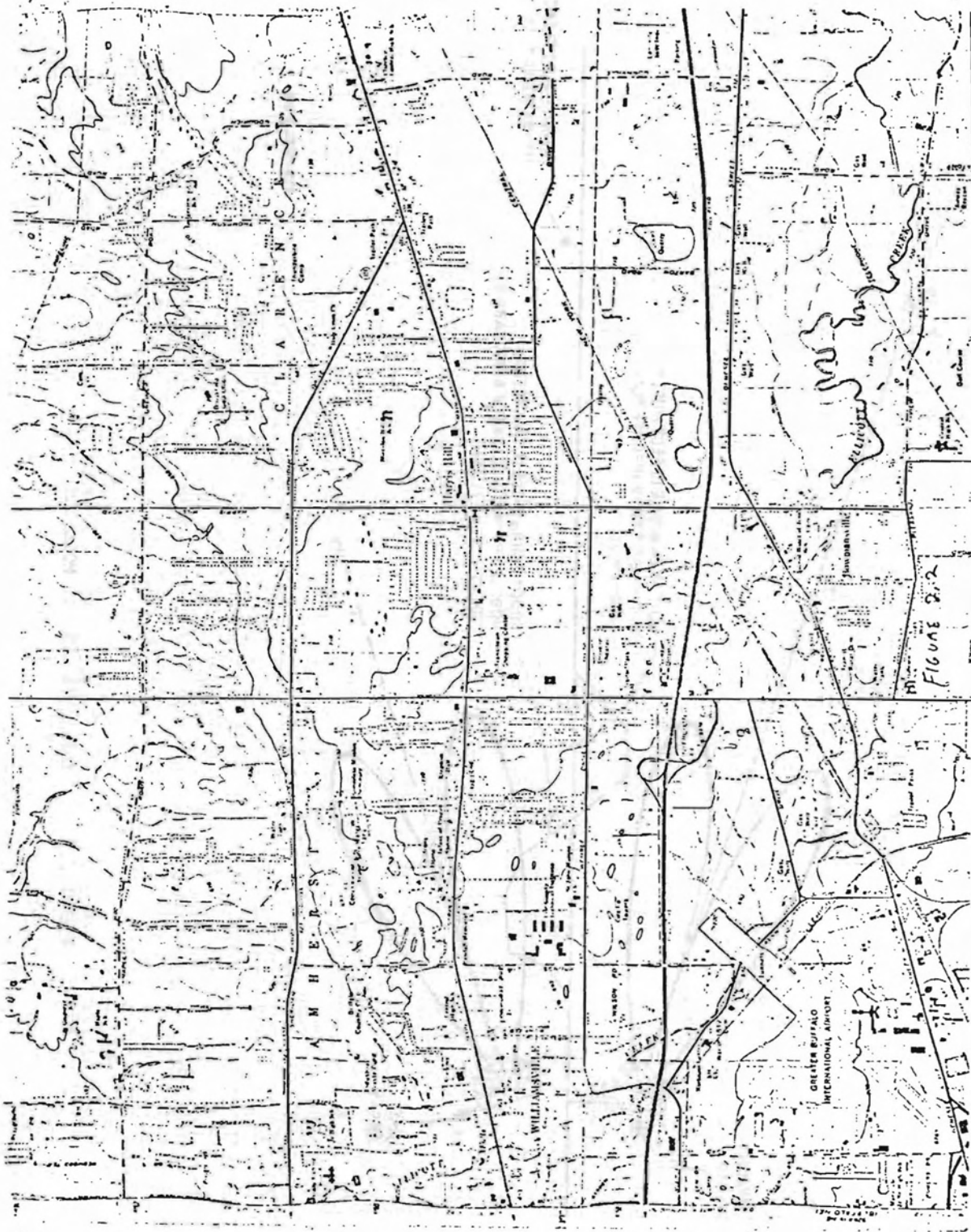
Figure 2.3 shows the strategy utilized in modeling non-flat terrain near the antenna.<sup>2.1</sup>

The effect of the non-flat ground is determined in three steps. As a first approximation, the terrain is assumed to be an infinite flat plane and image theory is used to calculate the field at the aircraft.

Second, the area which is occupied by the non-flat ground is modeled as a void. This is done by modeling the area represented by the dotted line in Figure 2.3 by pre-integrated flat plates. The effect of this flat area is then subtracted from the infinite flat plane approximation. Third, the non-flat portion is built up by pre-integrated plates and their effect is added to the previous calculation. If the pre-integrated flat plates are small enough, this method will result in an accurate prediction of the effect of terrain. Appendix A1 details the investigation of maximum plate size that will still insure accurate prediction. Since the non-flat terrain occurs only near the antenna, it was assumed that the pre-integrated plates were illuminated by direct radiation only. This is in contrast to the case of modeling mountains at great distance from the antenna where the pre-integrated plates are illuminated by direct and image radiation.



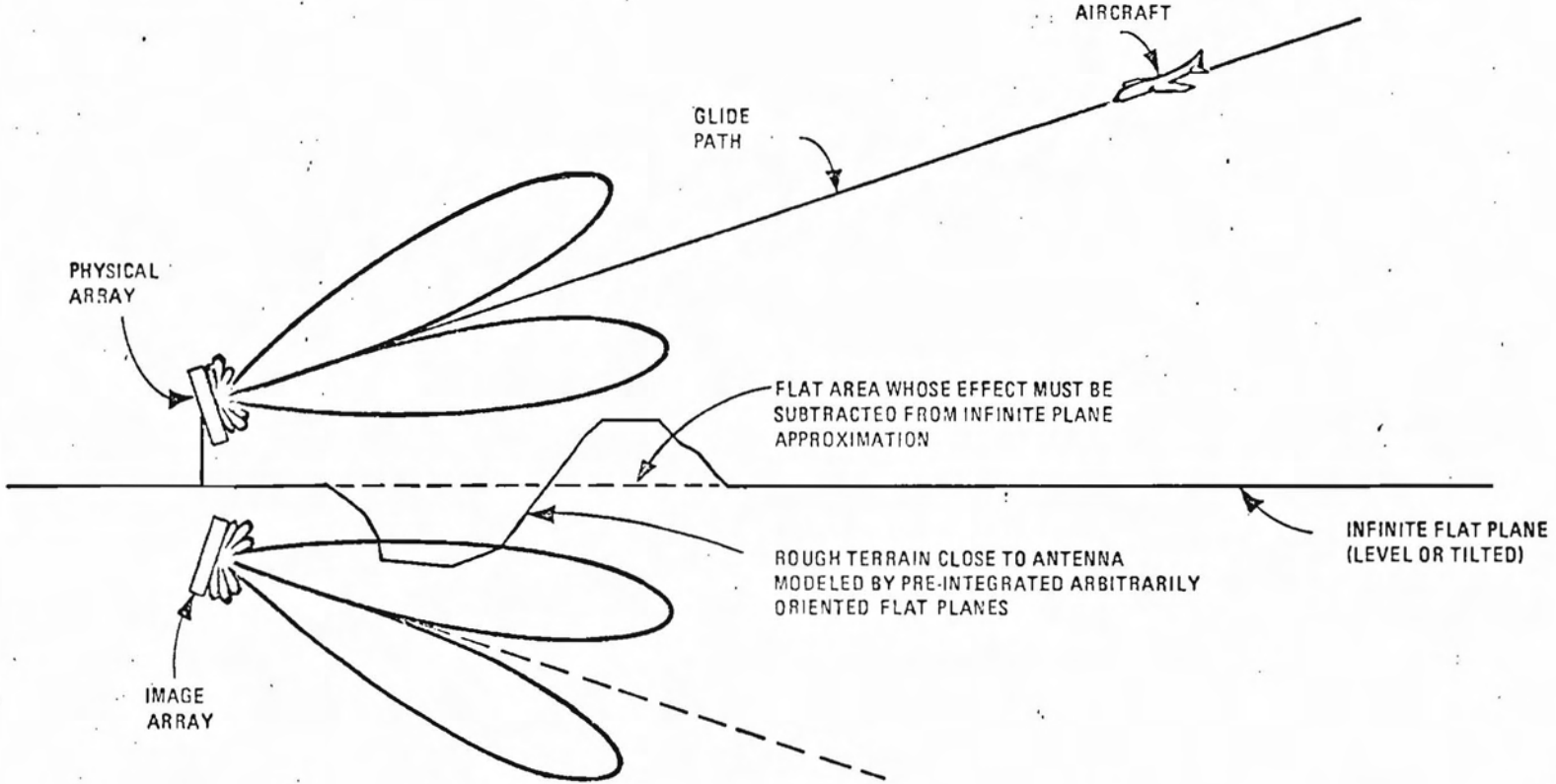
FIGURE 2.1 U.S. GEOLOGICAL SURVEY OF THE BUFFALO INTERNATIONAL AIRPORT AREA.



U.S. GEOLOGICAL SURVEY OF THE BUFFALO  
INTERNATIONAL AIRPORT AREA

FIGURE 2.2

2-4



S74-0934-VA-1

FIGURE 2.3 NON-LEVEL TERRAIN MODELING

In order for the structure output to be an accurate representation of what the pilot reads on the DDM indicator it is necessary to provide a scaling which is equivalent to the calibration used on the actual equipment. Figure 2.4 illustrates the calculation of the scaling or normalization factor.

$$N = \frac{75}{\frac{1}{2} \left| \mathcal{R}_e \left( \frac{S}{C} \right)_{+.35^\circ} \right| + \frac{1}{2} \left| \mathcal{R}_e \left( \frac{S}{C} \right)_{-.35^\circ} \right|}$$

S is the detected side band difference and C is the detected carrier level or sum. These are due to both direct and image radiation. The side band only power is adjusted until a path width of  $.7^\circ$  results. That is, the side band only power is adjusted until the pilot reads + 75 microamps at Point A and -75 microamps at Point B. The DDM in microamps can be written as:

$$DDM = N \left[ \mathcal{R}_e \left( \frac{S}{C} \right) \right]$$

S and C refer to the total detected side band and carrier signals received at the point of interest.

## 2.2 Uncompensated Pattern Matching

In 1967, several fly over runs were made at Buffalo with the waveguide antenna lying on its back. 6 dB and 0 dB coned antenna patterns were measured at an altitude of 15,000 feet. Using the computer, these measured patterns were duplicated. This was done by varying the efficiency of the antenna model about its approximate value of .5 until the difference between the measured and calculated antenna patterns was minimized. Figures 2.5 and 2.6 show the results of this minimization for 0 dB and 6 dB coning respectively. This concluded the model verification of those antenna characteristics which are independent of the terrain.

256

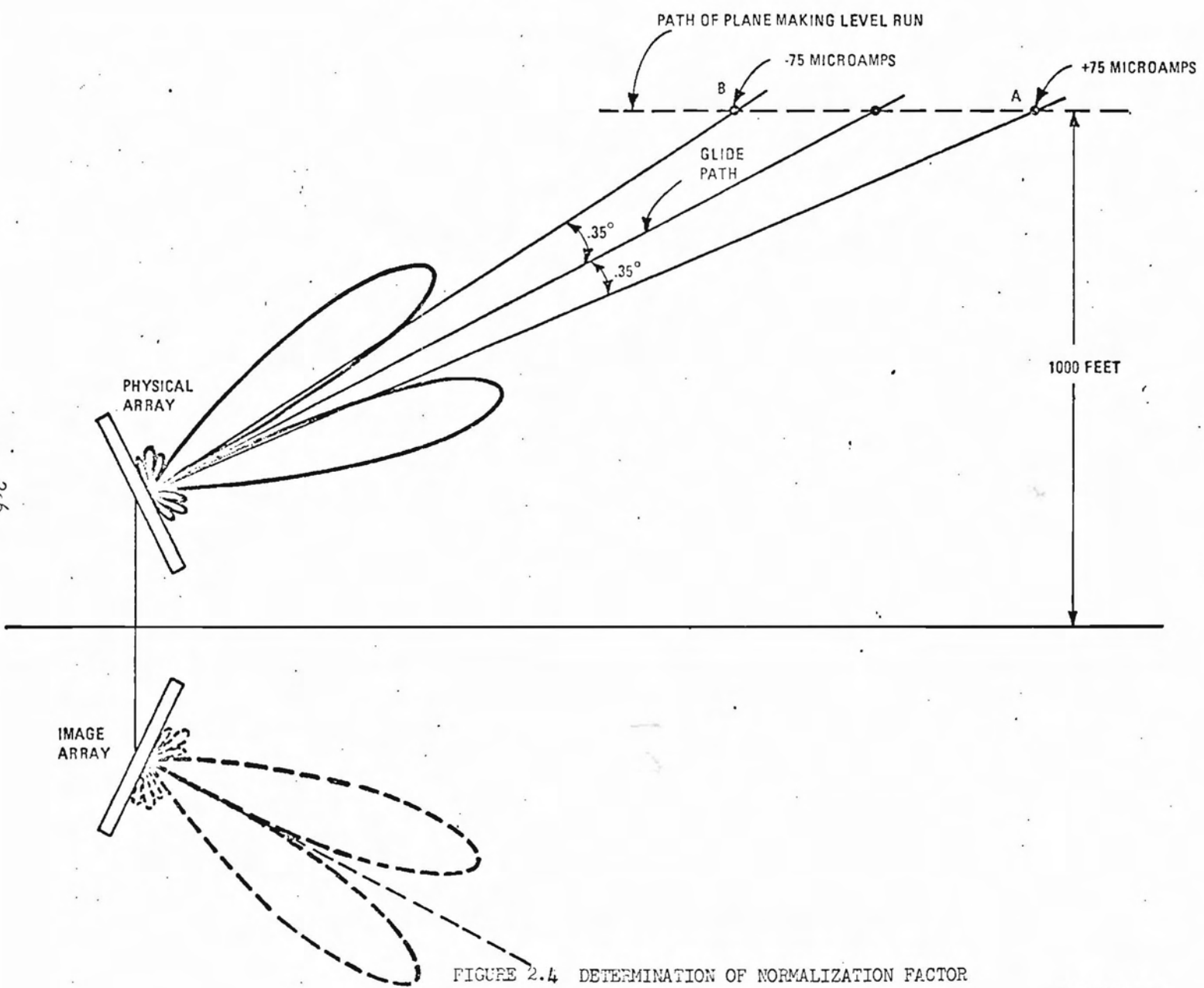


FIGURE 2.4 DETERMINATION OF NORMALIZATION FACTOR

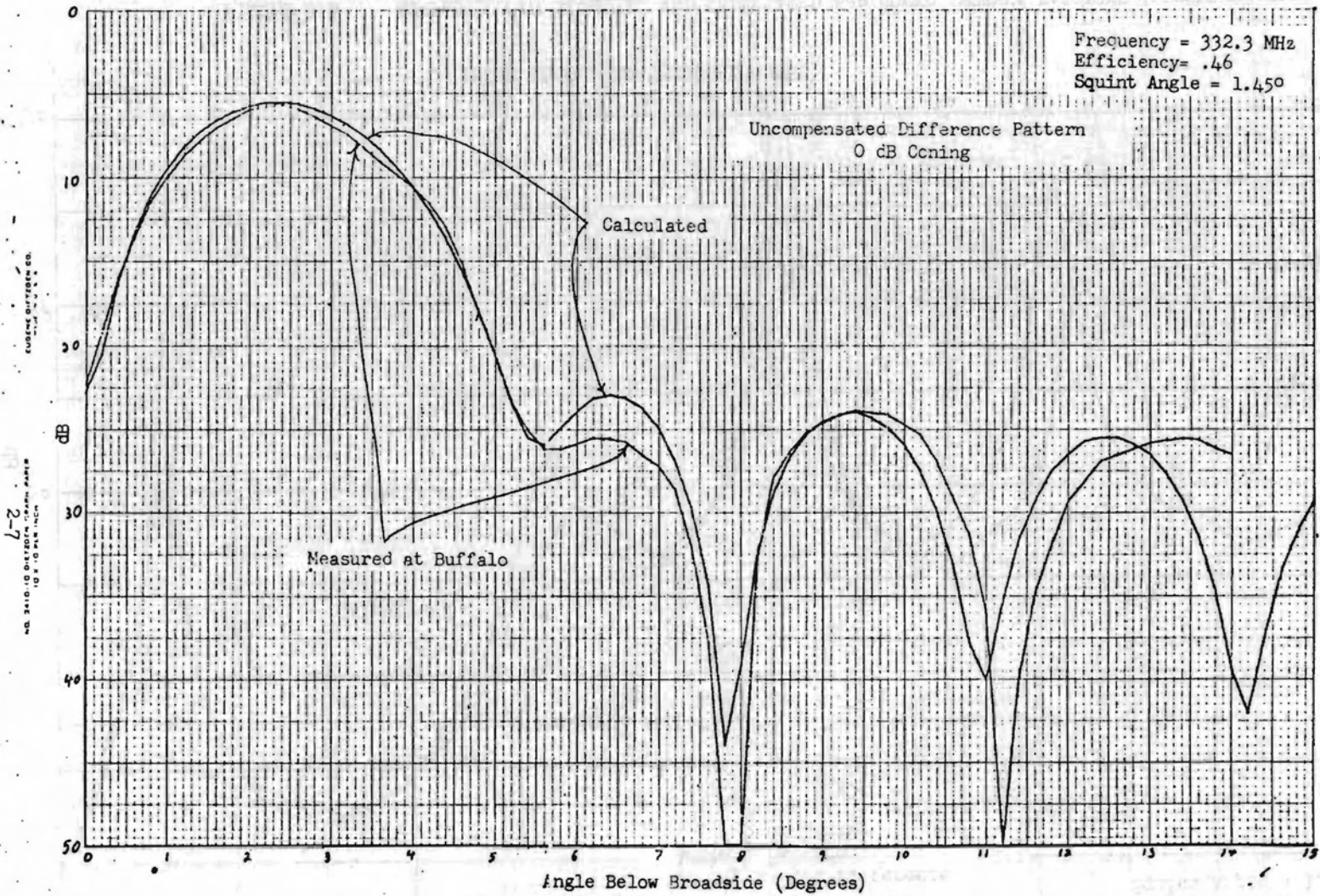


FIGURE 2.5 COMPARISON OF MEASURED AND CALCULATED 0dB CONED ANTENNA PATTERNS (UNCOMPENSATED)

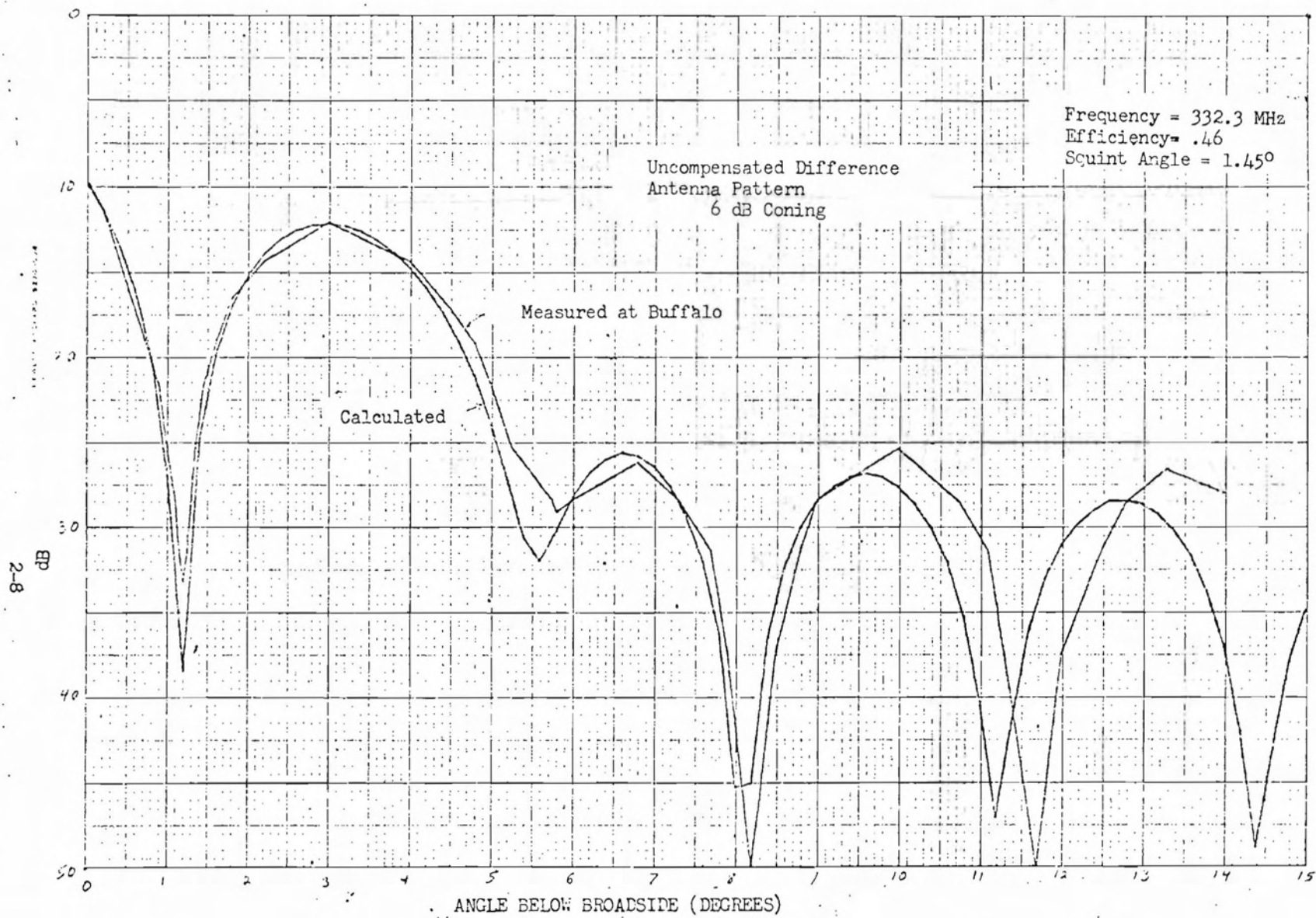


FIGURE 2.6 COMPARISON OF MEASURED AND CALCULATED 6dB CONED ANTENNA PATTERNS (UNCOMPENSATED)

### 2.3 Terrain Modeling

A great deal of structure data was taken at Buffalo in 1967. However, only a small portion of that data was obtained using an R.T.T. There were also two antenna heights. The earliest data was taken with the antenna phase center 67 feet above the ground but no R.T.T. data was taken at this antenna height. The antenna was lowered 30 feet on May 2, 1967 and R.T.T. measurements were made beginning on May 26, 1967. Table 1 shows a list of all the R.T.T. structure runs. Six of these runs were chosen for their legibility and because they were a representative cross-section of the conditions noted in Table 1. Data points from runs number 12, 42, 44, 78, 92 and 98 are plotted in Fig. 2.7 and an average curve drawn through these points to represent a long term trend. The inclusion of terrain effects in the computer model should duplicate this measured curve. Figure 2.8 is a structure run assuming the antenna phase center is situated 37 feet above an infinite flat plane. Since the area around Runway 23 is not an infinite flat plane one should not be surprised that Figure 2.8 does not agree with the measured data of Figure 2.7.

To further improve the similarity of the two curves, more explicit modeling was required. The first obvious choices were the runway embankment and the chain link fence running parallel to the runway. Figures 2.9 and 2.10 show the effect of both of these. Obviously, the long term trend exhibited by the measured data is not produced by either the fence or the embankment. As an additional refinement the terrain in front of the antenna was investigated to determine if any large scale terrain trends could be ascertained. Figure 2.11 is a cross-section of the ground in front of the antenna. As one can see, a general uptilt of about  $.25^\circ$  occurs. Figure 2.12 shows a fly-in with the inclusion of the ground tilt superimposed on the measured trend.

Upon examination of the measured data, possible periodic interference can be discerned. Fig. 2.13 illustrates how the measured curve can be divided into sections that appear to be half the period of some sinusoidal interference. This information can be used to calculate the location of possible derogating sources. Figure 2.14 explains how this was done. If the direct radiation and the derogating radiation add in phase at point A and subtract at point B, then the two signals must differ in phase by  $180^\circ$  at point B.

TABLE 1

<u>RUN NUMBER</u>	<u>DATE</u>	<u>CONING</u>	<u>REMARKS</u>
12	5/26/67	4 dB	
13	"	"	
14	"	"	
15	"	"	
32	5/27/67	"	
33	"	"	
34	"	"	
35	"	"	
39	"	"	1000 Feet Of Fence Next To Antenna Lowered
42	"	"	
44	"	"	
45	"	"	
46	"	"	
62	6/2/67	"	Additional 150 Feet Of Fence Lowered (Down To 50 Feet Behind Antenna)
66	"	"	150 Feet Of Fence Set Back Up
68	"	"	
70	"	"	Remove Guy Wires From Tower
71	"	"	
75	6/3/67	"	
77	"	"	
78	"	"	
80	"	"	
85	"	"	
90	"	"	
92	6/4/67	"	6 Short Screens Mounted 12 Feet Apart On 1000 Foot Light Station
93	"	"	
94	"	"	
98	"	"	Secondary Braces Removed From G. S. Tower
102	"	5 dB	Removed Screens
103	"	"	
106	6/5/67	4 dB	
107	6/5/67	4 dB	
2	6/21/67	"	Screens Installed Behind Antenna
4	"	"	
6	6/22/67	"	
9	"	"	Screens Behind Antenna Removed

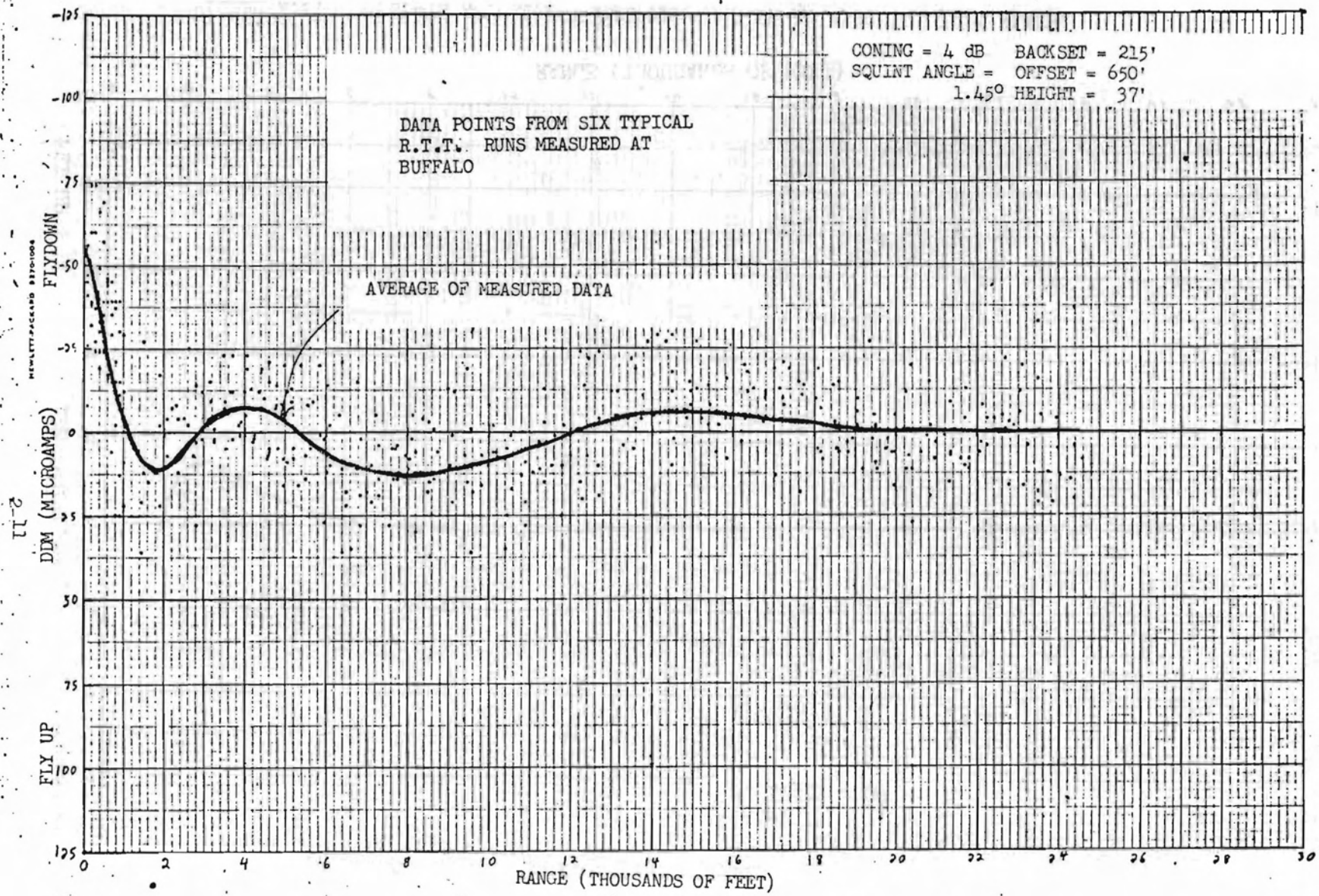


FIGURE 2.7 DATA POINTS FROM SIX TYPICAL R.T.T. MEASURED AT BUFFALO

FAA WJH Technical Center  
 00090251

2-12

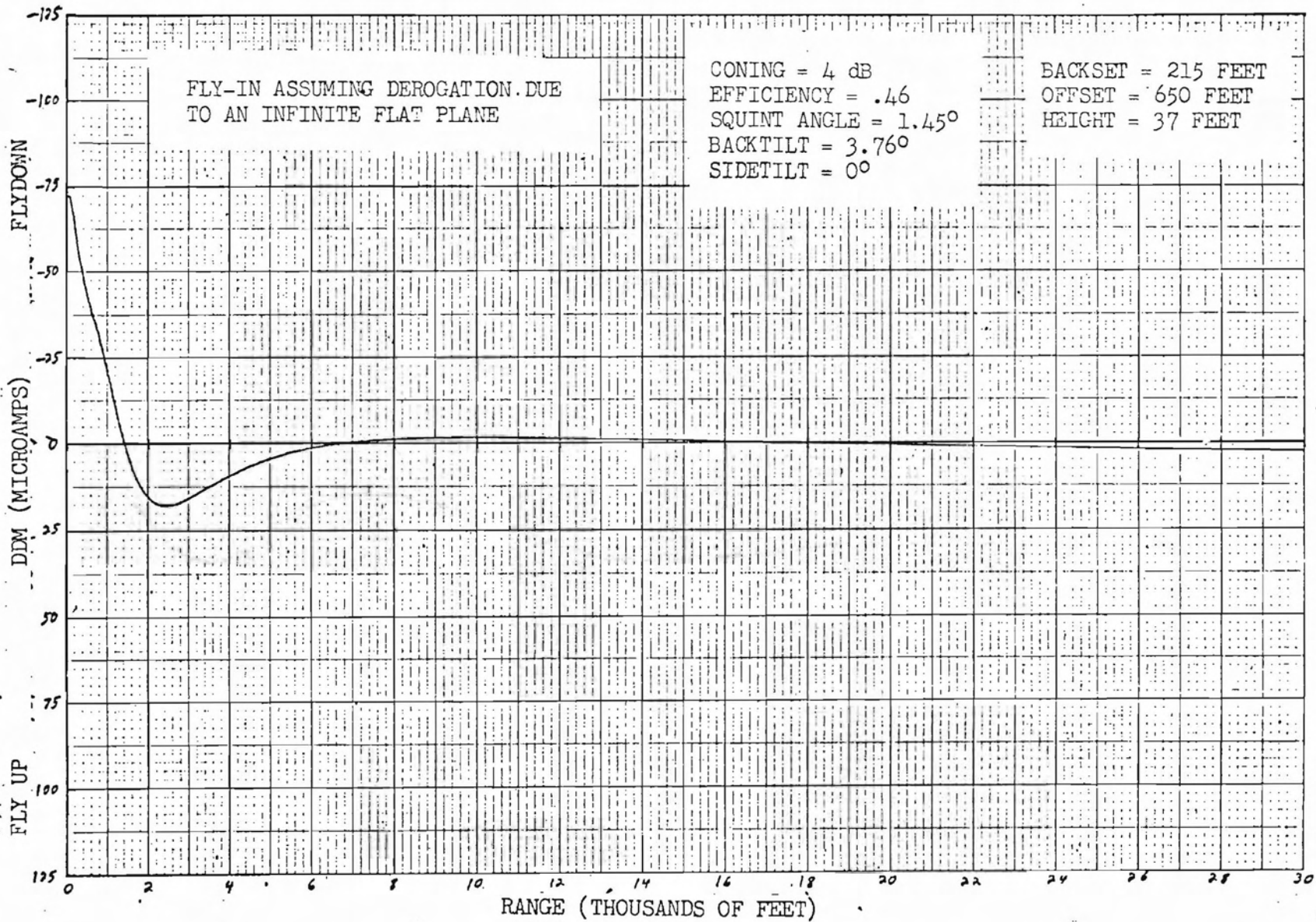


FIGURE 2.8. FLY-IN ASSUMING DEROGATION DUE TO AN INFINITE FLAT PLANE.

2-13

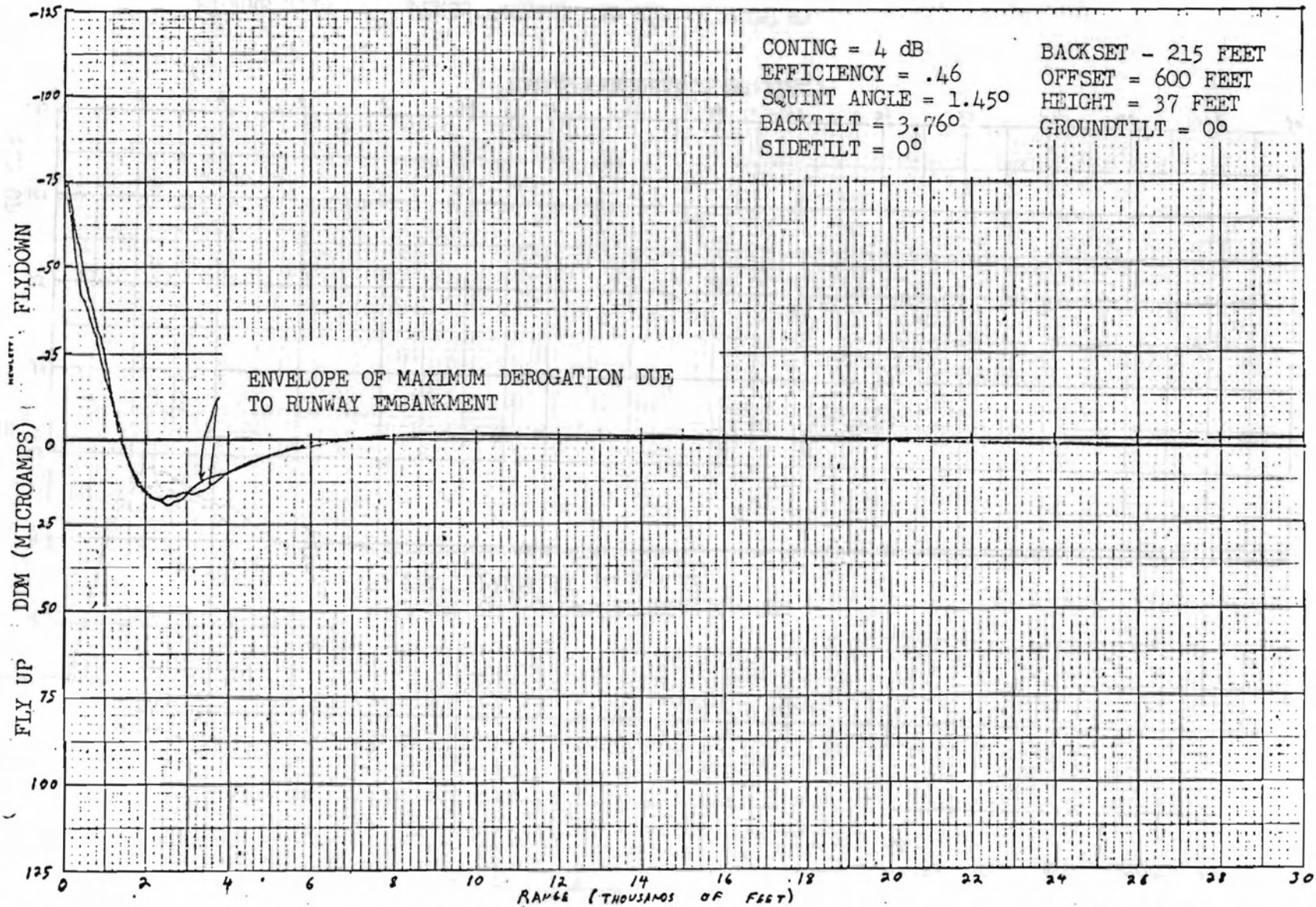


FIGURE 2.9 RUNWAY EMBANKMENT MODELED

214

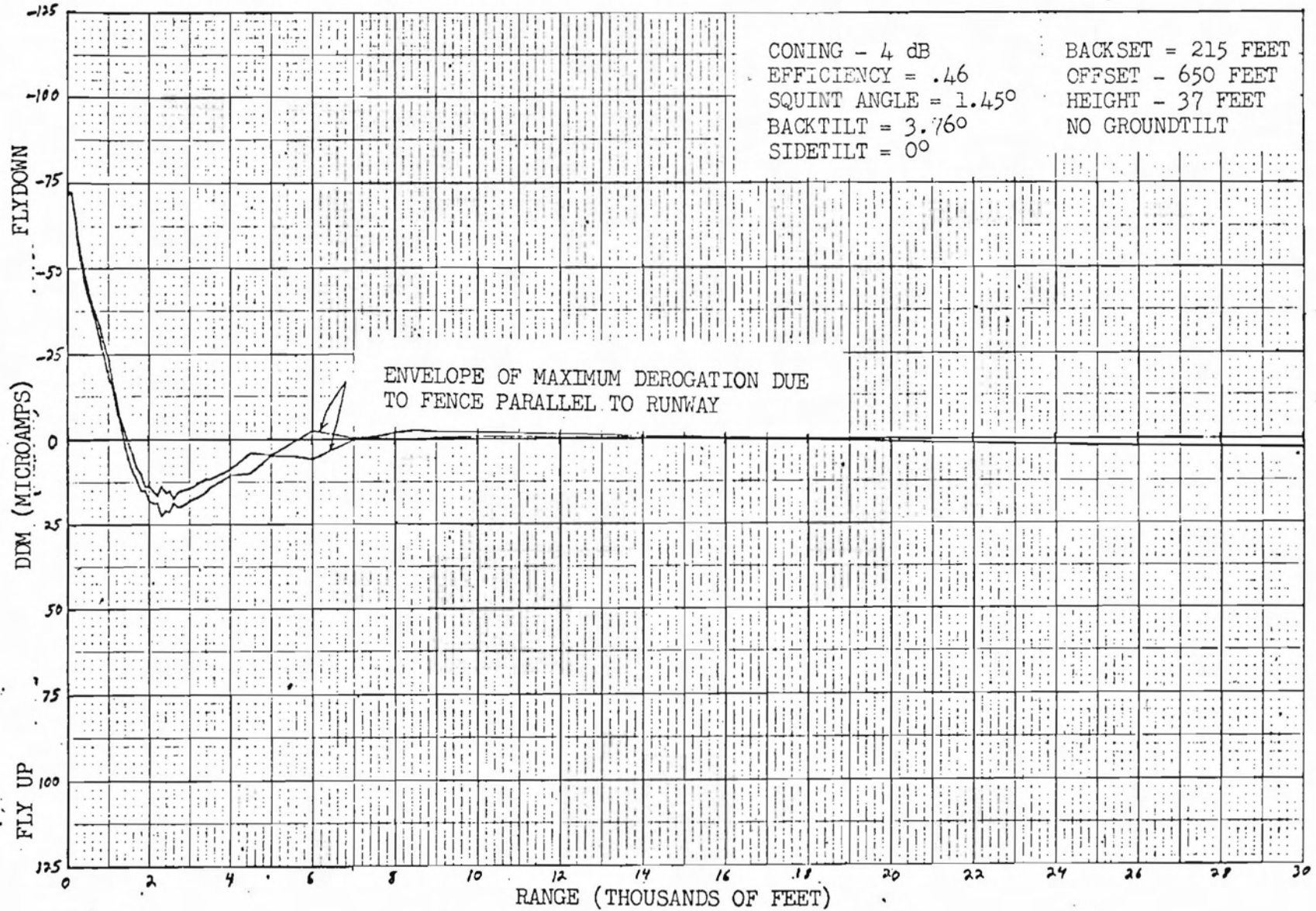


FIGURE 2.10

FENCE PARALLEL TO RUNWAY MODELED

2.15

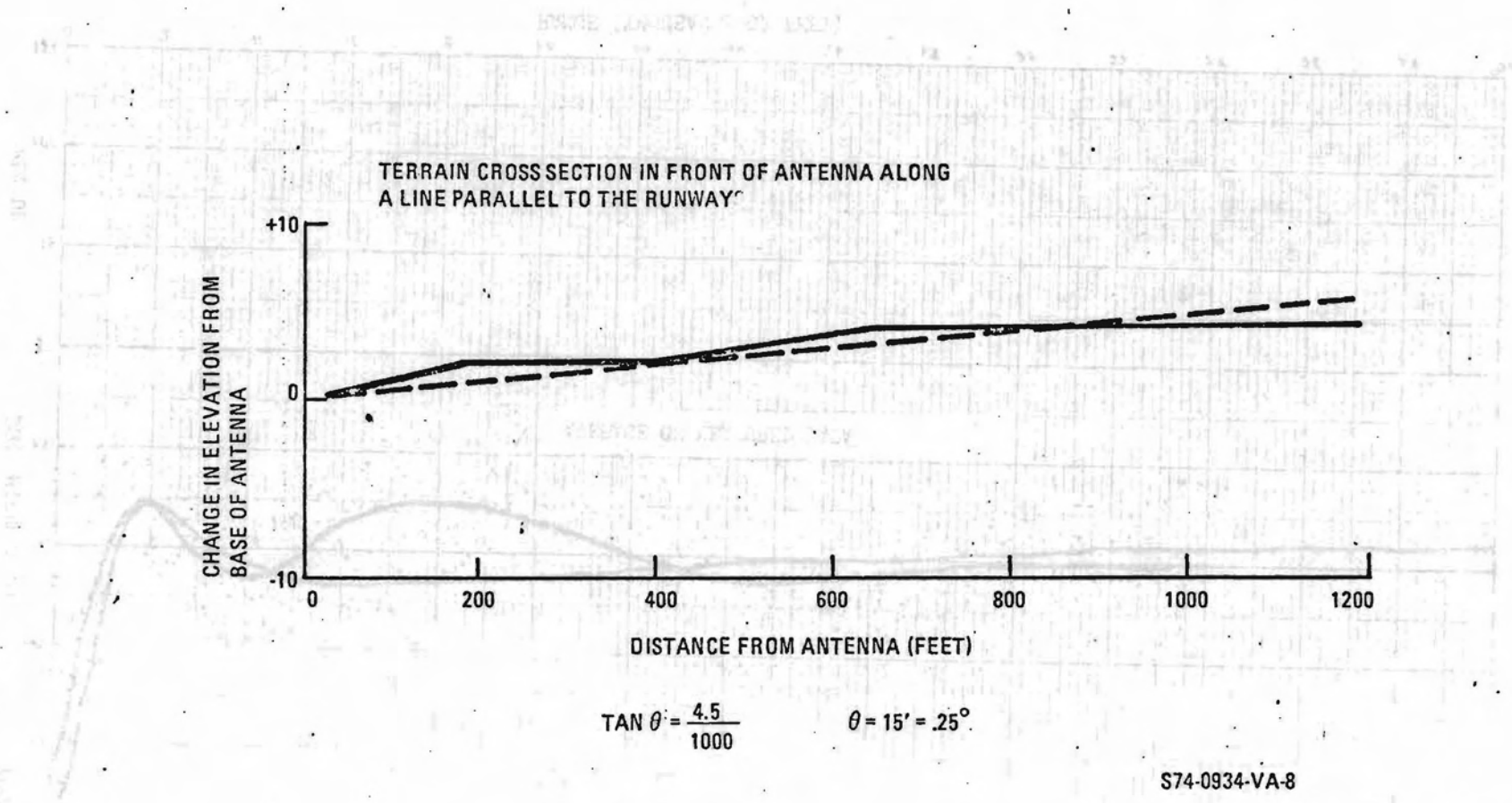


FIGURE 2.11 TERRAIN CROSS-SECTION IN FRONT OF ANTENNA

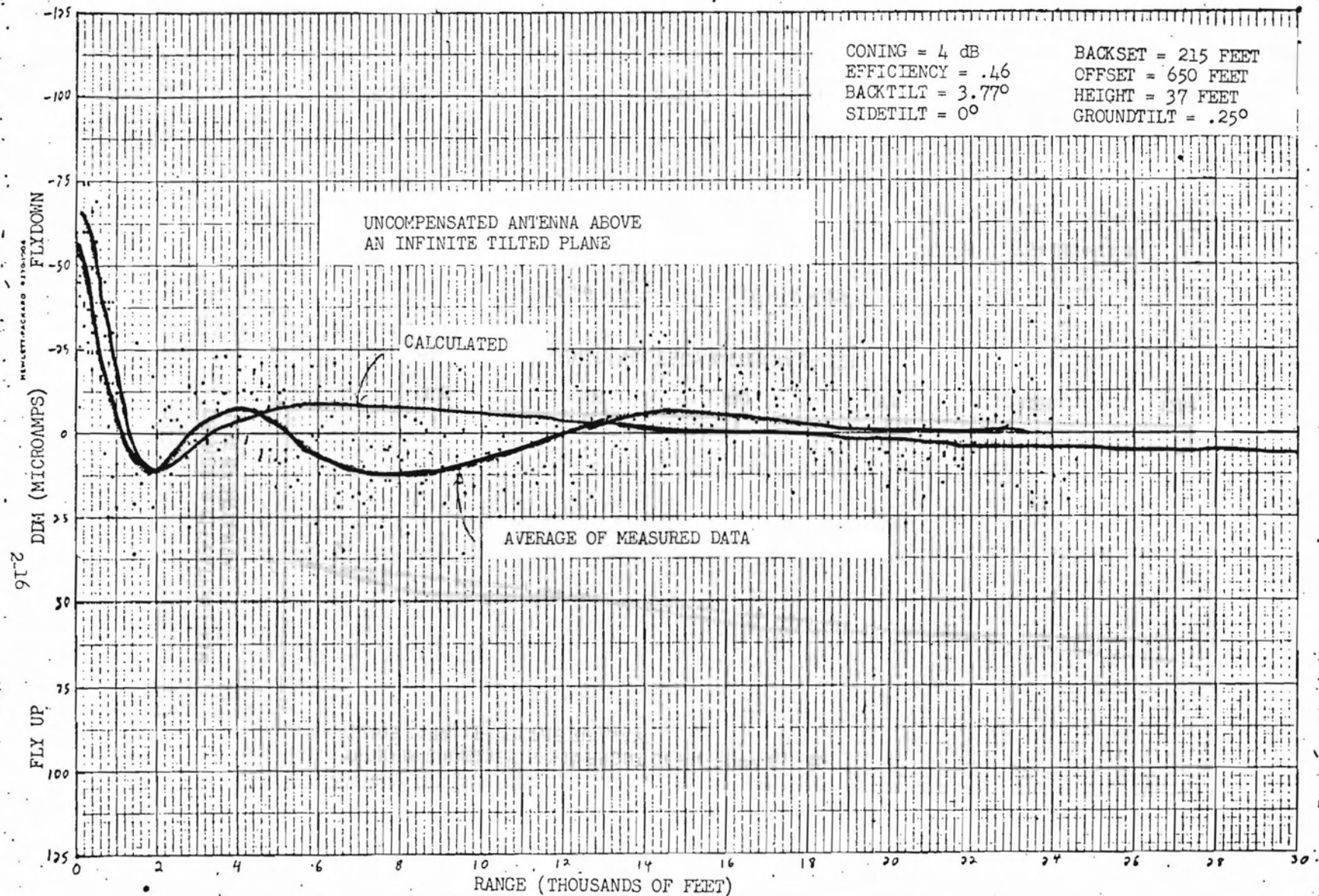


FIGURE 2.12. DEROGATION DUE TO AN INFINITE TILTED PLANE SUPERIMPOSED ON MEASURED DATA

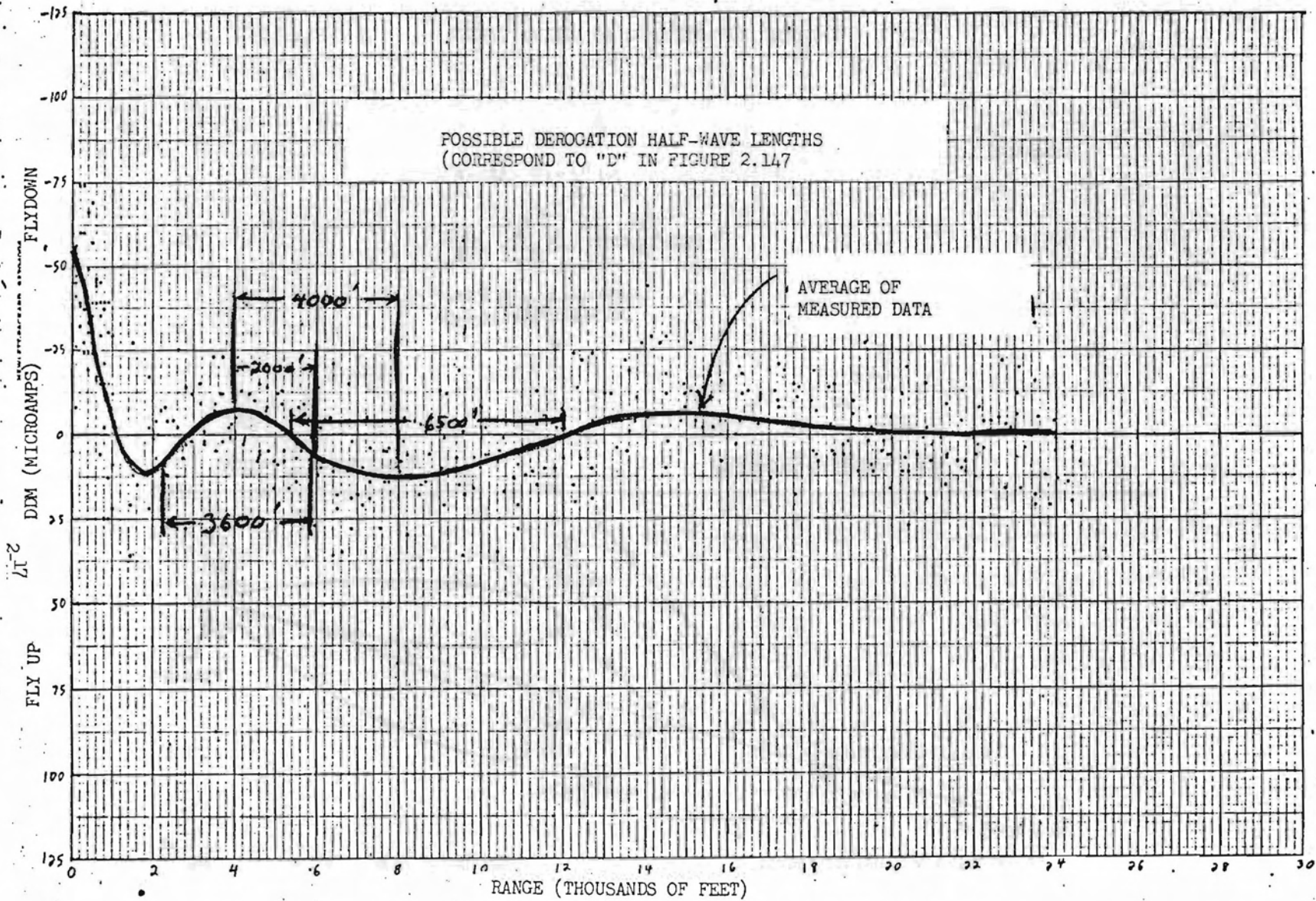
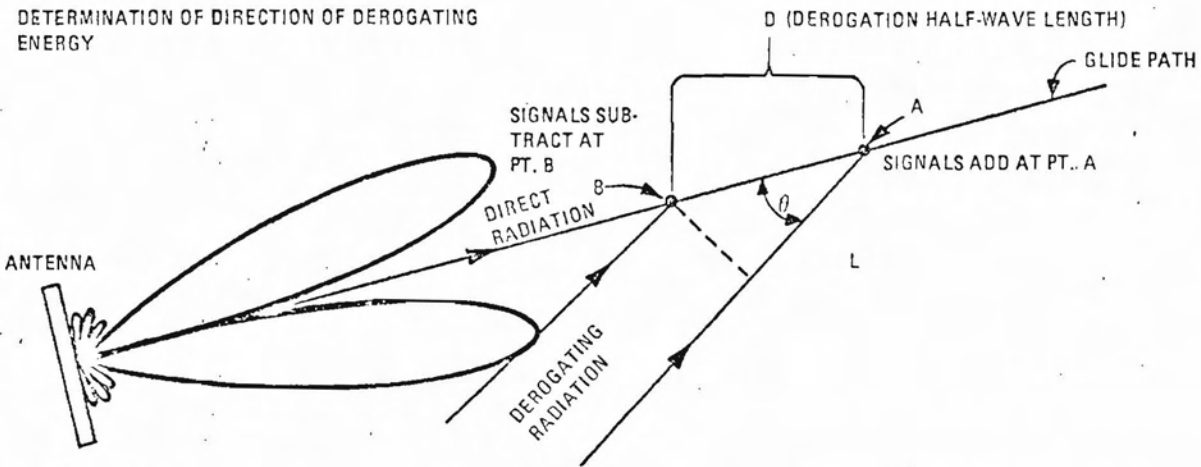


FIGURE 2.13 POSSIBLE DEROGATION HALF-WAVELENGTHS OCCURRING IN MEASURED DATA CURVE



DIRECT RADIATION PHASE

<u>PT. A</u>	<u>PT. B</u>
0	$0 - \frac{2\pi}{\lambda} D$

DEROGATING RADIATION PHASE

<u>PT. A</u>	<u>PT. B</u>
0	$0 - \frac{2\pi}{\lambda} L$

THE DIFFERENCE IN PHASE  
AT PT. B MUST BE  $\pi$  RADIANS

$$\frac{2\pi D}{\lambda} - \frac{2\pi L}{\lambda} = \pi \quad \text{ALSO } \frac{L}{D} = \cos \theta$$

$$\theta = \cos^{-1} \left( 1 - \frac{\lambda}{2D} \right)$$

S74-0934-VA-4

FIGURE 2.14 DETERMINATION OF DIRECTION OF DEROGATING ENERGY

The angle  $\theta$  can be determined and a cone in space is generated. The intersection of this cone with the ground will give the location of possible derogating sources. Figures 2.15, 2.16, 2.17 and 2.18 show areas of possible derogating sources superimposed on a map of Runway 23. All of these areas include the New York State Thruway. The modeling of the thruway is illustrated in Figure 2.19 and its effect on the fly-in is shown in Fig. 2.20 superimposed on the measured data. There is very good agreement, so it was felt that the verification of the complete computer model was established.

#### 2.4 Compensated Pattern Matching

The only model verification detail that remained was establishing the validity of compensated antenna patterns. Since the antenna at Buffalo had no compensating radiators, all measured compensated patterns were made at the Westinghouse antenna range. Figures 2.21 and 2.22 show comparisons of measured and calculated 6 dB and 9 dB compensated patterns. These calculated patterns were used in the prediction of antenna performance.

2.20

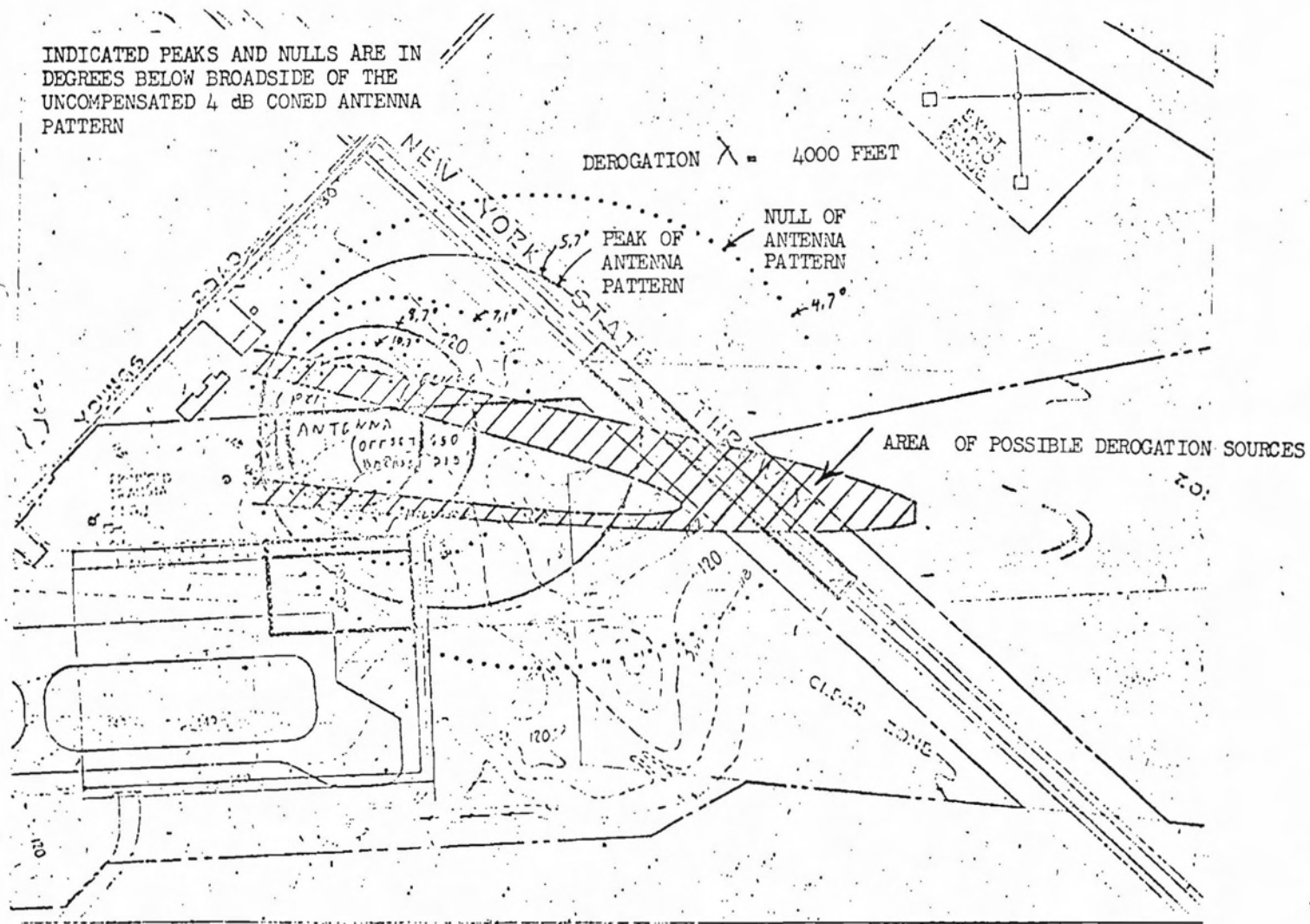


FIGURE 2.15

AREA OF POSSIBLE DEROGATION SOURCES DUE TO A DEROGATION WAVELENGTH OF 4000 FEET

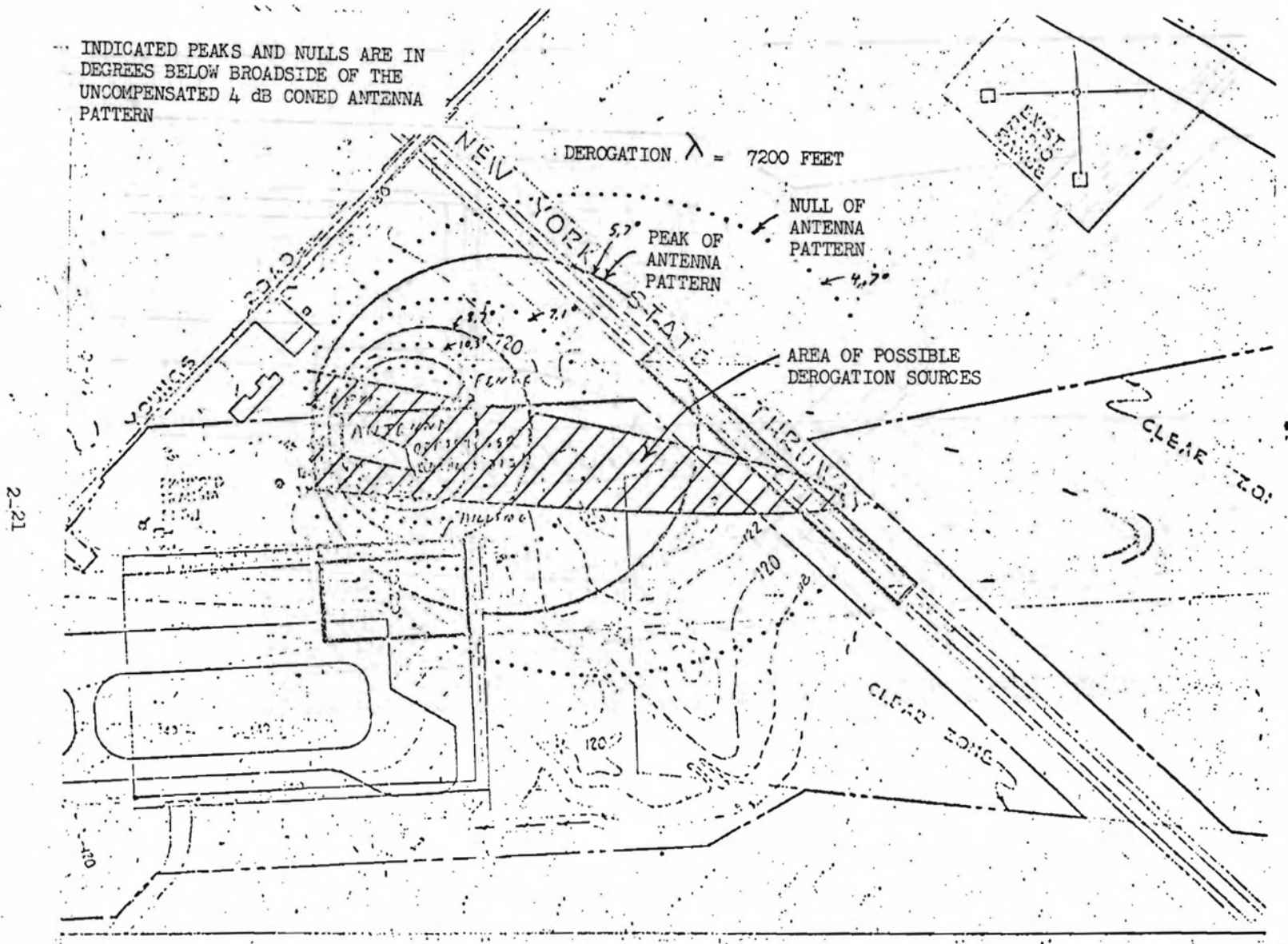


FIGURE 2.16. AREA OF POSSIBLE DEROGATION SOURCES DUE TO A DEROGATION WAVELENGTH OF 7200 FEET

INDICATED PEAKS AND NULLS ARE IN DEGREES BELOW BROADSIDE OF THE UNCOMPENSATED 4 dB CONED ANTENNA PATTERN

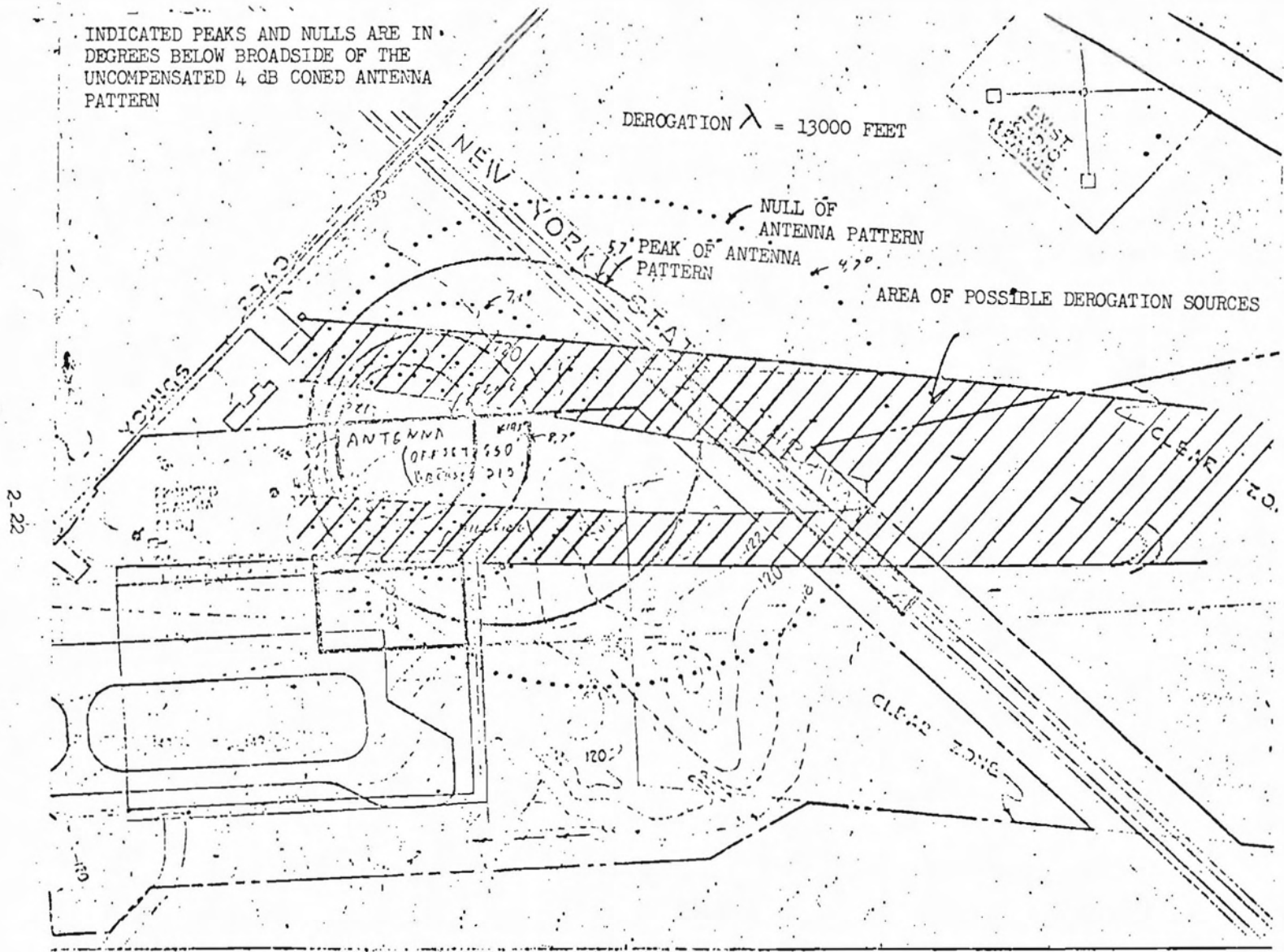
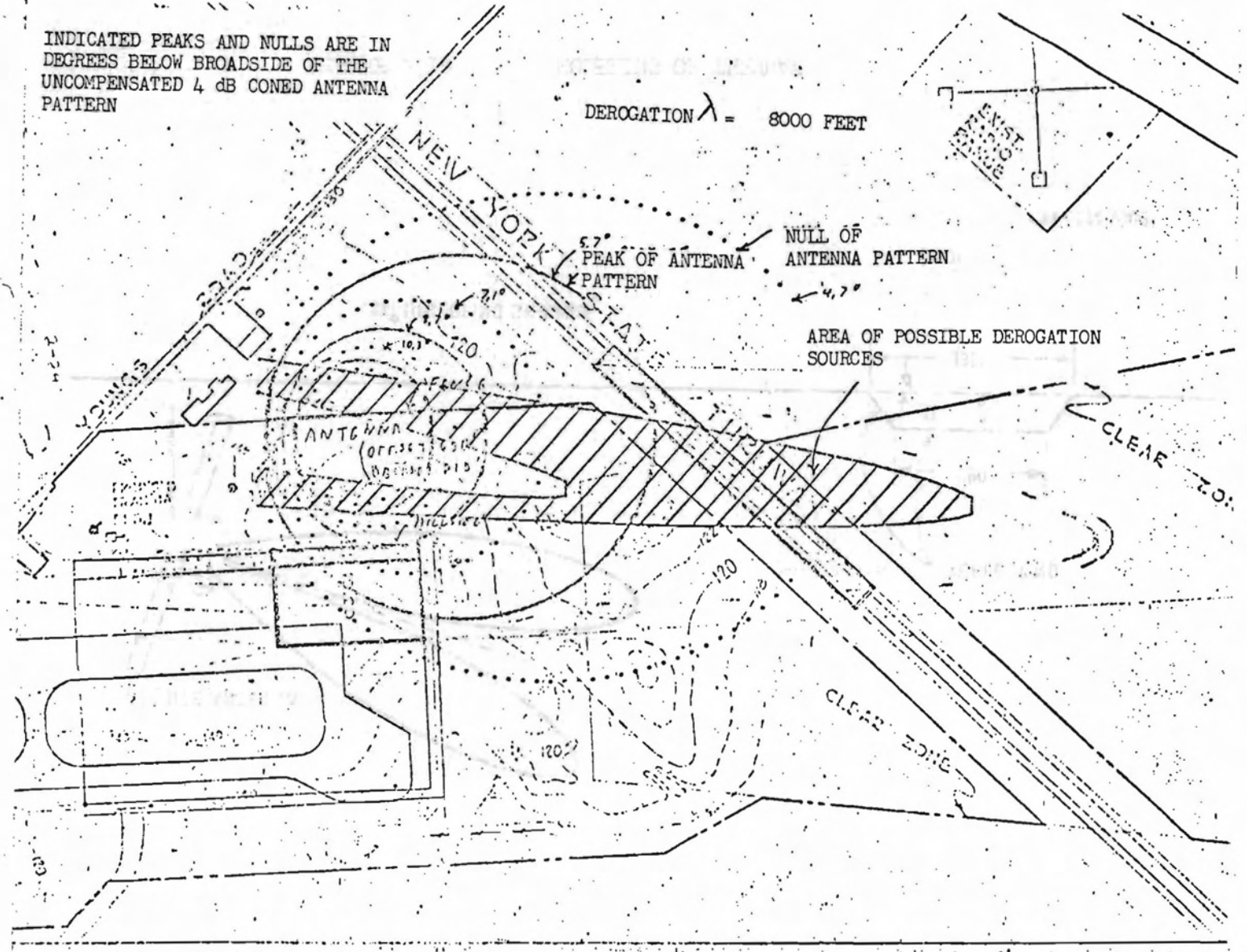
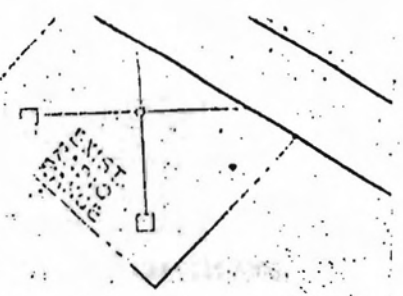


FIGURE 2.17

AREA OF POSSIBLE DEROGATION SOURCES DUE TO A DEROGATION WAVELENGTH OF 1300 FEET.

INDICATED PEAKS AND NULLS ARE IN DEGREES BELOW BROADSIDE OF THE UNCOMPENSATED 4 dB CONED ANTENNA PATTERN

DEROGATION  $\lambda = 8000$  FEET



2.23

FIGURE 2.18 AREA OF POSSIBLE DEROGATION SOURCES DUE TO A DEROGATION WAVELENGTH OF 8,000 FEET

2-24

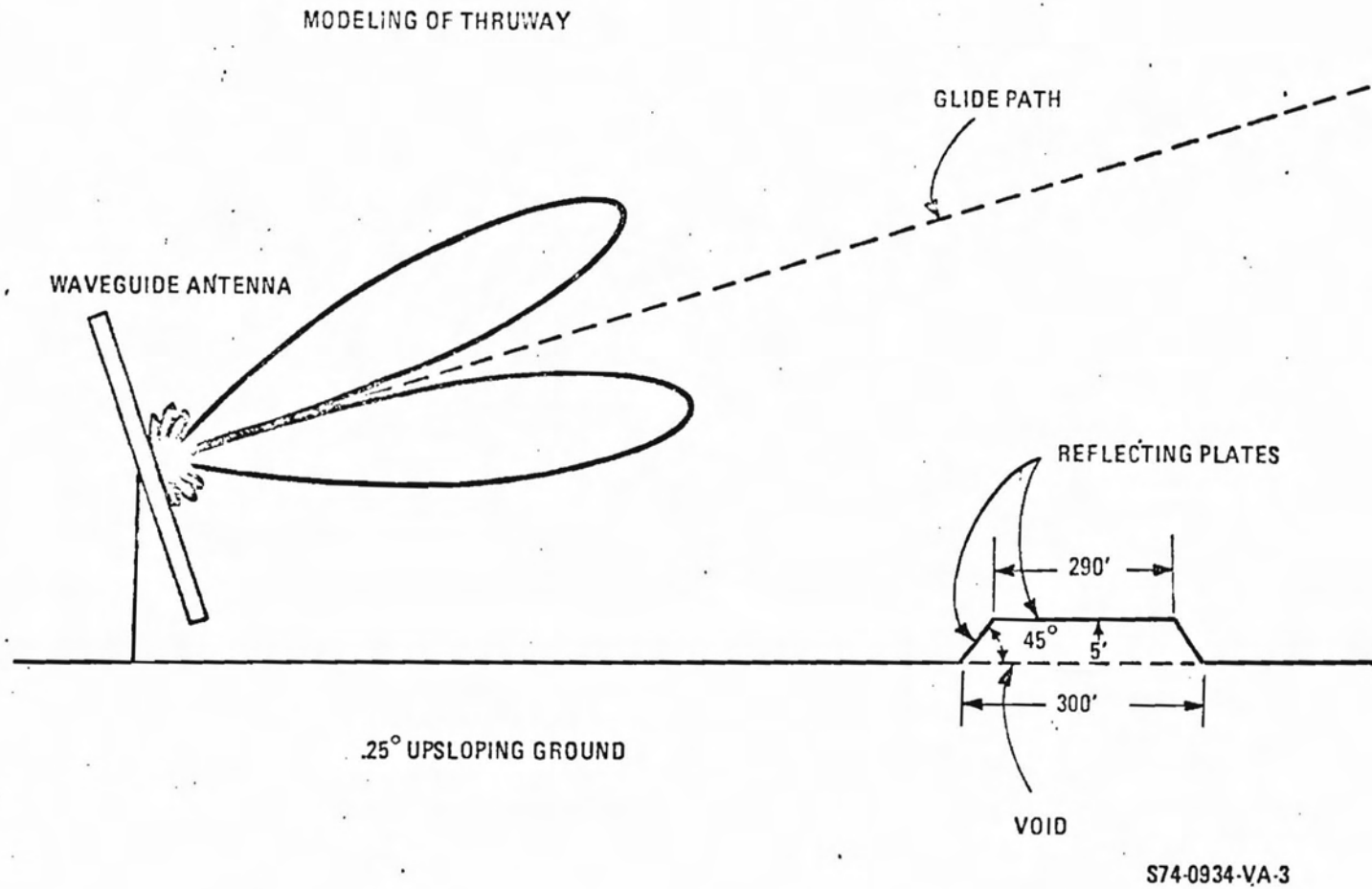


FIGURE 2.19

MODELING OF THRUWAY

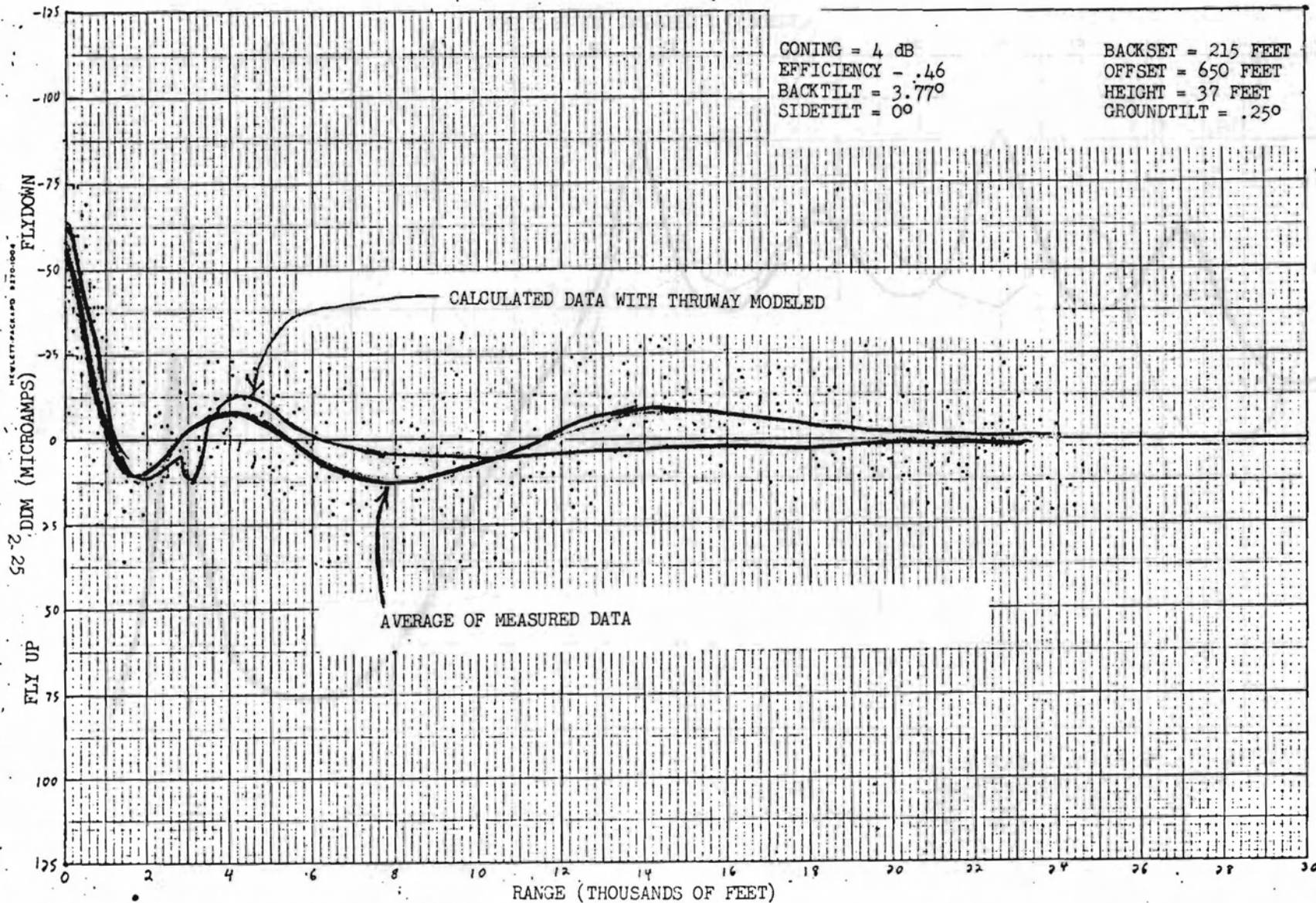


FIGURE 2.20 COMPARISON OF MEASURED DATA TO CALCULATED DATA WHEN THRUWAY MODELED

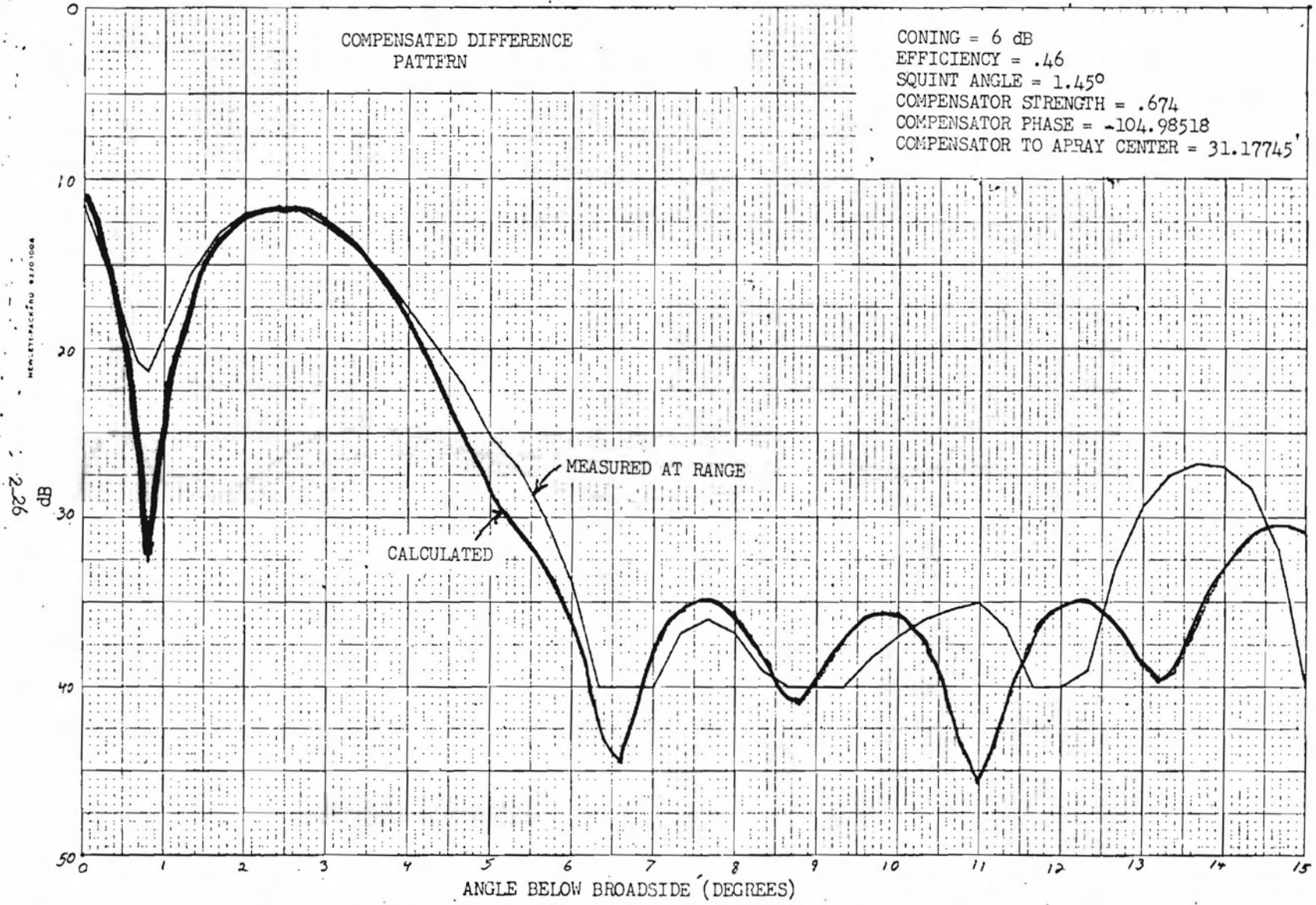


FIGURE 2.21 COMPARISON OF MEASURED AND CALCULATED 6 dB COMPENSATED ANTENNA PATTERNS

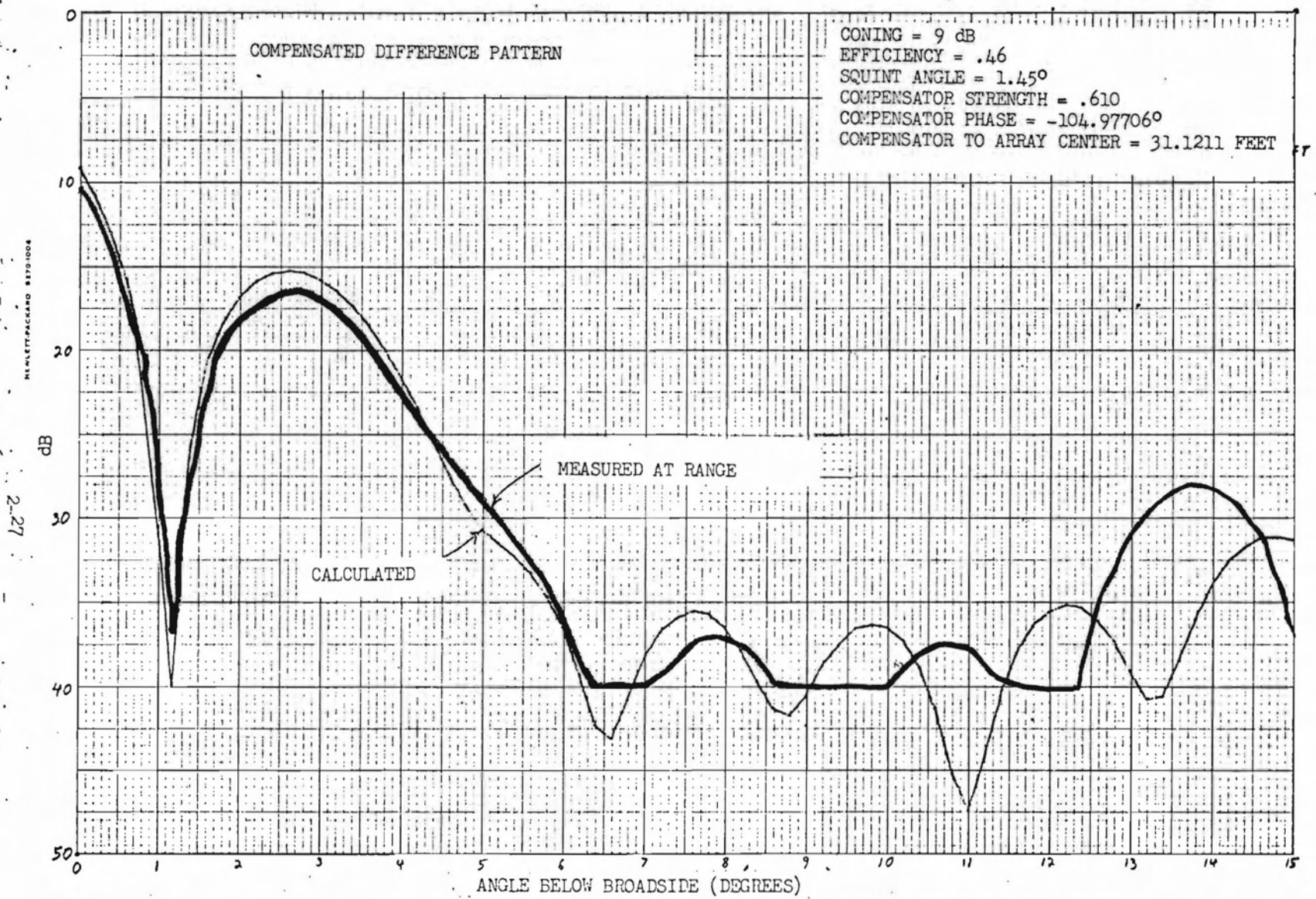


FIGURE 2.22 COMPARISON OF MEASURED AND CALCULATED 9dB COMPENSATED ANTENNA PATTERNS

## 3.1 Long Term Derogation

The antenna performance suffers because of unwanted reflections. Reflections due to sidelobe radiation can be reduced by compensation. However, since compensation barely affects the main lobe, reflections due to the main lobe are reduced by coning the antenna. A bad feature of coning is the inherent "flare" or fly-down signal near threshold. This can be somewhat alleviated by moving the antenna further back from threshold and side tilting the antenna. Taking all of this into consideration, the antenna should be as far from threshold as possible and coned as much as possible. As an indication of the improvement due to compensation, Fig. 3.1 compares the compensated and uncompensated fly-ins with the antenna at its original position of 215 feet backset, 650 feet offset and 37 feet height. There is considerable improvement but even further improvement can be realized by increased coning and a larger backset. In searching for the optimum condition, it was felt that an infinite tilted plane approximation would supply sufficient information for a site decision to be made. Once the antenna site was established, modeling of specific terrain features could be made to predict the expected flyability. This decision was made because of the large amount of computer time needed for complete modeling (about 250 seconds) wherea an infinite tilted plane approximation takes very little computer time (about 6 seconds). Figs. 3.2 to 3.12 illustrate fly-ins for various conditions. The position, height, sidetilt and coning were the variable parameters. Table 2 lists the condition of each of the fly-ins. The optimum antenna performance was obtained by locating the antenna 800 feet backset, 650 feet offset and a height of 43.1 feet (TCH of 55 feet). Figure 3.12 is a fly-in with all significant terrain features modeled. Category II limits are met by the long term trend.

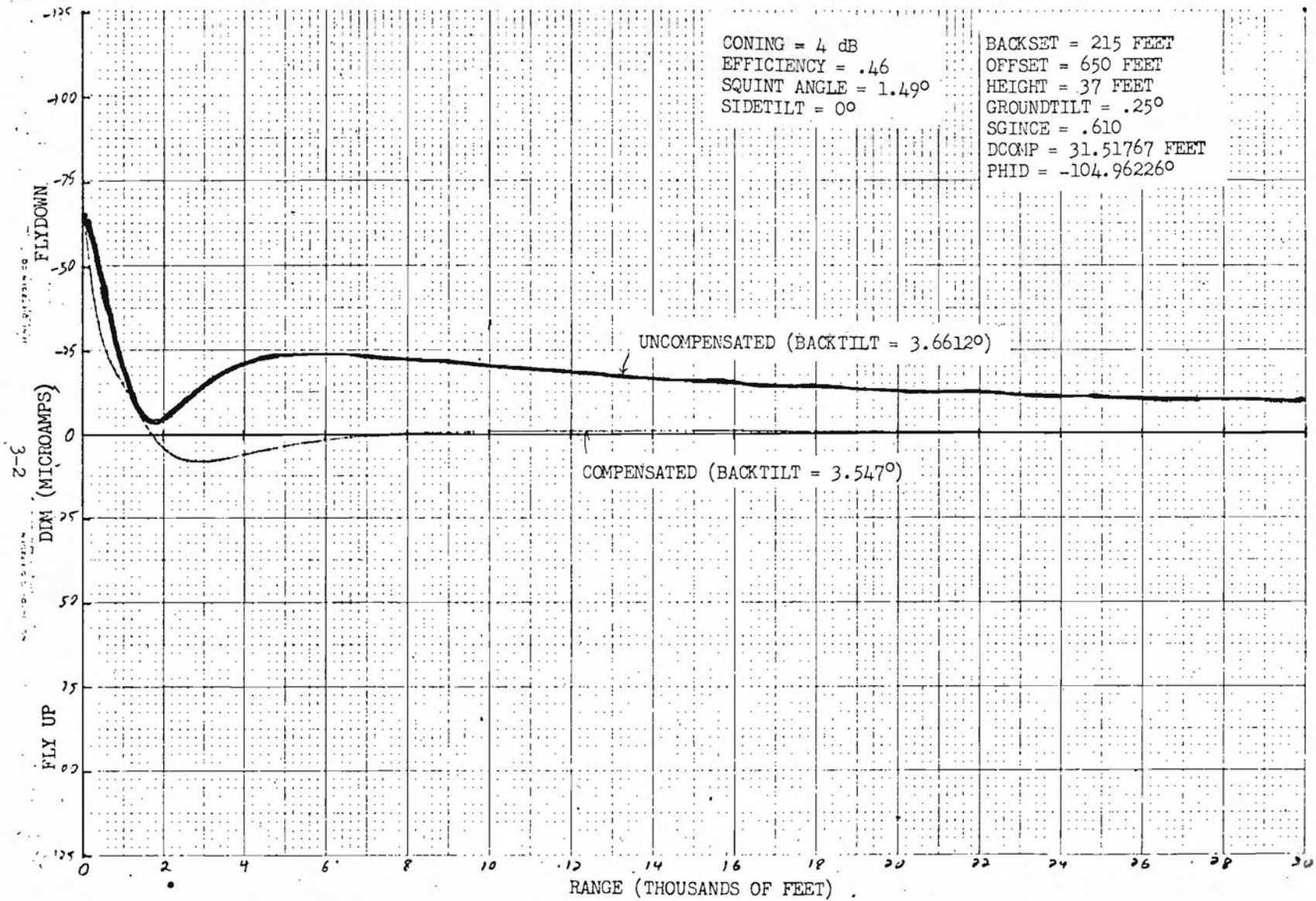


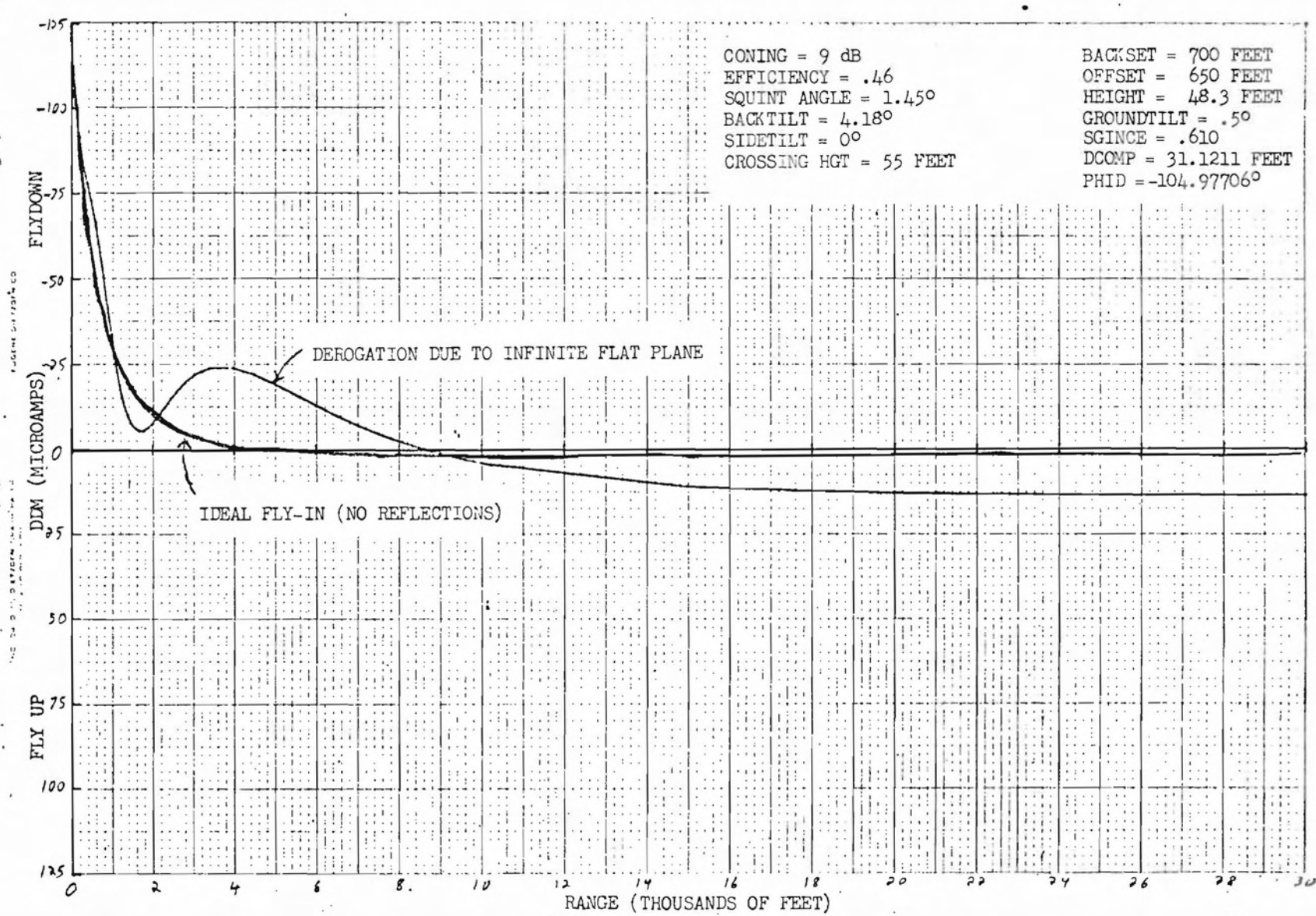
FIGURE 3.1 COMPARISON OF COMPENSATED AND UNCOMPENSATED FLY-INS AT ORIGINAL ANTENNA SITE AND WITH ORIGINAL ANTENNA CHARACTERISTICS

TABLE 2

FIGURE	POSITION							REMARKS
	BACKSET	OFFSET	HEIGHT	BACKTILT	SIDETILT	CONING	TCH	
3.2	700	650	48.3	4.18°	0	9 dB	55	Large flare can be reduced by larger backset, less coning, a lower TCH, and a small sidetilt
3.3	800	"	38.1	3.808°	.1°	6 dB	50	Looks good but fast term derogation may not be reduced sufficiently at the 6 dB of coning. One also needs to know the effect of terrain modeling. fence parallel to runway modeled
3.4	"	"	"	"	"	"	"	
3.5	"	"	"	"	"	"	"	Thruway modeled. Cat.II limits may be exceeded. It will probably be necessary to go to 9 dB coning.
3.6	"	"	"	"	"	9 dB	"	Large flare and large fly-up signal need to be reduced
3.7	"	"	38.1 41.1 43.1	4.16 4.13 4.14	"	"	50 53 55	Increasing the TCH reduces fly-up hump increasing sidetilt at a higher TCH should reduce the flare without increasing the fly-up hump too much
3.8	"	"	38.1 40.1 43.1	4.16 4.13 4.11	1.25 .25 .5	"	50 52 55	The .5° sidetilt and 55 ft TCH seem to be the best combination but modeling effects must be determined before a final decision is made
3.9	"	"	38.1	4.16	.1°	"	50	Thruway and Runway Embankment modeled.
3.10	"	"	40.1	4.13	.25°	"	52	"
3.11	"	"	43.1	4.11	.5	"	55	"
3.12	"	"	"	"	"	"	"	Comparison of uncompensated and compensated fly-ins for optimum antenna site

3-3

7-4



FLARE DUE TO CONING

FIGURE 3.2

1.

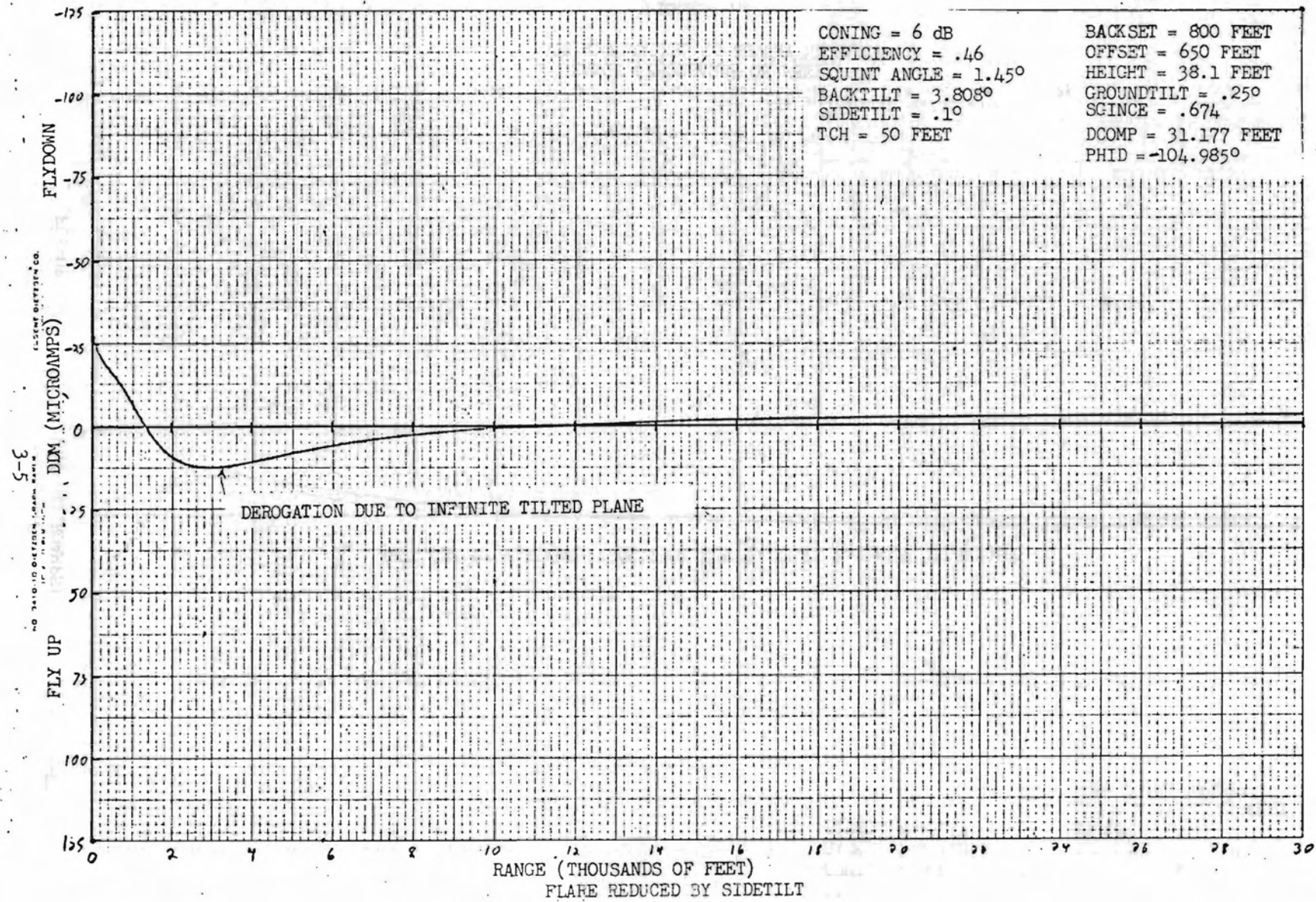


FIGURE 3.3

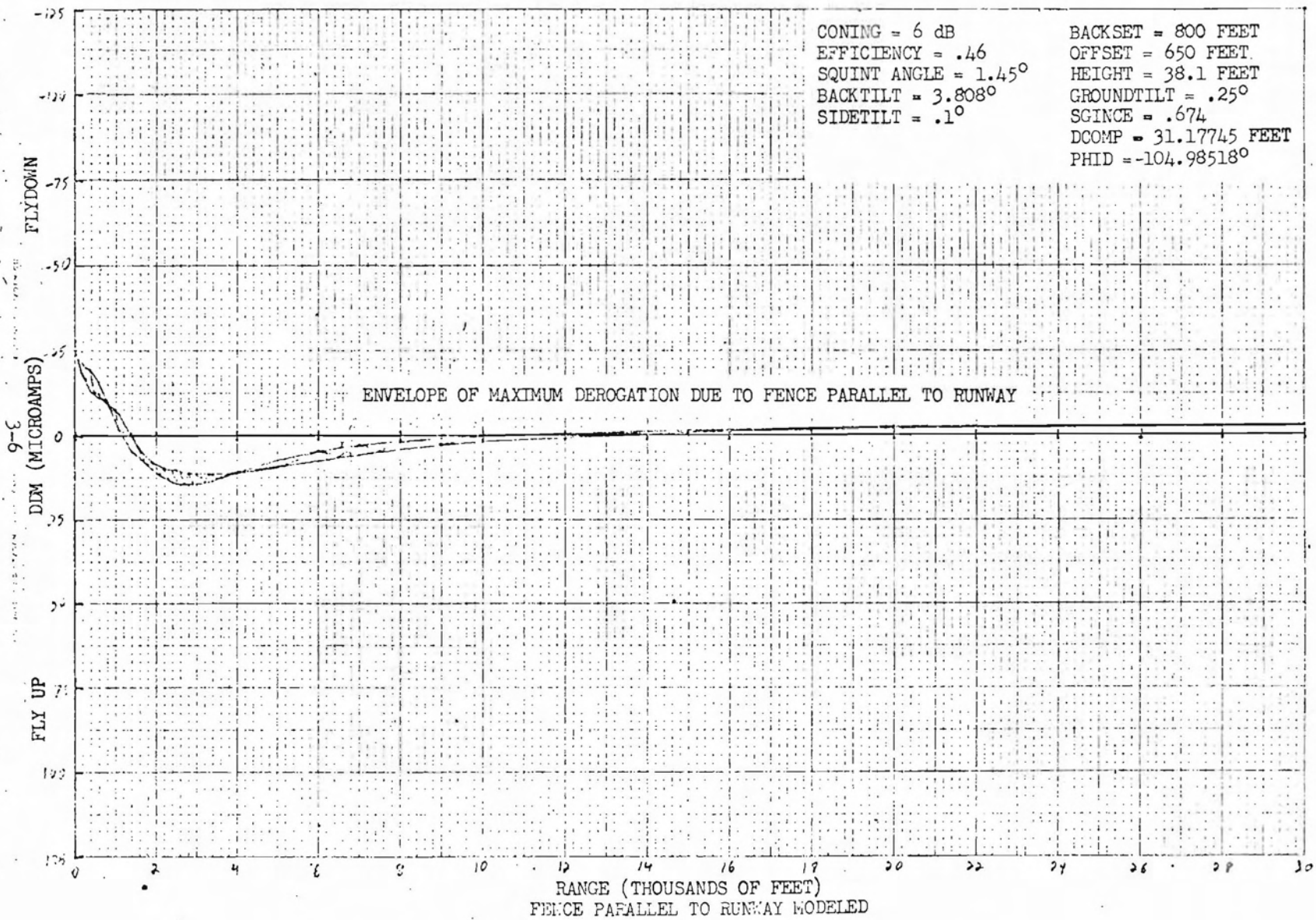


FIGURE 3.4

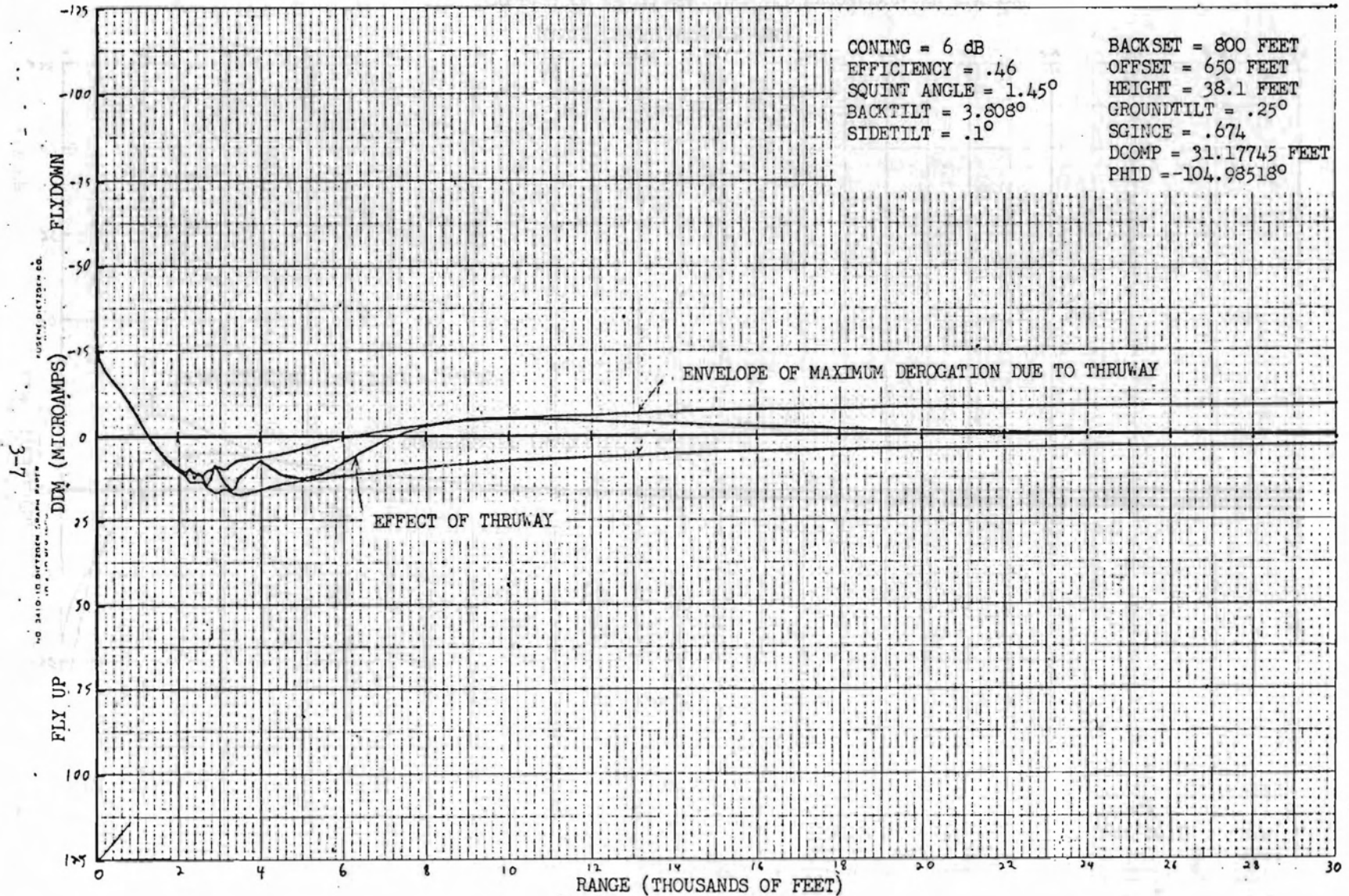
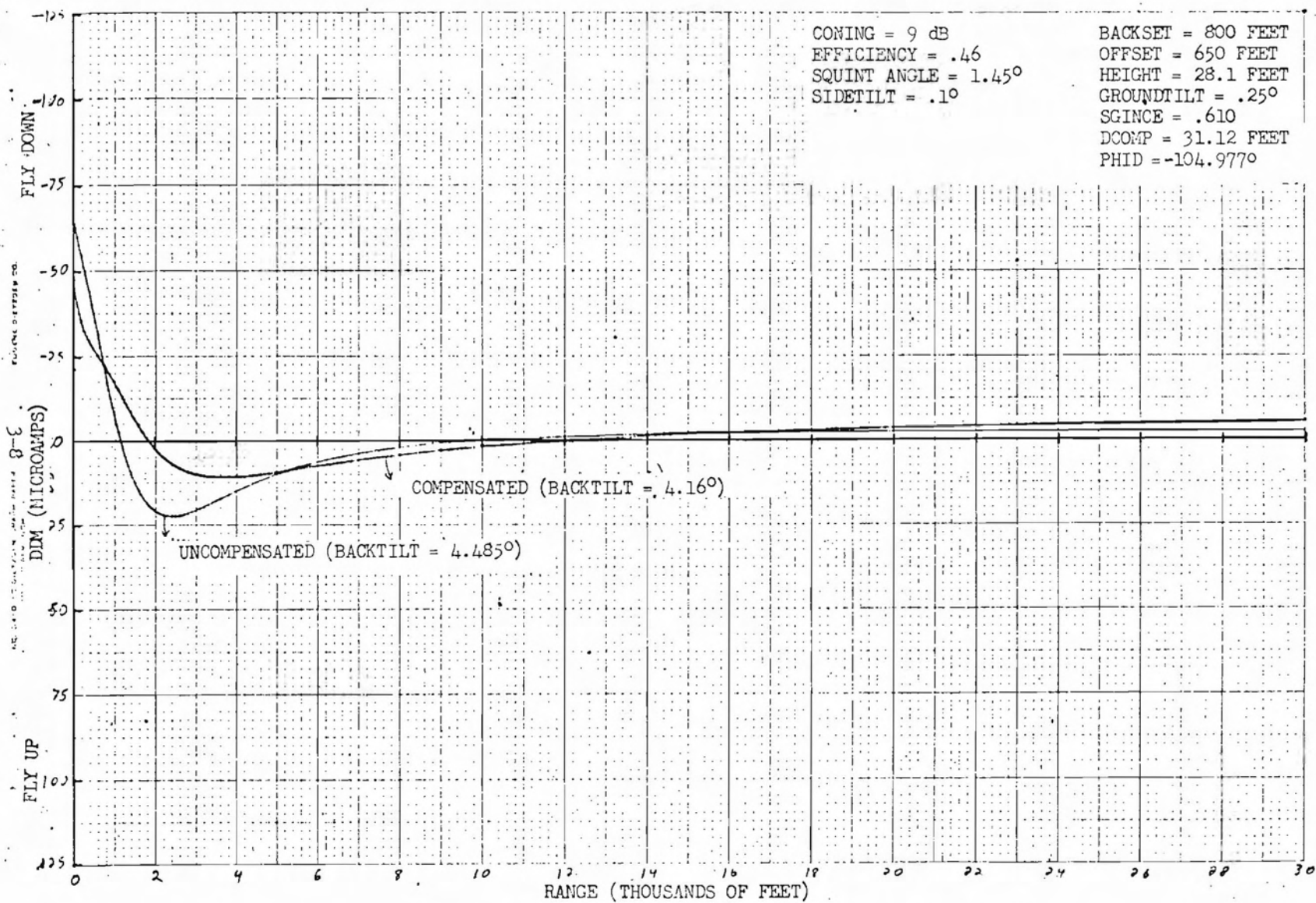


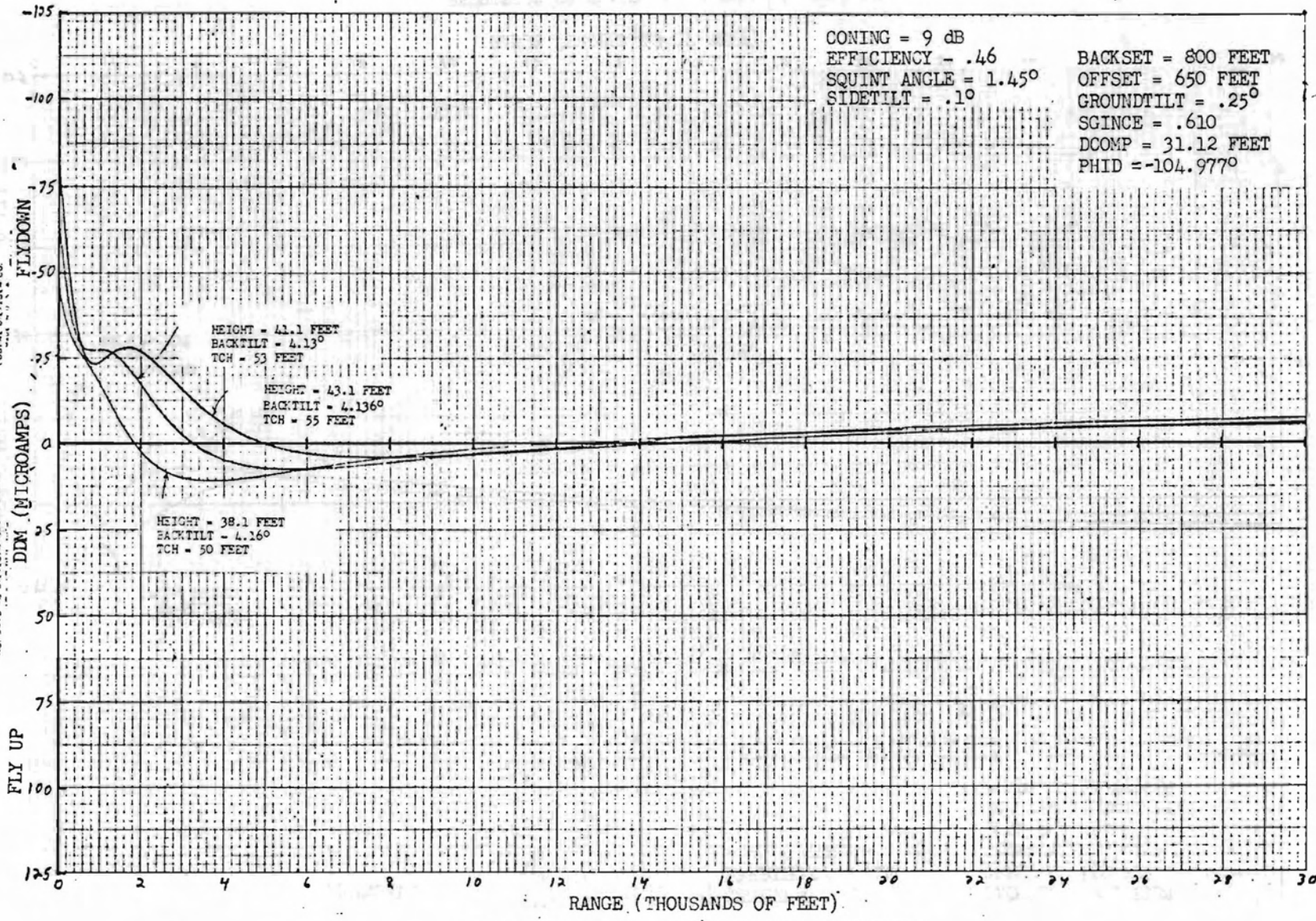
FIGURE 3.5



COMPARISON OF COMPENSATED AND UNCOMPENSATED FLY-INS

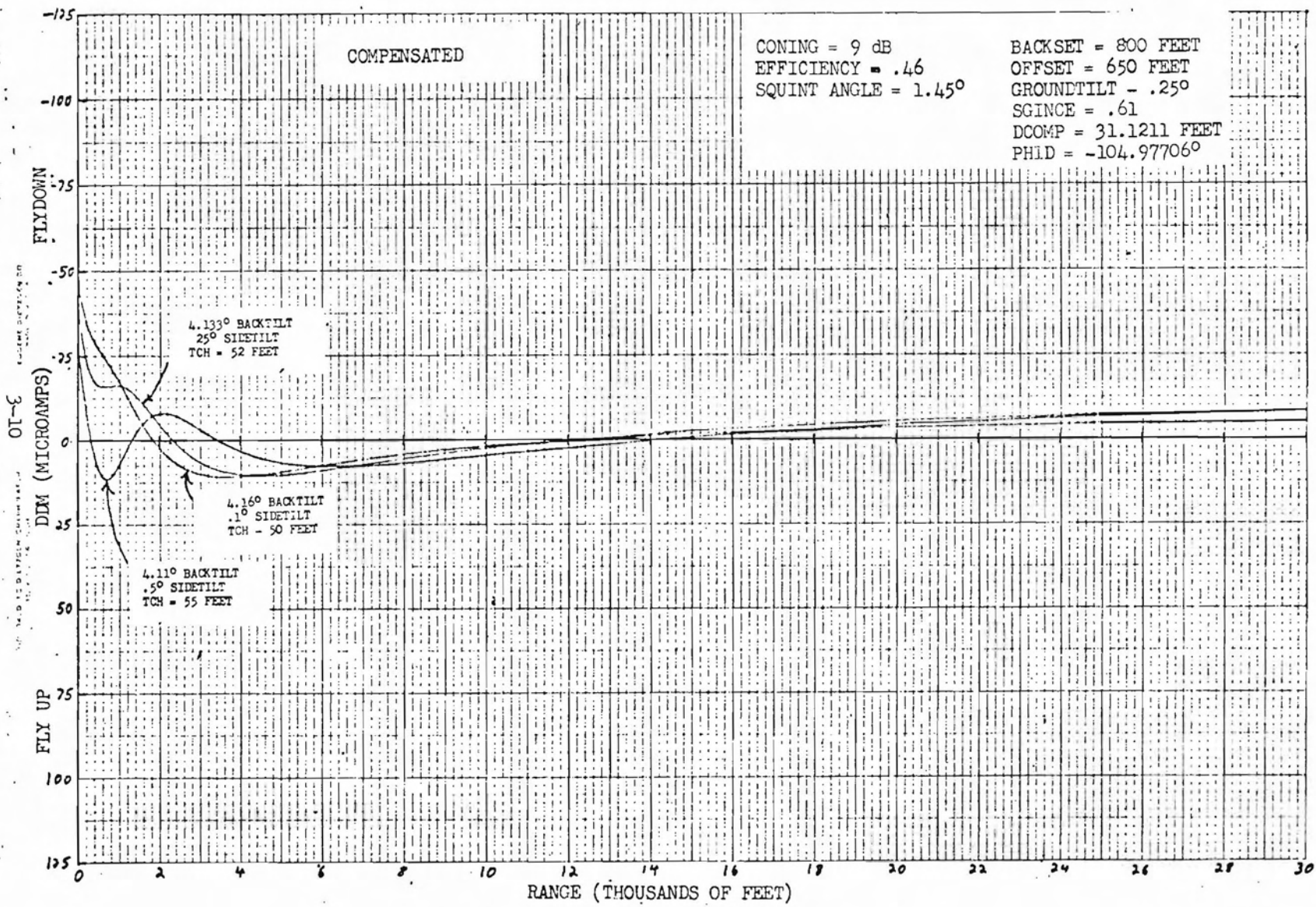
FIGURE 3.6

NO. 3410 10 DIVISION (100-100) SCALE  
 3-9  
 LOG-PLOT SYSTEM CO.



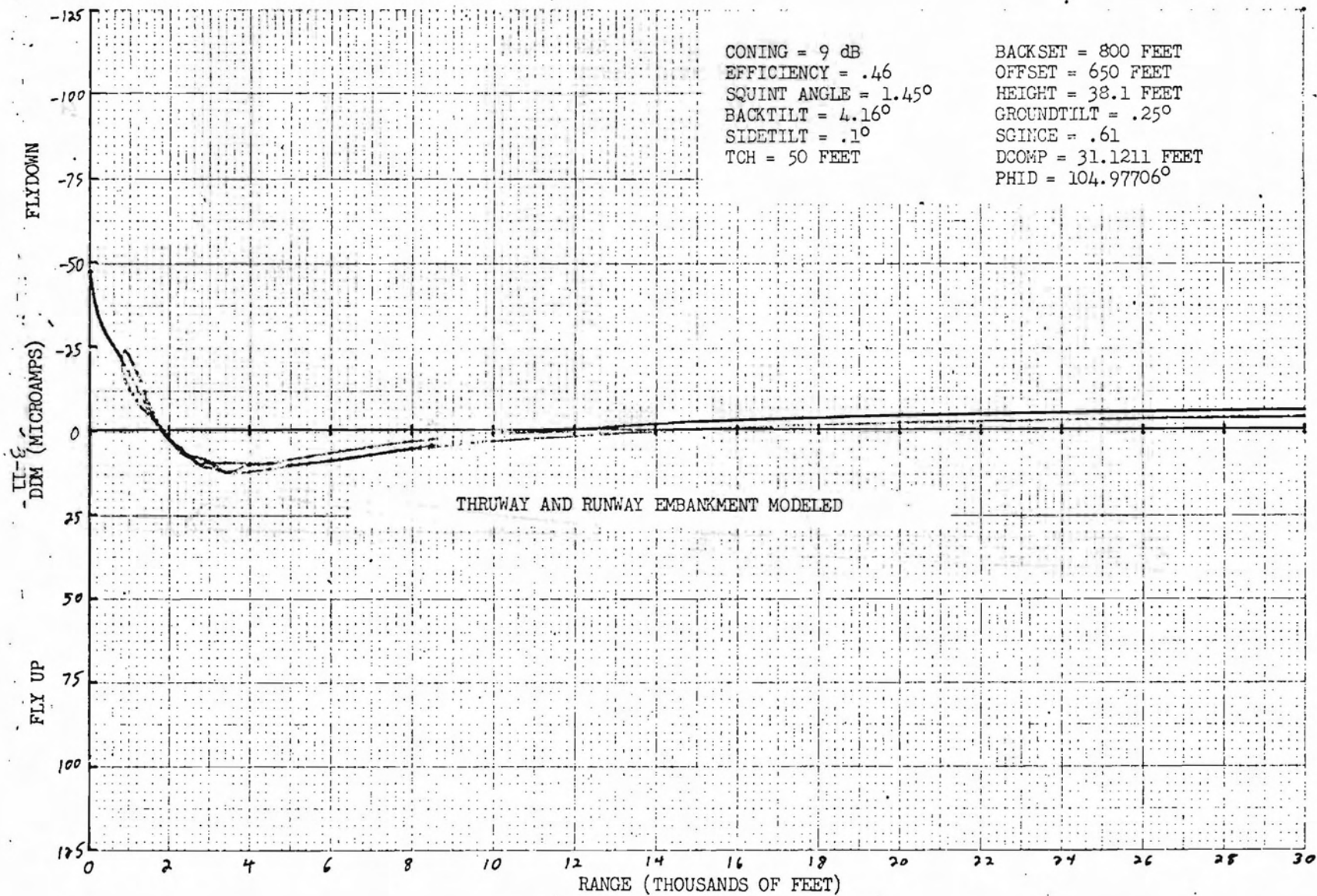
REDUCTION OF FLY-UP HUMP BY RAISING ANTENNA

FIGURE 3.7



REDUCTION OF FLARE BY INCREASING SIDETILT

FIGURE 3.8



THRUWAY AND RUNWAY EMBANKMENT MODELED

FIGURE 3.9

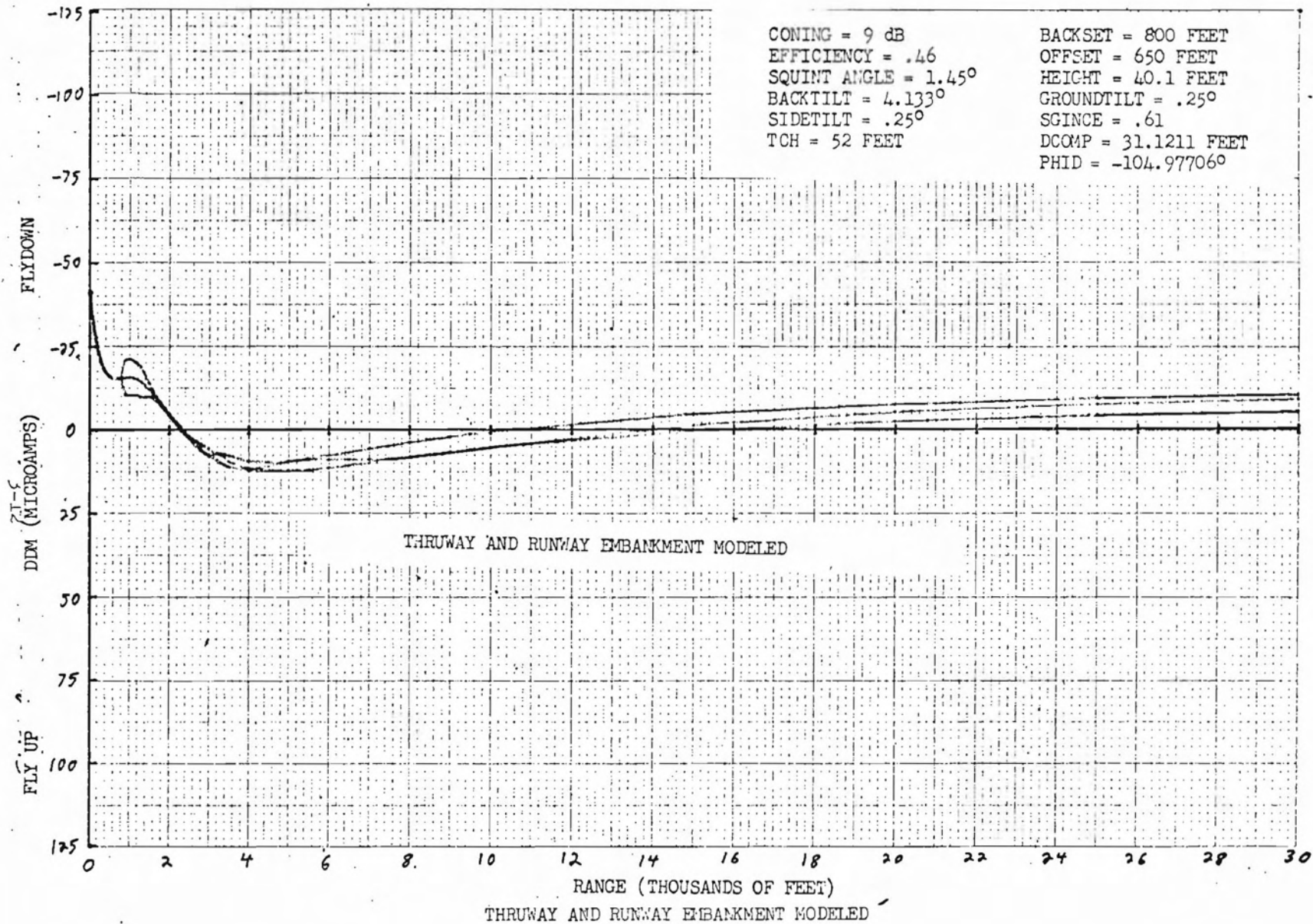
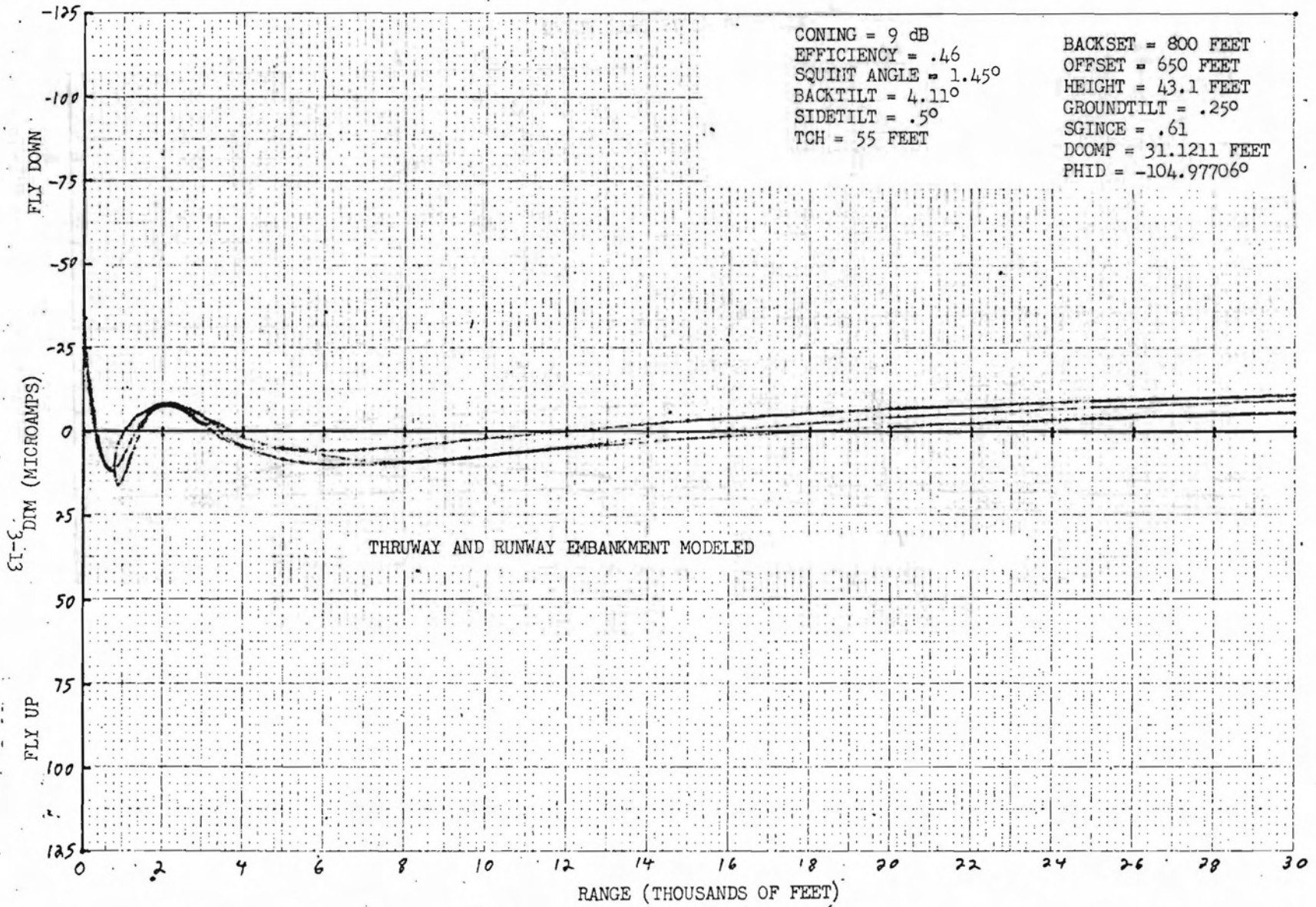
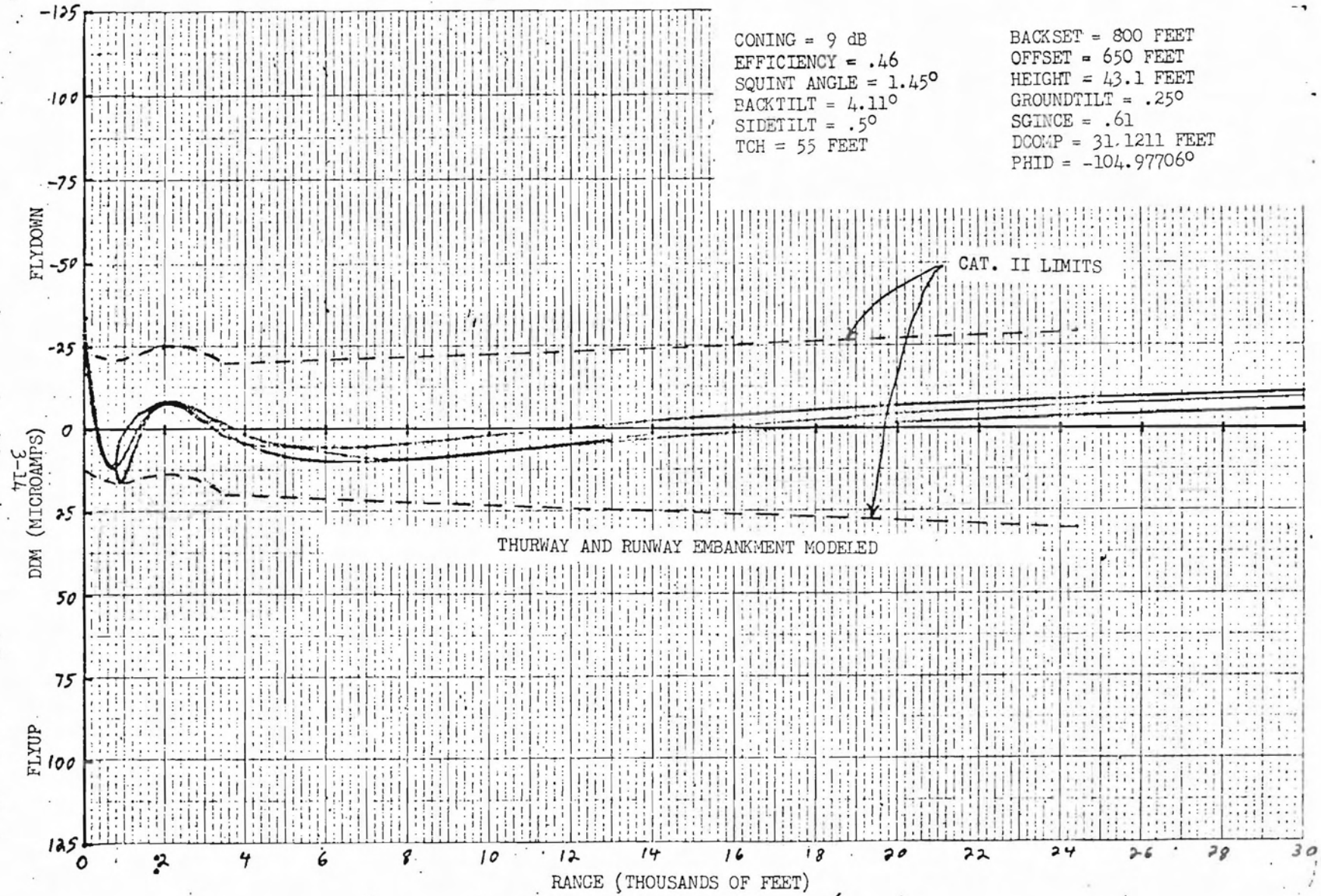


FIGURE 3.10



THRUWAY AND RUNWAY EMBANKMENT MODELED

FIGURE 3.11



THURWAY AND RUNWAY EMBANKMENT MODELED

FIGURE 3.12

### 3.2 Short Term Derogation

The bulk of fast term derogation is caused by spurious reflection of horizon radiation. Horizon radiation is main lobe radiation and is only reduced by increasing coning. An average of the maximum fast term derogation for the measured data was found to be 17 microamps. This was for 4 dB of coning. The expected reduction of the fast term derogation by coning can be obtained from a comparison of the uncompensated 4 dB antenna pattern and the compensated 9 dB antenna pattern. Figure 3.13 shows both antenna patterns and the location of the horizon illumination. The antenna patterns indicate an 8 dB reduction in horizon illumination. This will reduce the maximum average fast term derogation to 6.7 micro amps. This fast term derogation should not be large enough to put the antenna out of Category II limits.

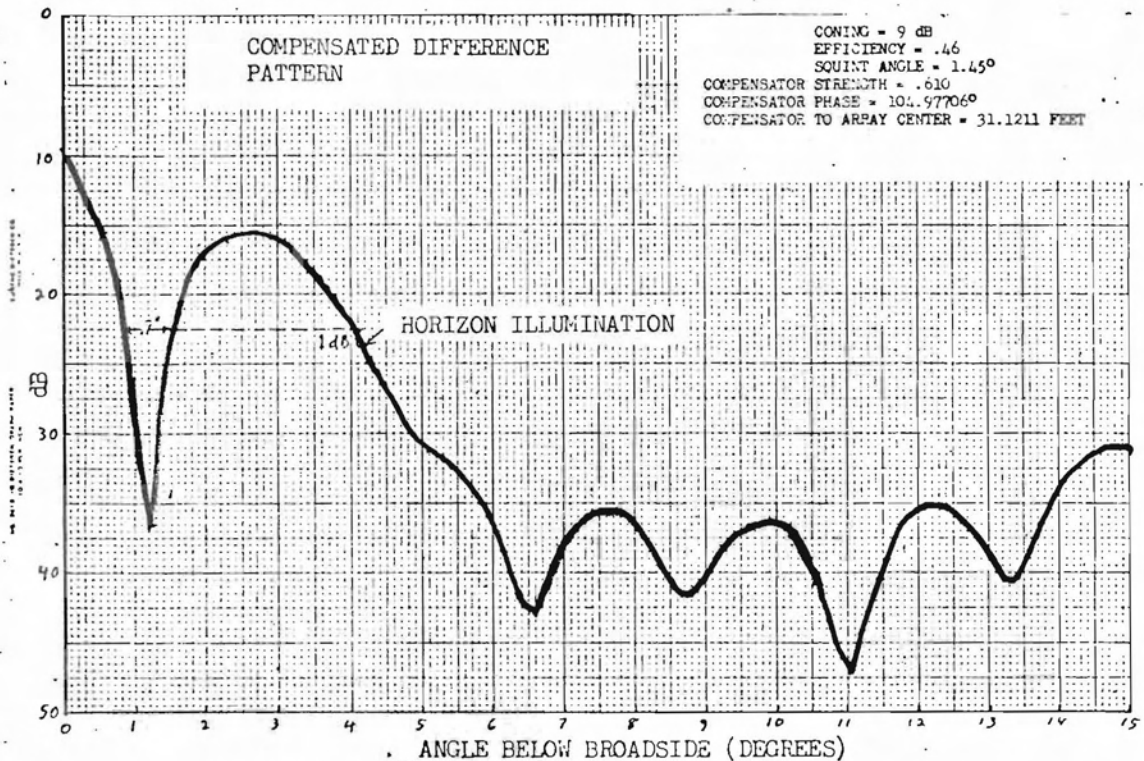
A trip was made to Buffalo on July 24, 1974 to investigate the antenna site in more detail. A small 6 or 7 foot high knoll that was not indicated on the available terrain maps was situated in front of the optimum antenna position. Other possible sites at less offset and nearly the same backset were felt to be reasonable alternatives since they had relatively uniform ground in front of them. The terrain was surveyed and this information was used to determine a final antenna site. Figure 3.14 shows the investigated positions and Figures 3.15 to 3.20 are the infinite tilted plane fly-ins for each of the positions. Figure 3.20 is the infinite tilted plane fly-in for the optimum site. Figure 3.21 is a fly-in for the optimum antenna site with all terrain modeled. Its position is shown in detail on the map in Figure 3.14. At this position, the antenna should meet Category II requirements.

### 3.3 Powerlines

The only remaining possible problem sources are the powerlines in the vicinity of Runway 23. These are located near the middle marker and at the corner of Main Street and Transit Road. Figure 3.22 shows the relation of the powerlines to the approach path of the aircraft.

The calculation of the reflected radiation from a powerline is described in appendix A.2.0. The equation for reflected radiation derived in appendix A.20 is:

$$\vec{E}_R = \sum_{m=-\infty}^{\infty} \left[ \frac{-E_0 j^m J_m(kR_0) H_m^{(1)}(kr) e^{j m \theta}}{H_m^{(1)}(kR_0)} \right] \hat{a}_z$$



AN 8 dB REDUCTION IN HORIZON ILLUMINATION IS ACHIEVED BY COMPENSATION AND INCREASED CONING

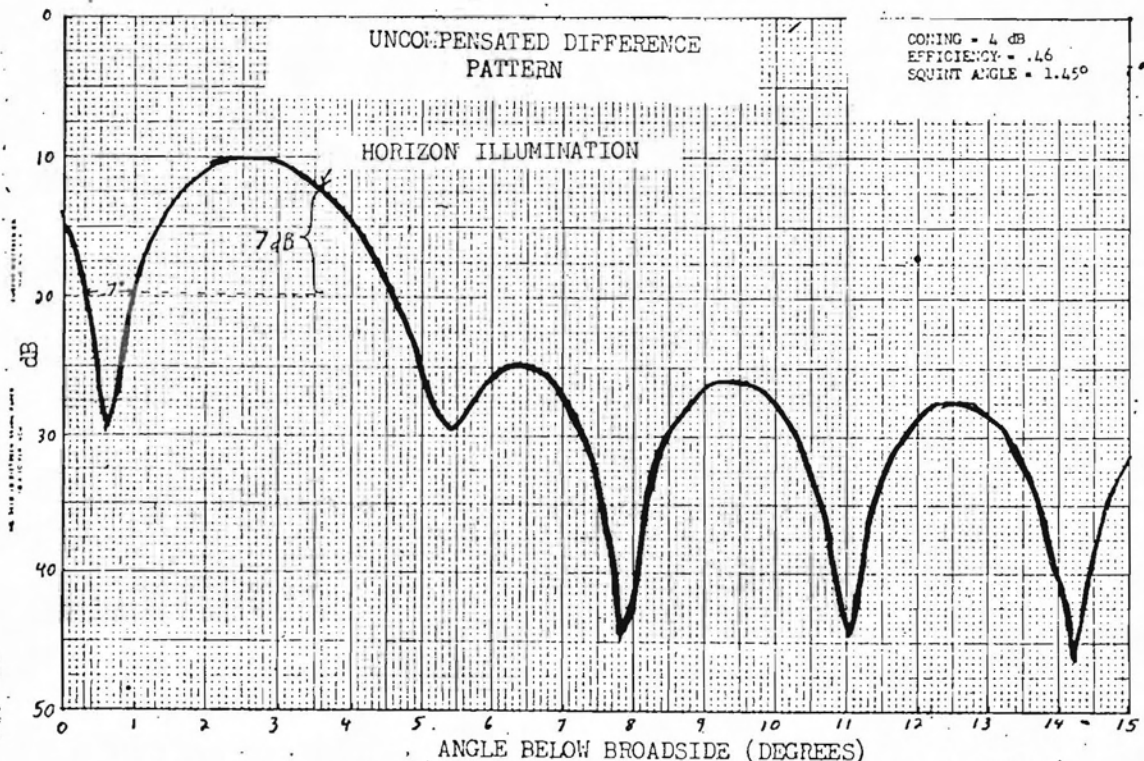


FIGURE 3.13. REDUCTION OF FAST TERM DEROGATION BY INCREASED CONING (4 dB to 9 dB)

3-17

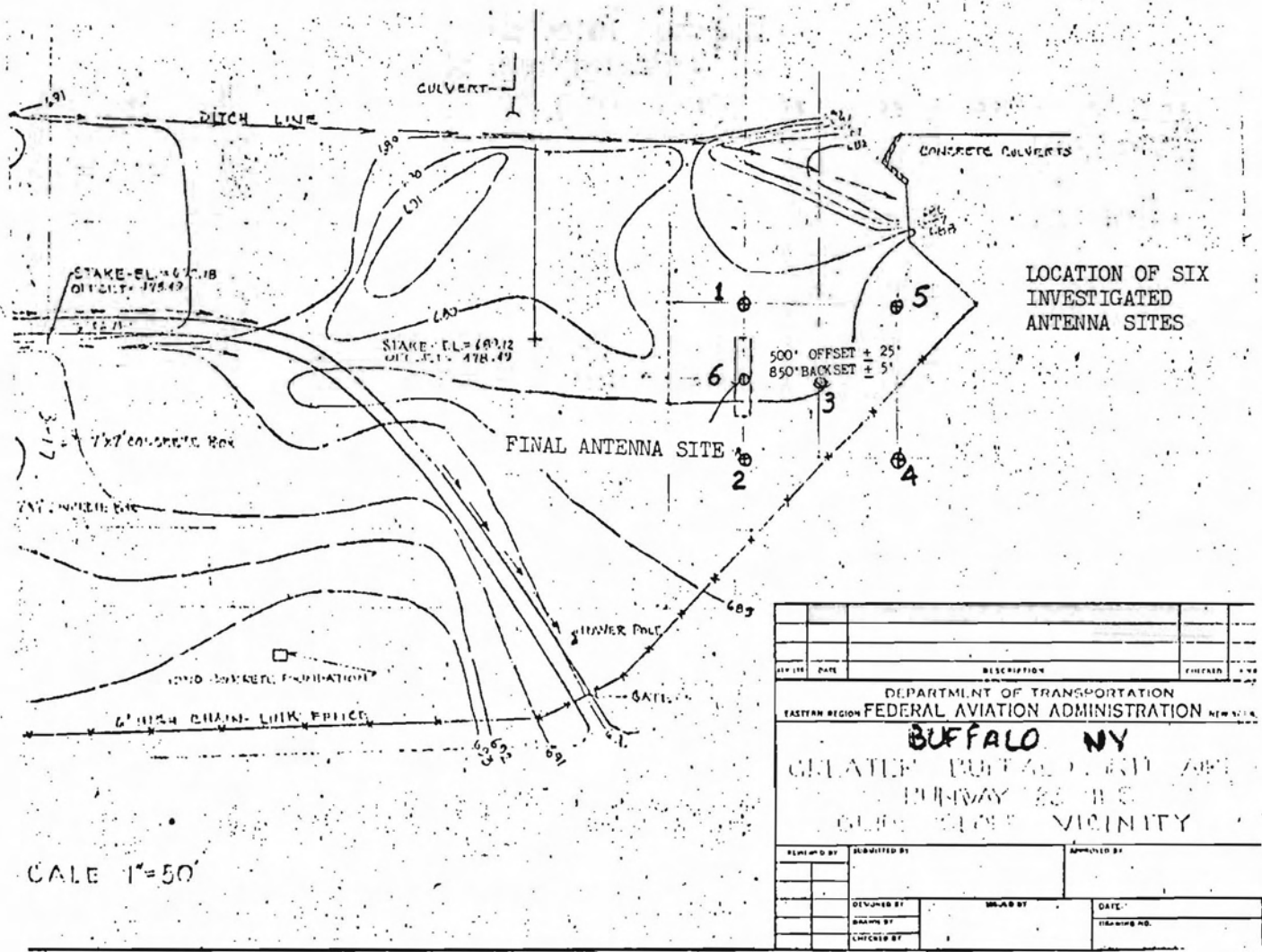


FIGURE 3-14 LOCATION OF SIX POSSIBLE ANTENNA SITES

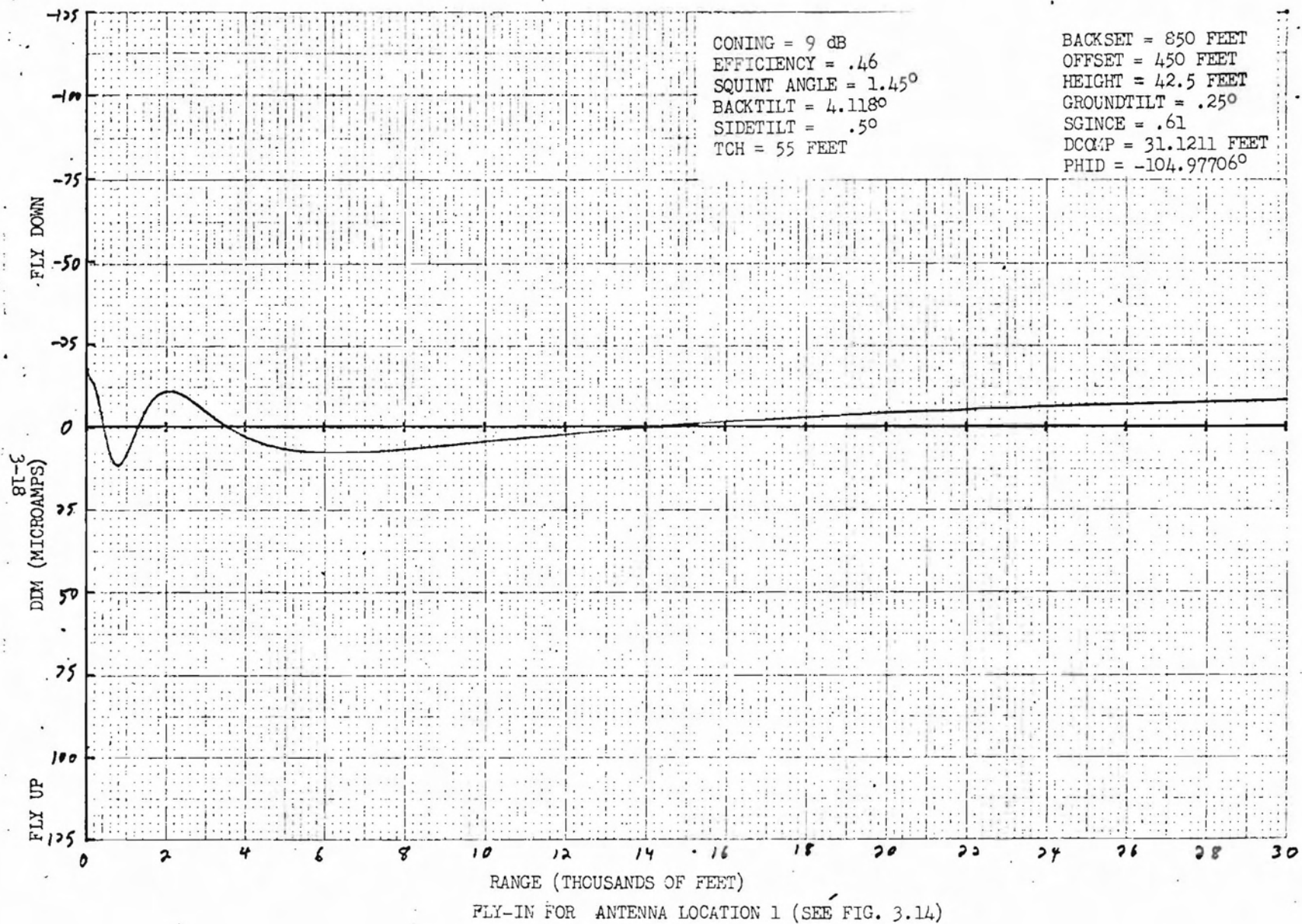
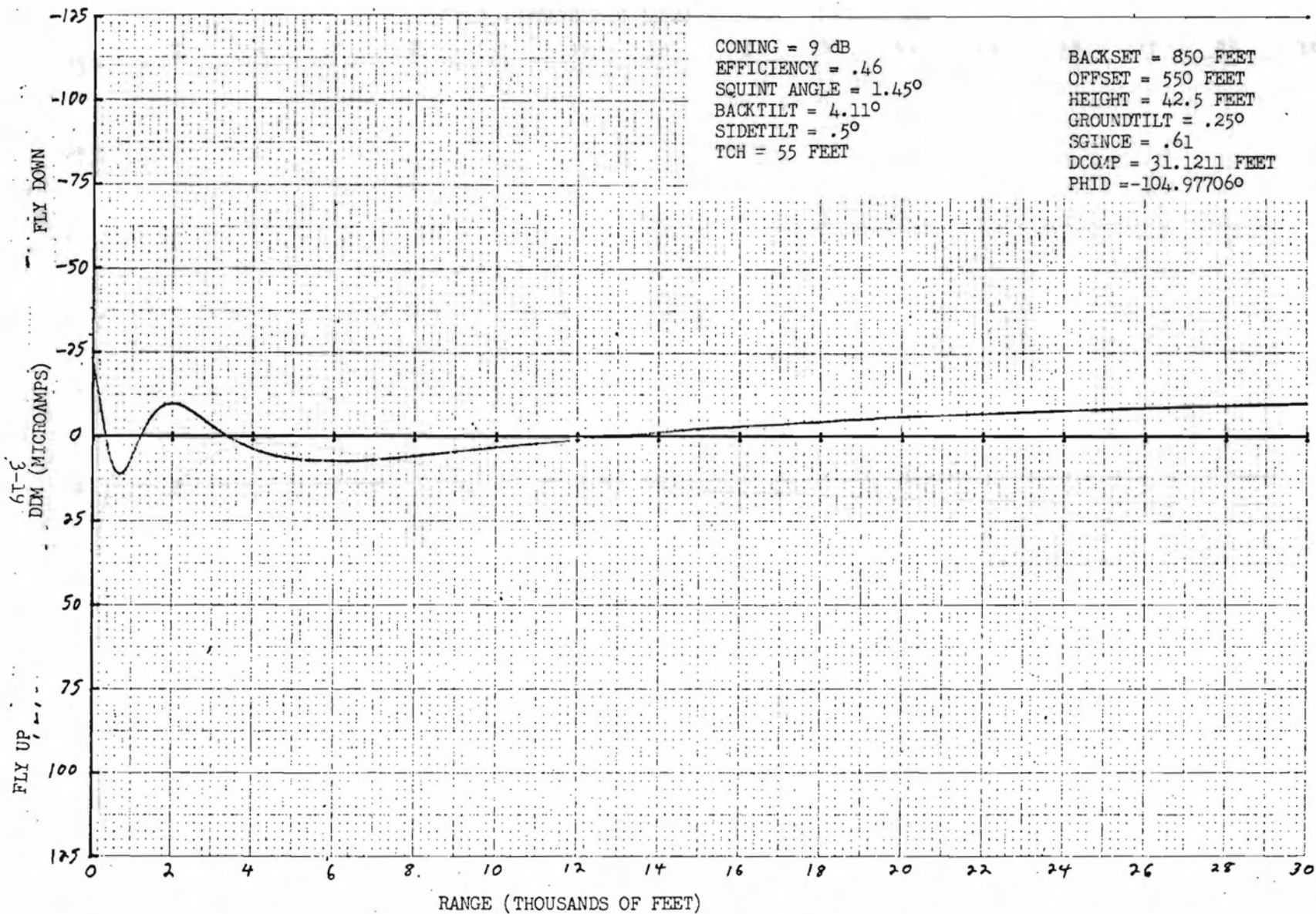
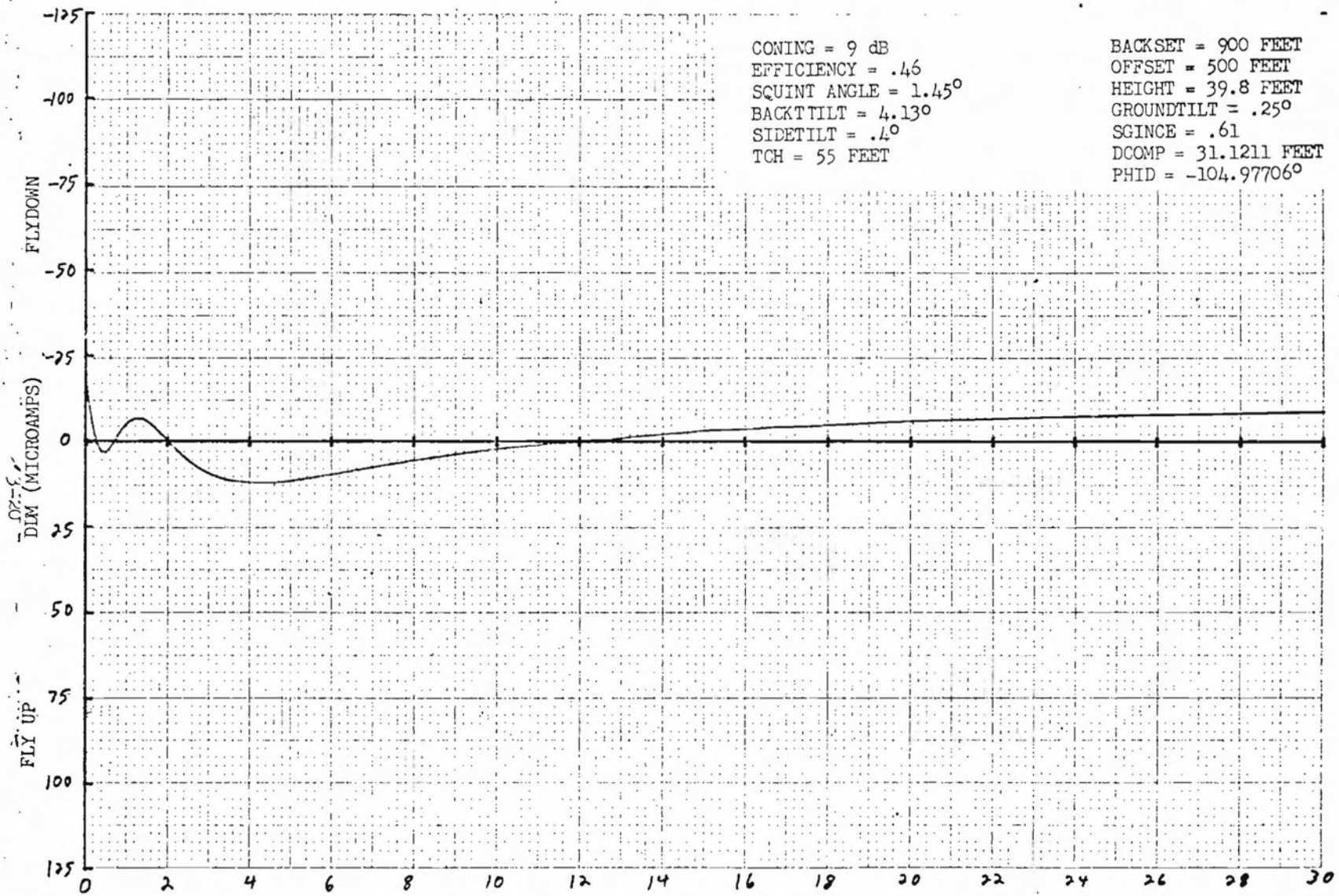


FIGURE 3.15



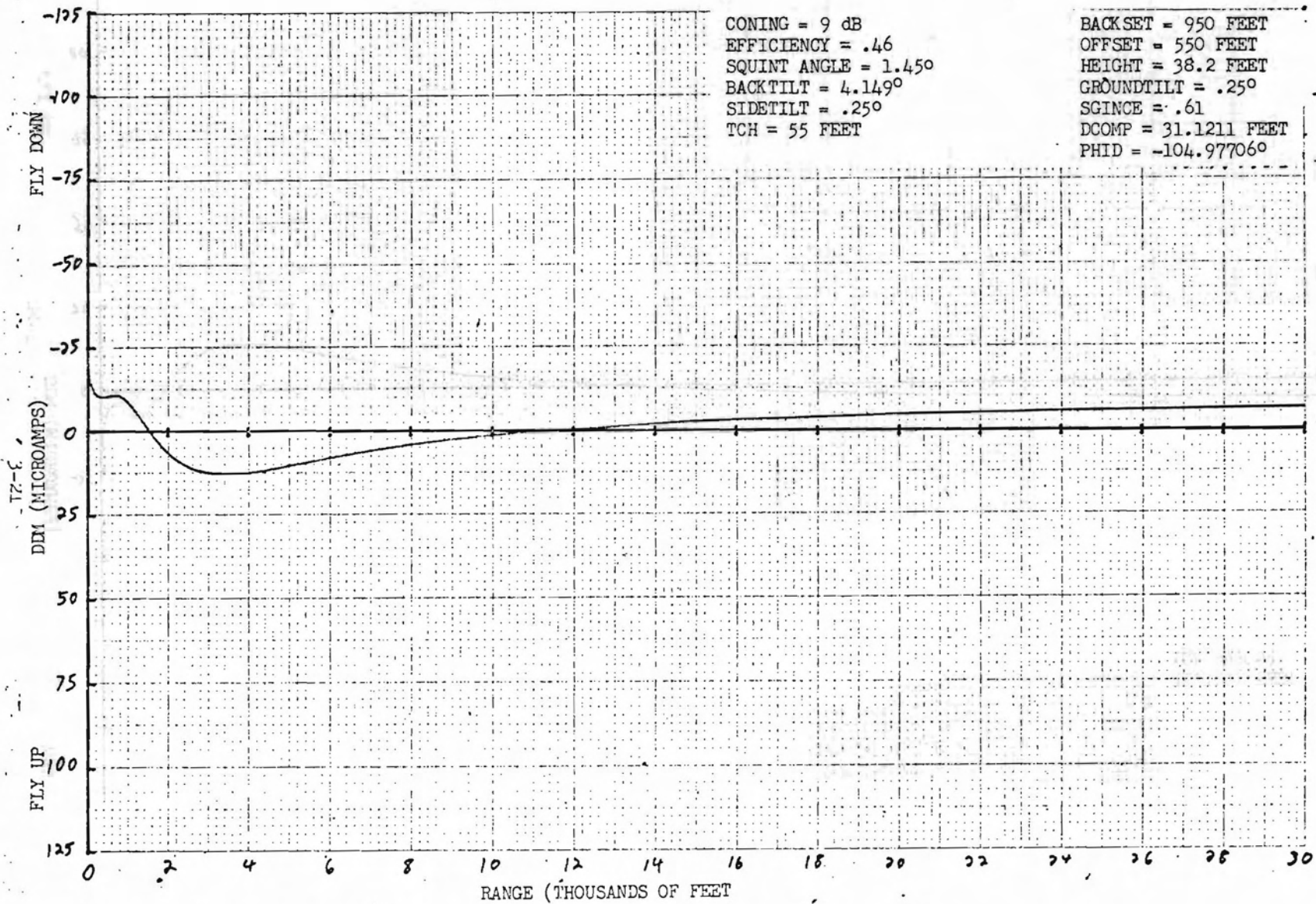
FLY-IN FOR ANTENNA LOCATION 2 (SEE FIG.3.14)

FIGURE 3.16



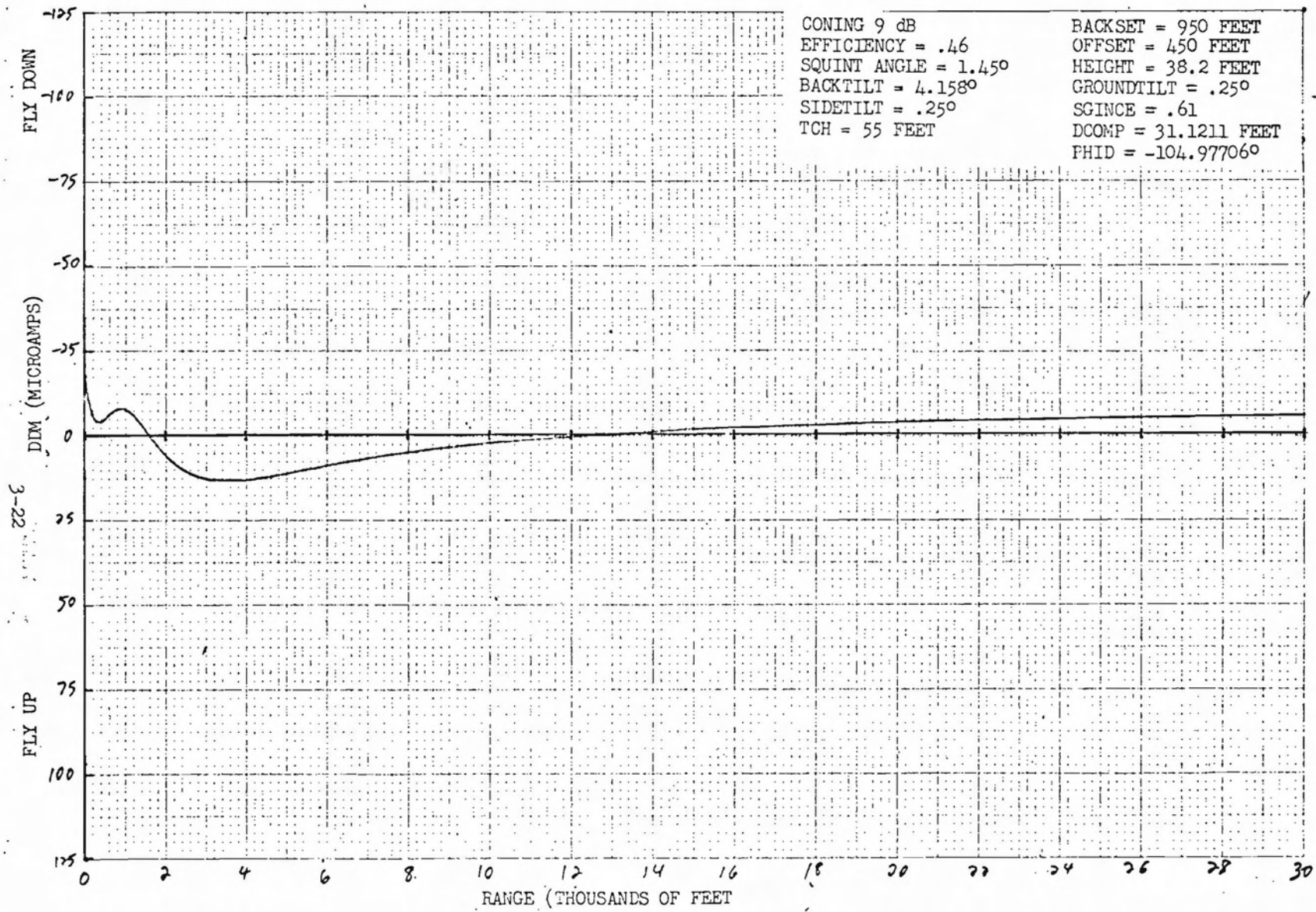
RANGE (THOUSANDS OF FEET)  
 FLY-IN FOR ANTENNA LOCATION 3 (SEE FIG.3.14)

FIGURE 3.17



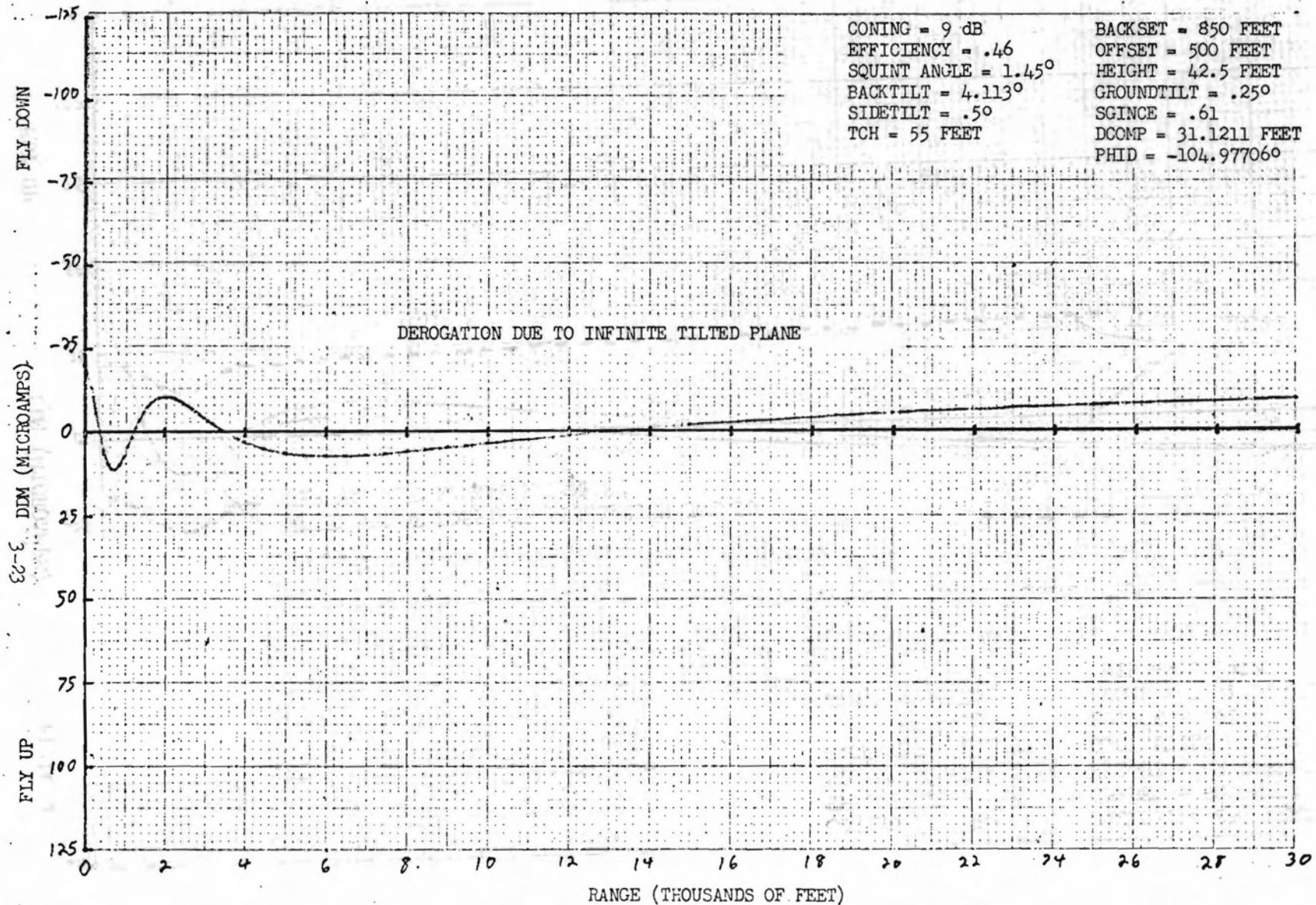
FLY-IN FOR ANTENNA LOCATION 4 (SEE FIG.3.14)

FIGURE 3.18



FLY-IN FOR ANTENNA LOCATION 5 (SEE FIG. 3.14)

FIGURE 3.19



FLY-IN FOR ANTENNA LOCATION 6 (SEE FIG.3.14)

FIGURE 3.20

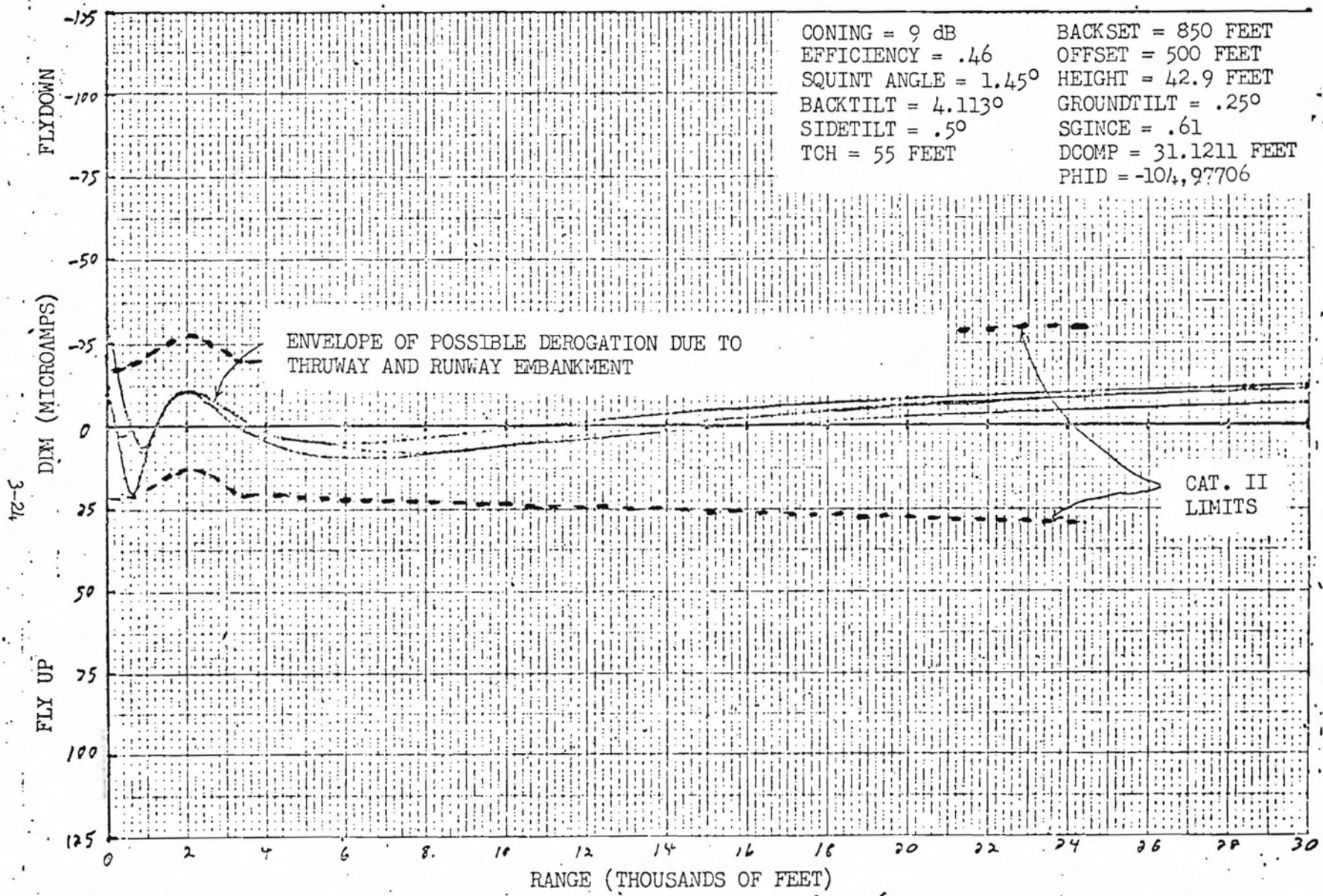
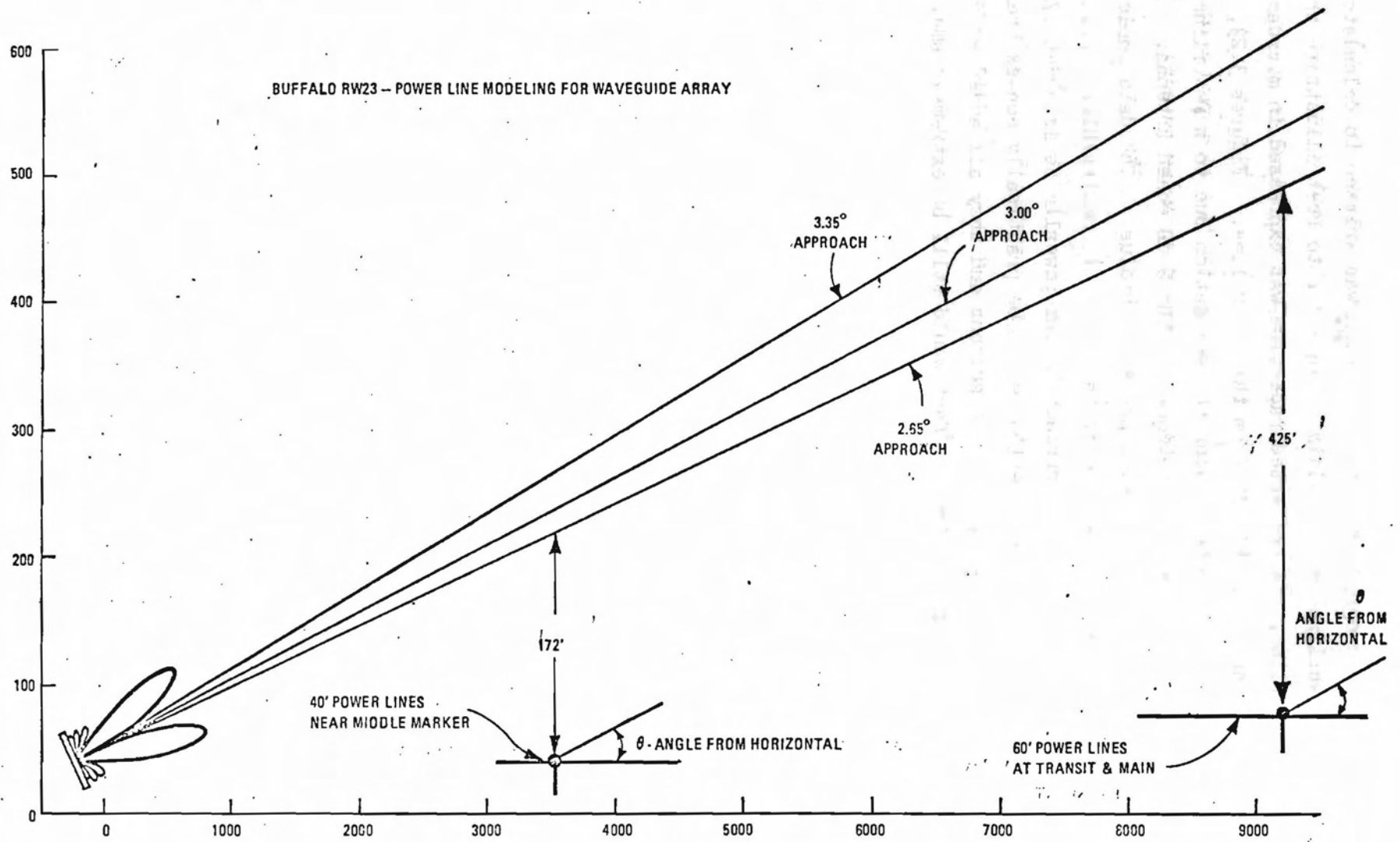


FIGURE 3.21 OPTIMUM FLY-IN WITH ALL SIGNIFICANT TERRAIN MODELED.

3-25



S74-0934-VA-9

FIGURE 3.22 RELATION OF AIRCRAFT PATH TO POWERLINES

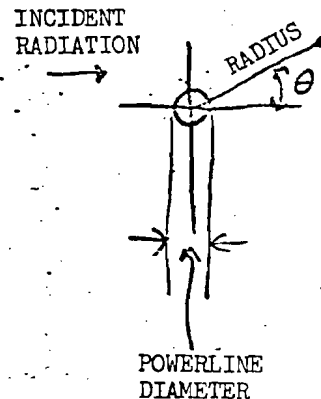
A computer program using this equation was written to calculate the effect of a powerline on flyability. In order to best illustrate the effect of the powerline, the reflected radiation was expressed in microamps of DDM derogation at various distances from the power line. Figures 3.23, 3.24 and 3.25 are computer printouts showing the derogation due to a powerline illuminated by both the 4 dB coned antenna and the 9 dB coned antenna. Each of these printouts are for a different powerline radius. The data indicates that beyond 10 feet from the powerlines, the effect is negligible. Figure 2.62 shows that the aircraft's closest approach to the powerlines is about 172 feet. At this range the effect of one powerline would be practically non-existent. Even if a large number of powerlines were present and they all added in phase at the aircraft (highly unlikely) their effect would still be extremely small.

RADIUS OF POWERLINE (INCHES) =

2 .125

RADIUS (FEET)	ANGLE ABOVE HORIZONTAL (DEGREES)	DDM DEGRADATION (MICROAMPS)	
		9DB Conting	4DB Conting
.01	.1	57.5750	124.7459
.01	30.0	57.7321	125.0561
.01	60.0	58.1752	126.0483
.01	90.0	58.7857	127.3691
.01	120.0	59.3963	128.6919
.01	150.0	59.8394	129.6521
.01	180.0	59.9965	129.9924
1.00	.1	8.8496	19.1741
1.00	30.0	8.8496	19.1742
1.00	60.0	8.8497	19.1744
1.00	90.0	8.8499	19.1747
1.00	120.0	8.8500	19.1750
1.00	150.0	8.8501	19.1752
1.00	180.0	8.8501	19.1753
3.00	.1	.5338	1.1568
3.00	30.0	.5338	1.1567
3.00	60.0	.5339	1.1567
3.00	90.0	.5339	1.1569
3.00	120.0	.5340	1.1570
3.00	150.0	.5340	1.1571
3.00	180.0	.5340	1.1571
5.00	.1	.0145	.0313
5.00	30.0	.0145	.0313
5.00	60.0	.0145	.0313
5.00	90.0	.0145	.0313
5.00	120.0	.0145	.0313
5.00	150.0	.0145	.0313
5.00	180.0	.0145	.0313
10.00	.1	.0007	.0016
10.00	30.0	.0007	.0016
10.00	60.0	.0007	.0016
10.00	90.0	.0007	.0016
10.00	120.0	.0007	.0016
10.00	150.0	.0007	.0016
10.00	180.0	.0007	.0016

STOP



SS 22.533 SECS.

RUN COMPLETE.

FIGURE 3.23

DEGRADATION DUE TO POWERLINE OF .25 INCH DIAMETER

RADIUS OF POWERLINE (INCHES) 2

2 .25

RADIUS (FEET)	ANGLE ABOVE HORIZONTAL (DEGREES)	DDM DEROGATION (MICROAMPS)	
		9DB <i>Coating</i>	4DB <i>Coating</i>
.02	.01	52.7340	122.9236
.02	30.00	57.0508	123.6097
.02	60.00	57.9779	125.8167
.02	90.00	59.2889	128.4117
.02	120.00	60.5550	131.2048
.02	150.00	61.4632	133.2136
.02	180.00	61.7999	133.8997
1.00	.01	10.1447	21.9802
1.00	30.00	10.1449	21.9305
1.00	60.00	10.1453	21.9815
1.00	90.00	10.1459	21.9829
1.00	120.00	10.1468	21.9842
1.00	150.00	10.1470	21.9852
1.00	180.00	10.1472	21.9855
3.00	.01	.6955	1.5070
3.00	30.00	.6956	1.5071
3.00	60.00	.6958	1.5076
3.00	90.00	.6961	1.5032
3.00	120.00	.6964	1.5033
3.00	150.00	.6986	1.5092
3.00	180.00	.6965	1.5094
5.00	.01	.0215	.0465
5.00	30.00	.0215	.0465
5.00	60.00	.0215	.0465
5.00	90.00	.0214	.0465
5.00	120.00	.0214	.0464
5.00	150.00	.0214	.0454
5.00	180.00	.0214	.0464
10.00	.01	.0012	.0027
10.00	30.00	.0012	.0027
10.00	60.00	.0012	.0027
10.00	90.00	.0012	.0027
10.00	120.00	.0012	.0027
10.00	150.00	.0012	.0027
10.00	180.00	.0012	.0027

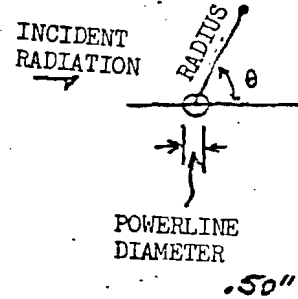
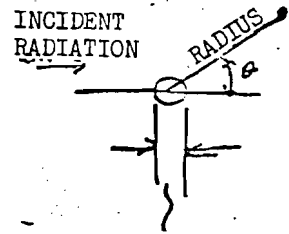


FIGURE 3.24 DEROGATION DUE TO POWERLINE OF .50 INCH DIAMETER

RADIUS OF POWERLINE (INCHES)

RADIUS (FEET)	ANGLE ABOVE HORIZONTAL (DEGREES)	DDM DEROGATION (MICROAMPS)	
		9DB <i>Coupling</i>	4DB <i>Coupling</i>
.03	-01	55.5615	120.3533
.03	30.00	56.0258	121.3892
.03	60.00	57.4352	124.4494
.03	90.00	59.4191	128.7414
.03	120.00	61.4000	133.0334
.03	150.00	62.8124	138.0938
.03	180.00	63.2767	137.3995
1.00	-01	11.0857	24.0190
1.00	30.00	11.0861	24.0198
1.00	60.00	11.0372	24.0222
1.00	90.00	11.0337	24.0255
1.00	120.00	11.0982	24.0257
1.00	150.00	11.0913	24.0311
1.00	180.00	11.0917	24.0320
3.00	-01	.8279	1.7937
3.00	30.00	.8281	1.7941
3.00	60.00	.8288	1.7953
3.00	90.00	.8293	1.7969
3.00	120.00	.8300	1.7984
3.00	150.00	.8305	1.7996
3.00	180.00	.8308	1.8000
5.00	-01	.0279	.0604
5.00	30.00	.0279	.0604
5.00	60.00	.0279	.0604
5.00	90.00	.0273	.0603
5.00	120.00	.0273	.0603
5.00	150.00	.0273	.0603
5.00	180.00	.0273	.0602
10.00	-01	.0017	.0038
10.00	30.00	.0017	.0038
10.00	60.00	.0017	.0038
10.00	90.00	.0017	.0038
10.00	120.00	.0017	.0038
10.00	150.00	.0017	.0038
10.00	180.00	.0017	.0038
STOP			



POWERLINE  
DIAMETER .75"

SS 22.505 SECS.

RUN COMPLETE.

FIGURE 3.25 DEROGATION DUE TO POWERLINE OF .75 INCH DIAMETER

4.00      REFERENCES

- 2.1    R.A.Moore, G. Moussally, T. Parker, S.F.Peyer,  
      "Analysis of Instrument Landing System Glide Slope Broadside Antennas"  
      Phase I, Interim Report  
      CONTRACT FAA-RD-72-139
- A.1.1 (same as above)
- A.2.1 J.A.Stratton, "Electromagnetic Theory", McGraw-Hill Book Company, Inc.,  
      New York, 1961, pp 364-372

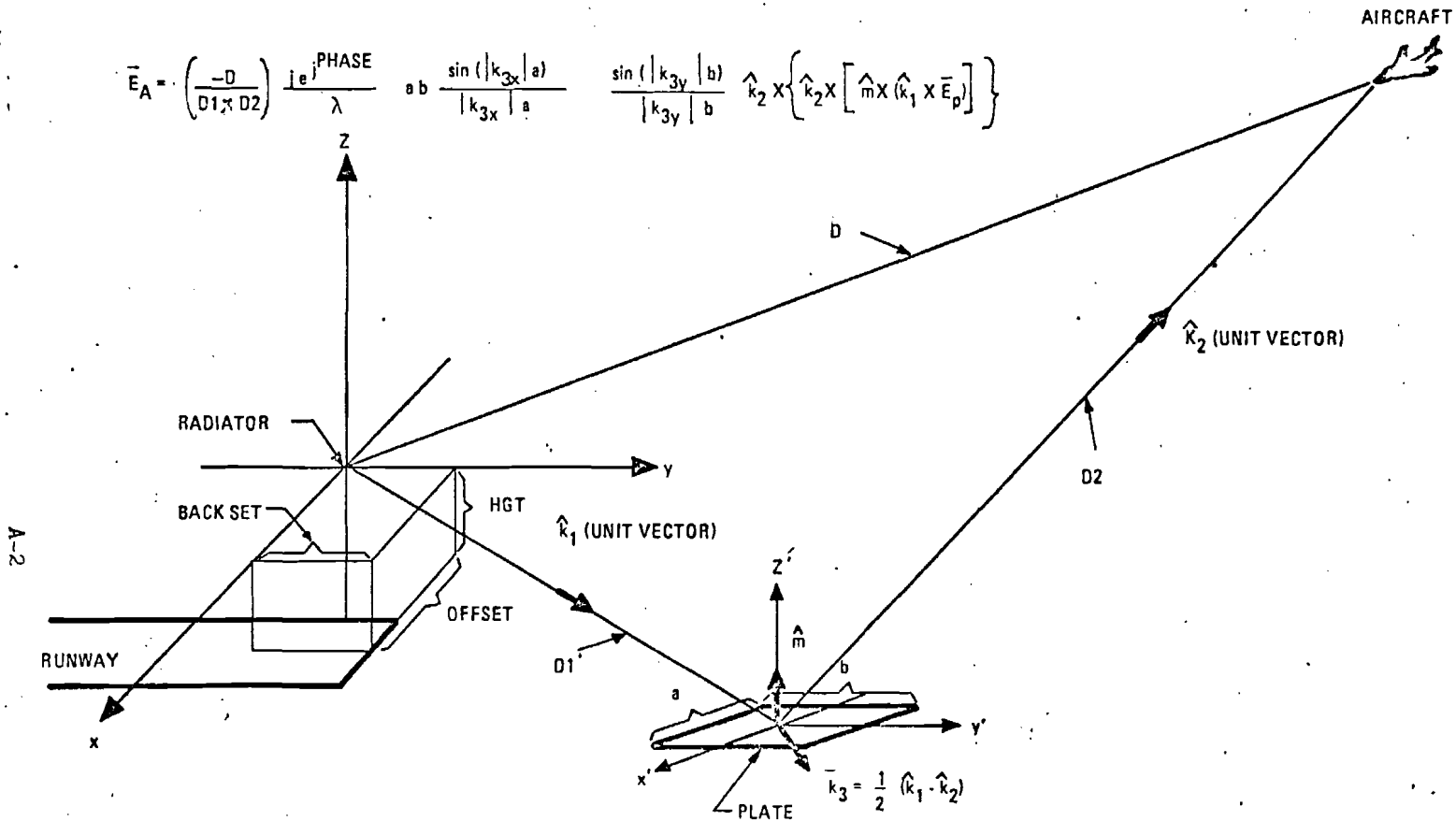
A. 1.0 DETERMINATION OF MAXIMUM PLATE SIZE FOR TERRAIN MODELING

The method of physical optics involves modeling the non-uniform terrain as arbitrarily oriented flat plates and calculating the effect at the aircraft by the equation: A.1.1

$$\bar{E}_A = \left( \frac{-D}{D1 \cdot D2} \right) j \frac{e^{j \text{PHASE}}}{\lambda} a b \frac{\sin(|k_{1x}|a)}{|k_{1x}|a} \frac{\sin(|k_{2y}|b)}{|k_{2y}|b} \hat{k}_2 \cdot \left\{ \hat{k}_1 \cdot [\hat{m} \times (\hat{k}_1 \times \bar{E}_p)] \right\}$$

Figure A.1.1 explains the terms used in the above equation. This equation was derived by assuming the radiation illuminating the plate is a plane wave. At finite distances from the radiator this is not exactly correct. However, good accuracy can be achieved by breaking the plate into rectangles small enough that the incident radiation appears to be a plane wave. The problem is then to determine the maximum plate size that will still ensure accuracy. In order to solve this problem empirically, it was necessary to compare the calculated approximation to a known solution. The simplest problem was to calculate the reflected radiation due to a point charge of unit magnitude above an infinite flat plane. Figure A.1.2 illustrates the geometry of the problem. There are two variables that must be determined: the maximum plate size and the minimum area needed to accurately model an infinite plane. The number of Fresnel zones was decided upon as a measure of area. The minimum plate size is a function of the radiation wavelength and the distance from the radiator to the reflecting surface. The criteria for determining if a receiver is in the far-field of a dipole is also a function of the distance from the receiver to the dipole, the separation of the radiators constituting the dipole, and the wavelength. This is expressed by distance =  $2D^2/\lambda$  where D is the separation of the radiators. The plate size is analogous to the radiator separation and can be expressed by  $D = \sqrt{\frac{\text{DIST} \times \lambda}{2}}$  This will ensure that the antenna is in the far-field of the plate but it does not necessarily mean that the plate size will give accurate modeling information. However, the "2" can be replaced by a variable "x" and as x increases the plate size will decrease and more accuracy will result. Figure A.1.2 also shows the results of varying plate size and modeled area. The plate size was varied while keeping the modeled area constant. Accuracy did not seem to improve satisfactorily with decreased plate size until the modeled area encompassed 20 Fresnel zones. The maximum plate size decided upon was:  $D = \sqrt{\frac{\text{DIST} \times \lambda}{8}}$  . This give about 5% error and any further decrease in plate size does not appreciably increase accuracy but does increase computer time and storage.

GRAPHICAL DESCRIPTION OF COMPONENTS OF PHYSICAL OPTICS EQUATION



$$\bar{E}_A = \left( \frac{-D}{D1 \times D2} \right) \frac{e^{j \text{PHASE}}}{\lambda} \frac{1}{ab} \frac{\sin \left( \frac{|k_{3x}| a}{|k_{3x}|} \right)}{|k_{3x}|} \frac{\sin \left( \frac{|k_{3y}| b}{|k_{3y}|} \right)}{|k_{3y}|} \hat{k}_2 \times \left\{ \hat{k}_2 \times \left[ \hat{m} \times (\hat{k}_1 \times \bar{E}_p) \right] \right\}$$

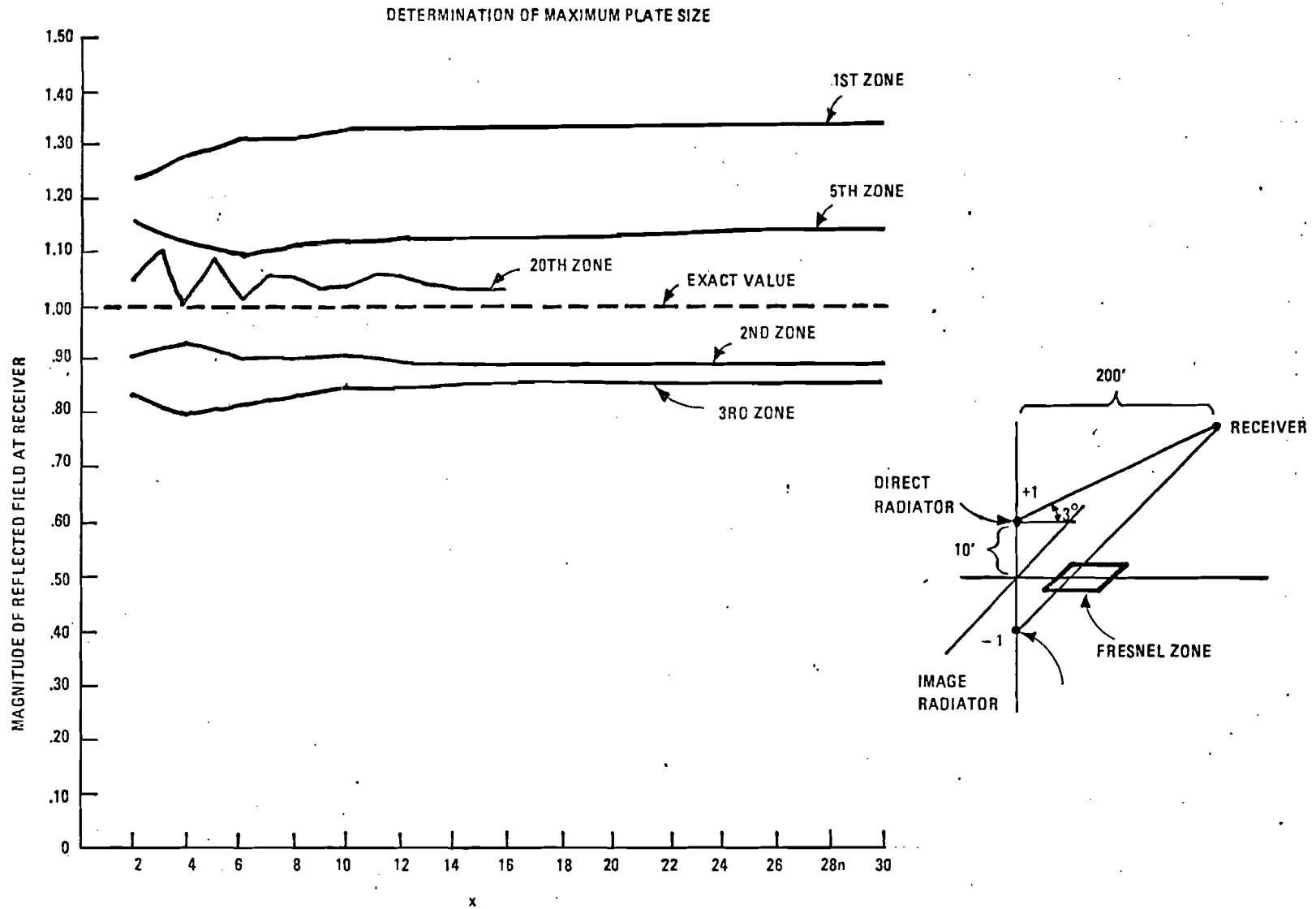
$\lambda$  = WAVELENGTH OF RADIATION  
 PHASE = PHASE AT AIRCRAFT

$\hat{m}$  = UNIT NORMAL TO PLATE ( $\hat{z}'$ )  
 $K_{3x}$  = X COMPONENT OF  $\vec{K}_3$  IN PLATE CO-ORDINATE SYSTEM (PRIMED)  
 $K_{3y}$  = Y COMPONENT OF  $\vec{K}_3$  IN PLATE CO-ORDINATE SYSTEM (PRIMED)  
 $\bar{E}_A$  = FIELD AT AIRCRAFT  
 $\bar{E}_p$  = FIELD INCIDENT TO PLATE

S74-0934-VA-5

FIGURE A.1.1

DESCRIPTION OF COMPONENTS OF PHYSICAL OPTICS EQUATION



'A MAXIMUM PLATE SIZE =  $\sqrt{D \times \lambda / x}$

$\lambda$  (WAVELENGTH) = 2.96 FT.

D = DISTANCE IN FEET FROM DIRECT RADIATOR TO NEAREST POINT ON MTH FRESNEL ZONE

FIGURE A.1.2

DETERMINATION OF MAXIMUM PLATE SIZE

A.2.0 POWERLINE MODELING

In order to accurately model the powerlines, the mathematical model must be as close as possible to the situation occurring in nature. However, to reduce the complexity of the problem it is necessary to make a few simplifying assumptions. The powerline can be thought of as an infinitely long, perfectly conducting cylinder immersed in free space. In this particular problem, the incident radiation can be assumed to be a plane wave since the distance from the antenna to either set of powerlines is very large compared to the radii of typical powerlines. The powerlines are assumed to be perpendicular to the direction of propagation and are parallel to the E field since the waveguide antenna radiates horizontally polarized waves. This is illustrated in Figure A.2.1.

The geometry of the problem suggests using cylindrical coordinates. A.2.1

$$\nabla^2 \bar{E} + k^2 \bar{E} \quad \text{is the wave equation in free space ( } k = 2\pi/\lambda \text{ ).}$$

The general solution to this equation in cylindrical coordinates is

$$E(r, \theta) = \sum A_n Z_n(kr) e^{j(m\theta - \omega t)} \quad \text{where } Z_n \text{ are Bessel functions or combinations of Bessel functions.}$$

In order to solve the boundary value problem, it will be necessary to represent the incident plane wave in the form of Bessel functions. A plane wave traveling in the  $x$  direction in free space can be represented by:

$$\bar{E}(x, y, z, t) = \bar{E}_0 e^{j(kx - \omega t)} = \bar{E}(r, \theta, z, t) = \bar{E}_0 e^{j(kr \cos \theta - \omega t)}$$

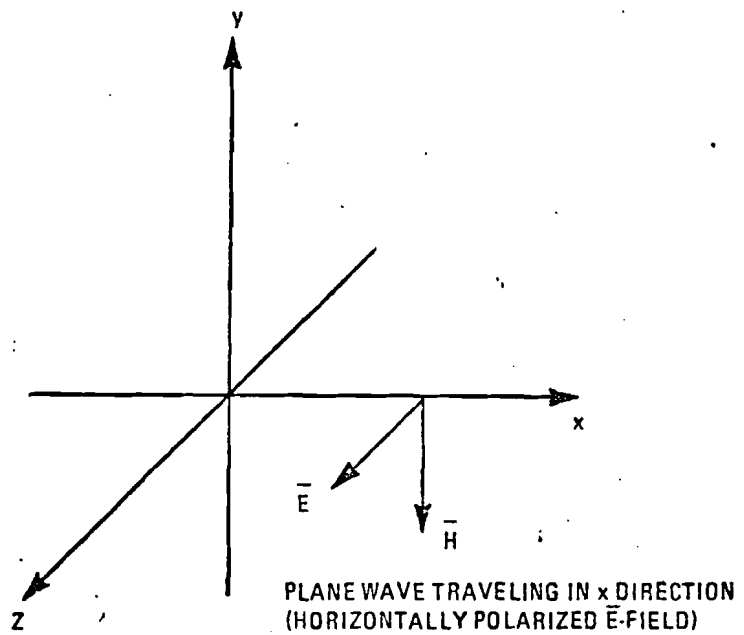
This function of  $r$  and  $\theta$  is periodic in  $\theta$  and can be expanded in a Fourier series whose coefficients are functions of  $r$  alone.

$$f(r, \theta) = \sum f_n(r) e^{im\theta}$$

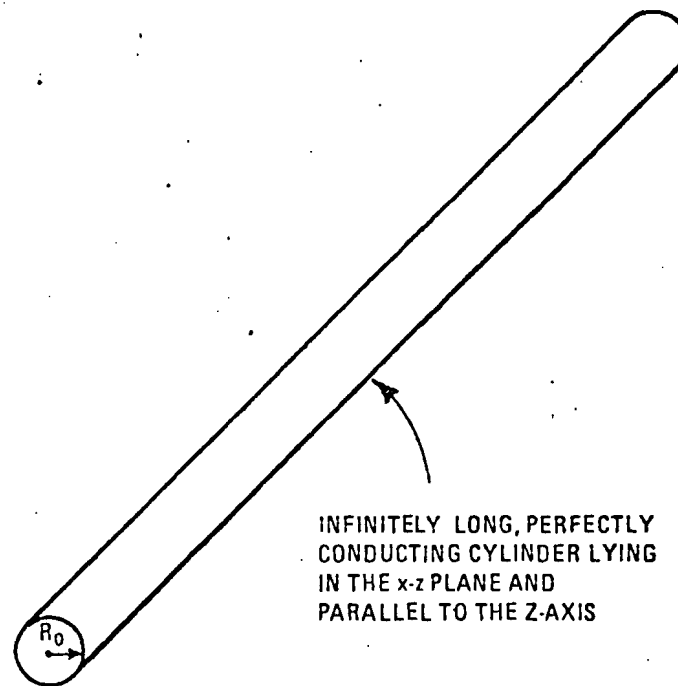
$$\text{WHERE } f_n(r) = \frac{1}{2\pi} \int_0^{2\pi} f(r, \theta) e^{-im\theta} d\theta$$

IDEALIZED REPRESENTATION OF A POWERLINE ILLUMINATED BY A PLANE WAVE

A-5



$$\vec{E}(x,y,z,t) = E_0 e^{j(kx - \omega t)} \hat{z}$$



S74-0934-VA-6

FIGURE A.2.1 IDEALIZED REPRESENTATION OF A POWERLINE ILLUMINATED BY A PLANE WAVE

In this problem,

$$f_m(r) = \frac{E_0}{2\pi} \int_0^{2\pi} e^{i(kr \cos \theta)} e^{-im\theta} d\theta$$

This integral must be evaluated in order to get  $f(r, \theta)$

An identity exists that has a form very similar to the above integral. This identity is an integral representation of the Bessel function of the first kind.

$$J_m(\rho) = \frac{i^{-m}}{2\pi} \int_0^{2\pi} e^{i\rho \cos \theta + im\theta} d\theta$$

where  $m$  is an integer

$f_m(r)$  can now be written as:

$$E_0 i^m \left[ \frac{i^{-m}}{2\pi} \int_{\theta=0}^{\theta=2\pi} e^{i kr \cos \theta - im\theta} d\theta \right]$$

LET  $\theta = -\phi$

$$\text{THEN } f_m(r) = E_0 i^m \left[ \frac{i^{-m}}{2\pi} \int_{\phi=0}^{\phi=-2\pi} e^{i kr \cos(-\phi) + im\phi} (-d\phi) \right]$$

The integral from 0 to  $-2\pi$  is the negative of the integral from 0 to  $2\pi$

Also,  $\cos(-\phi) = \cos \phi$

so

$$f_m(r) = E_0 i^m \left[ \frac{i^{-m}}{2\pi} \int_0^{2\pi} e^{i kr \cos \phi + im\phi} d\phi \right]$$

$$f_m(r) = E_0 i^m J_m(kr)$$

$$f(r, \theta) = \sum_{m=-\infty}^{\infty} E_0 i^m J_m(kr) e^{im\theta}$$

This is a plane wave expressed as an infinite sum of Bessel functions of the first kind.

The radiation in the powerline problem can be divided into incident radiation and reflected radiation.

Incident radiation:

$$\bar{E}_I = \bar{E}_0 \sum_{m=-\infty}^{\infty} j^m J_m(kr) e^{j^m \theta} \hat{a}_z$$

reflected radiation:

$$\bar{E}_R = \sum_{m=-\infty}^{\infty} H_m^{(1)}(kr) a_m$$

where  $H_m^{(1)}$  is a Hankel function and  $a_m$  is a constant to be determined.

The boundary conditions are:

$$E \text{ tangential} = 0$$

$$B \text{ normal} = 0$$

The E field inside a perfect conductor is zero, so at  $r = R_0$

$$g(r, \theta) = \bar{E}_I + \bar{E}_R = 0$$

$$g(R_0, \theta) = E_0 \sum_{m=-\infty}^{\infty} j^m J_m(kR_0) e^{j^m \theta} + \sum_{m=-\infty}^{\infty} H_m^{(1)}(kR_0) a_m e^{j^m \theta} = 0$$

In order to evaluate  $a_m$ ,  $g(r, \theta)$  is multiplied by  $e^{-j^p \theta}$  and integrated over  $\theta$  from 0 to  $2\pi$

$$\int_0^{2\pi} g(R_0, \theta) e^{-j^p \theta} d\theta = 0$$

$$\frac{1}{2\pi} \left[ \int_0^{2\pi} E_0 \sum_{m=-\infty}^{\infty} j^m J_m(kR_0) e^{j(m-p)\theta} d\theta + \int_0^{2\pi} \sum_{m=-\infty}^{\infty} a_m H_m^{(1)}(kR_0) e^{j(m-p)\theta} d\theta \right] = 0$$

$$\frac{1}{2\pi} \sum_{m=-\infty}^{\infty} \left\{ [E_0 j^{-m} J_m(kR_0) + a_m H_m^{(1)}(kR_0)] \int_0^{2\pi} e^{j(m-p)\theta} d\theta \right\} = 0$$

$$\int_0^{2\pi} e^{j(m-p)\theta} d\theta = \begin{cases} 0 & \text{if } m \neq p \\ 2\pi & \text{if } m = p \end{cases}$$

$$E_0 j^p J_p(kR_0) + a_p H_p^{(1)}(kR_0) = 0$$

$$a_p = \frac{-E_0 j^p J_p(kR_0)}{H_p^{(1)}(kR_0)}$$

reflected radiation:

$$\vec{E}_R = \sum_{m=-\infty}^{\infty} \left[ -\frac{E_0 j^m J_m(kR_0)}{H_m^{(1)}(kR_0)} H_m^{(1)}(kr) e^{j m \theta} \right] \hat{a}_z$$